LATERAL CONTINUITY OF THE EAGLE FORD GROUP STRATA IN LOZIER CANYON AND ANTONIO CREEK, TERRELL COUNTY, TEXAS

A Thesis

by

RAND DAVID GARDNER

Submitted to the Office of Graduate and Professional Studies of
Texas A&M University
in partial fulfillment of the requirements for the degree of

MASTER OF SCIENCE

Chair of Committee,	Michael C. Pope
Committee Members,	Arthur Donovan
	Walter B. Ayers
Head of Department,	John R. Giardino

December 2013

Major Subject: Geology

ABSTRACT

Understanding of the local lateral heterogeneity within the Eagle Ford Group, a prolific mudstone reservoir on the Texas Gulf Coast, is hindered by a lack of well-preserved outcrops in close proximity to one another. Misinformation or over simplistic assumptions about relevant horizontal reservoir heterogeneities can lead to sub-optimal or uneconomical exploitation. High-resolution correlation of individual beds in the Eagle Ford Group over several miles in Lozier Canyon and Antonio Creek in Terrell County, West Texas, was used to document lateral variation in thickness, composition, sedimentary structures, and gamma ray response of these strata on a local scale. Physical tracing of the beds on outcrops and within Gigapan photomosaics, hand-held spectral gamma-ray scintillometer profiles, and examination of polished hand samples and thin sections were used to correlate Eagle Ford Group strata across Lozier Canyon and Antonio Creek. The results add value by increasing the understanding of local horizontal heterogeneities and the depositional environments of Eagle Ford Group strata and potentially influencing how and where wells are drilled and completed.

Five distinct lithostratigraphic units, termed A-E from the base up, and their subunits, are laterally continuous over several miles in terms of thickness, lithology, and spectral gamma ray response. However, there are notable differences in thickness and sedimentary structures in units A and B. Unit A has the largest difference in thickness (7%), suggesting higher accommodation in the southeast part of the study area. Moreover, sedimentary structures and bed morphology of skeletal packstone beds in unit

B, the primary target of horizontal wells in the subsurface, vary over a 4-mi interval from discontinuous lenses to laterally continuous stacked beds. Simulated wireline logs obtained from outcrop exposures suggest that spectral gamma ray data is superior to total gamma ray data in correctly identifying the most desirable sub units for completion. Geochemical data and trace fossil abundance suggest primarily anoxic bottom water conditions during deposition of the Lower Eagle Ford Formation and oxic conditions during deposition of the Upper Eagle Ford Formation. Widespread zones of deformed bedding within the Eagle Ford Group strata typify certain units and were likely caused by paleoseismicity. Laterally extensive bedding plane exposures in Antonio Creek provide three-dimensional views of macrofossils and the bedform morphology that were previously only described from two-dimensional outcrops. Sedimentary structures suggest that units A, C, D, and E were deposited above storm wave base; and deposition of unit B was episodically above storm wave base.

ACKNOWLEDGEMENTS

I would like to thank my committee chair, Dr. Pope, and my committee members, Dr. Donovan, and Dr. Ayers, for their guidance and support throughout the course of this research.

I also want to extend my gratitude to the BP America Corporation, which provided the funds, equipment, and logistical support for this study. Field assistance was generously provided by Nicole Gardner, Matthew Wehner, Aris Pramudito, Scott Staerker, Abram Barker and Bryce Gardner. Thanks to Jacob Grosskopf for help identifying ichnofossils.

TABLE OF CONTENTS

LIST OF FIGURES

LIST OF TABLES

1. INTRODUCTION

The development of unconventional mudstone reservoirs like the Eagle Ford, Gothic, Marcellus, Utica, Haynesville, and Woodford formations and similar "shale plays" illustrate the need of understanding and predicting horizontal variability in mudstone reservoirs on the scale of a single lateral well. The horizontal component of a typical Eagle Ford well is 4,500 ft (1,400 m) long and contains 15 hydraulic fracture stages. The optimization of a horizontal drilling program depends on positioning and completing the lateral portion of a well in a way that maximizes revenue over the duration of well production. The outcrops of the Eagle Ford Group in Lozier Canyon and Antonio Creek (Fig. 1), Terrell County, Texas provide an opportunity to study lateral variability on this scale.

Based on work at the initial Lozier Canyon research site 1 (Fig. 1) in Lozier Canyon, Donovan et al. (2012) divided the Eagle Ford Group into four depositional sequences and illustrated the complex vertical variability of these strata. Furthermore, using petrophysical, biostratigraphic, and geochemical data, they suggested that the sequences and surfaces defined at the Lozier Canyon 1 site could be correlated into the subsurface and used to explain the thickness and facies distribution of the Eagle Ford Group unconventional reservoirs in South Texas. This work, however, did not address the lateral continuity or variability of individual beds within each of the four sequences defined within the Eagle Ford succession.

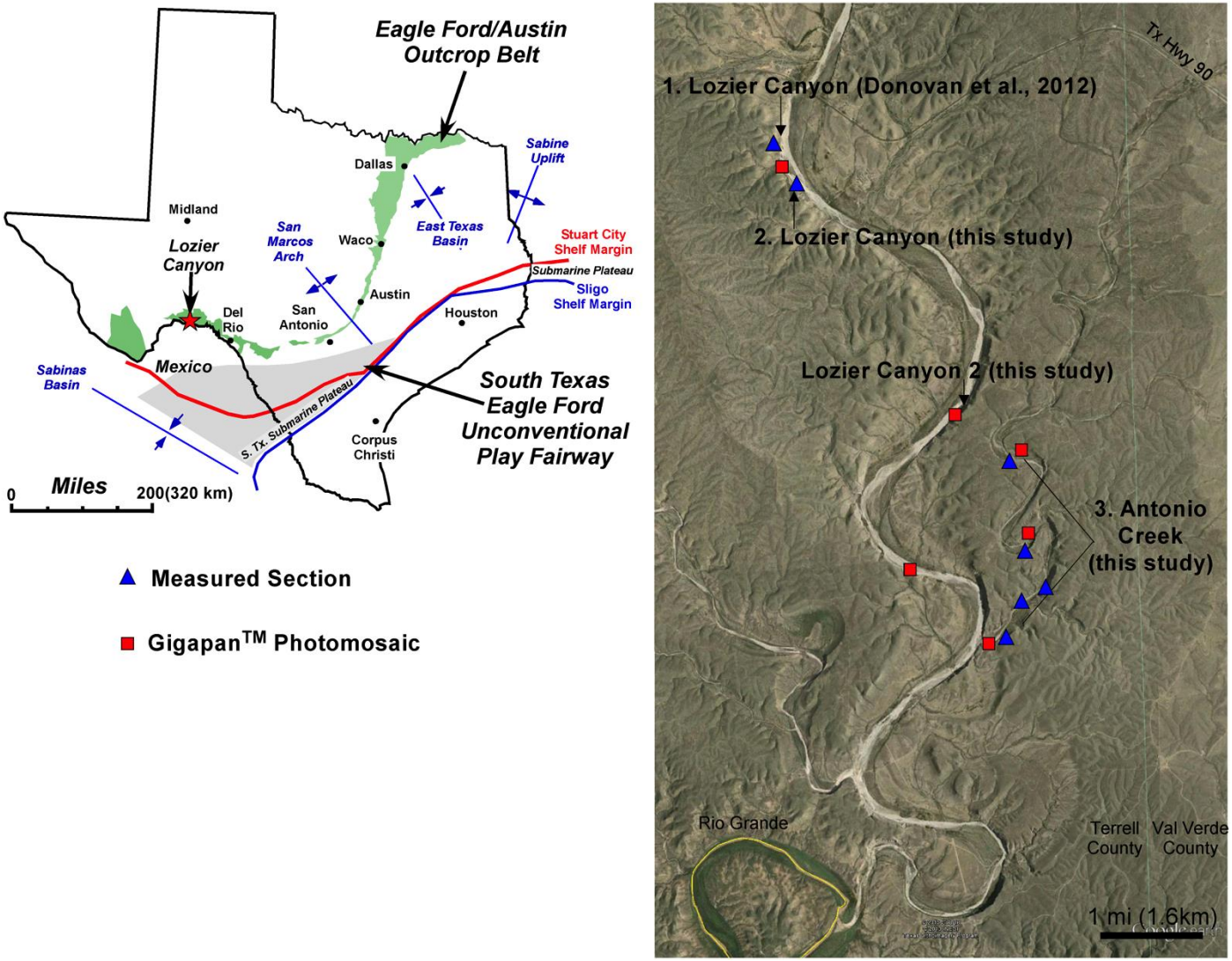

Figure 1. Location of the Study Area. State map modified after Donovan et al., 2012.

Eagle Ford Group outcrops in Lozier Canyon occur as semi-continuous cut-bank exposures along an approximate 8-mi (13-km) stretch from Texas Highway 90 to the U.S.-Mexico international border along the Rio Grande River. Typically, each of these cut-bank exposures is thousands of feet long and hundreds of feet high, providing good cross-sectional (2D) perspectives of bedding within the Eagle Ford. Recently, a new research site (#3) at Antonio Creek, a tributary to Lozier Canyon (Fig. 1), was studied. At this site, canyon floor exposures provide a unique opportunity to examine bedding plane exposures of most of the Eagle Ford Group strata, and an unparalleled opportunity to inspect 3D bedforms and fracture sets within the most prolific unconventional mudstone reservoir in the subsurface of south Texas.

2. GEOLOGIC SETTING

Sloss (1963) designated the Middle Jurassic through latest Cretaceous succession of North American as his unconformity-bounded Zuni Sequence, with the Cenomanian through Turonian portion of the Cretaceous section occurring at or near the maximum flooding surface of this first-order sequence. It was during this major marine incursion of the Zuni Sequence in the Cretaceous, that the Eagle Ford Group and equivalent (Woodbine) strata were deposited across Texas. Over much of Texas during the Early Cretaceous and earliest Late Cretaceous a well-developed carbonate platform developed. Hill (1887) referred to this carbonate-prone succession as the Comanche Series and named the overlying more siliciclastic-prone overlying Upper Cretaceous strata of Texas the Gulfian Series. Within south and west Texas the contact between the Buda Formation and Eagle Ford Group marks the boundary between Hill's (1887) Comanche and Gulfian Series (Fig. 2).

A well-developed carbonate platform, referred to as the Comanche Platform, developed during the Albian and early Cenomanian across much of central Texas. In south and west Texas, the platform-margin reef buildups on the Comanche Platform (Fig. 3) are commonly referred to as the Stuart City and Santa Elena trends; these reef buildups greatly influenced the inherited physiography of the overlying Eagle Ford Group succession.

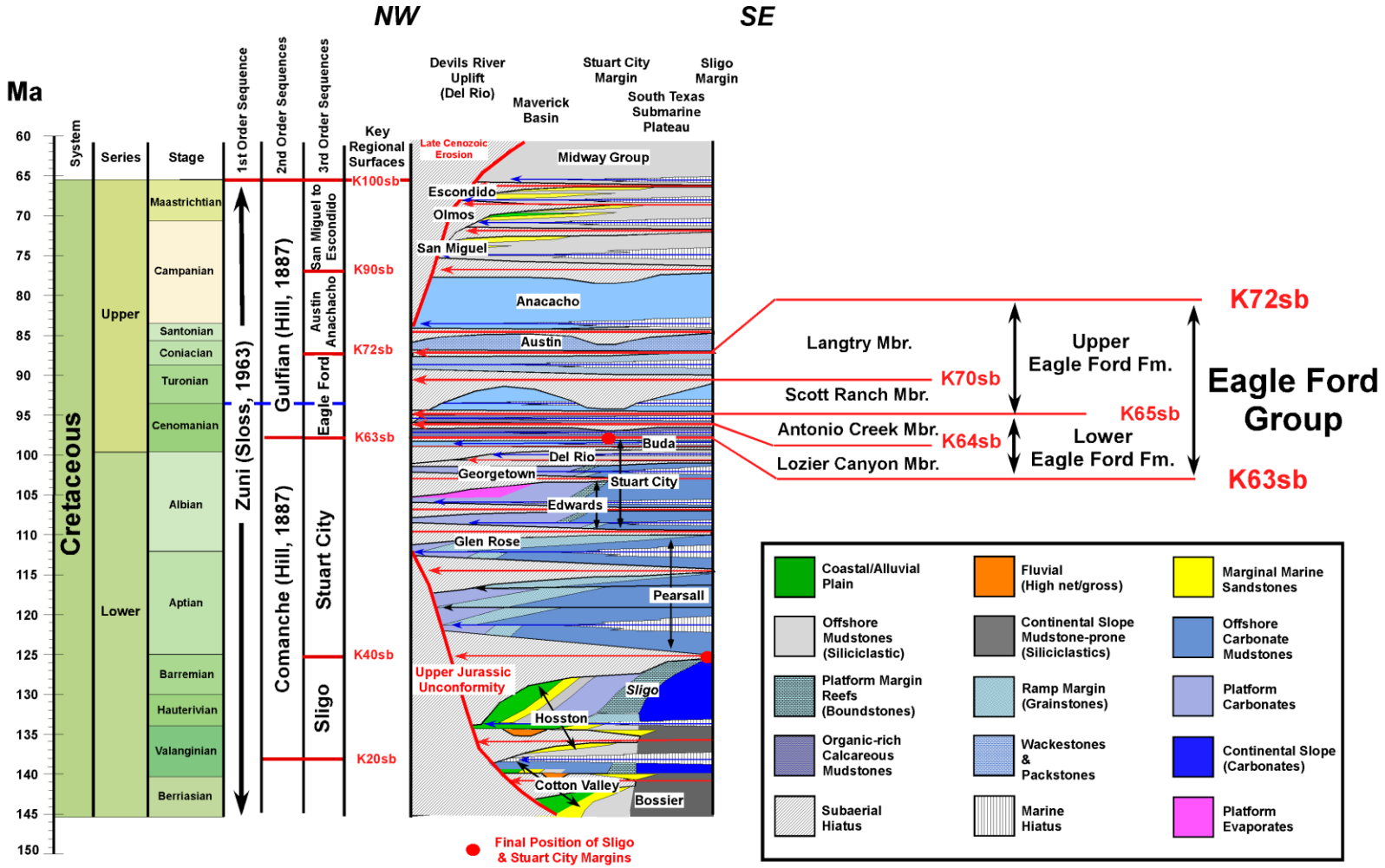

Figure 2. Cretaceous Chronostratigraphy of South Texas. Modified after Donovan et al., 2012

3. PREVIOUS WORK

The Eagle Ford Group outcrops of West Texas, which are also referred to as the Boquillas Formation, were studied by a number of previous workers. Key works on the stratigraphy of the Eagle Ford include Hazzard (1959), Freeman (1961, 1968), Pessagno (1969). Many aspects of the lithologies and sedimentology of the Eagle Ford Group were covered by Trevino (1988), as well as Lock and Peschier (2006). Key biostratigraphic papers on the Eagle Ford Group include Pessagno (1969) and Smith (1981). Donovan and Staerker (2010) utilized much of this previous work to subdivide the vertical facies succession observed in these outcrops into five basic lithostratigraphic units, which they termed A to E from the base up. This work was expanded and refined based on additional lithologic, biostratigraphic, geochemical, sedimentological, and petrophysical properties of these strata (Donovan et al., 2012), to further sub-divide the five units into 16 sub-units. These units and sub-units were then used to define four distinct depositional sequences within the Eagle Ford (K63, K64, K65, K70), each of which the authors suggested could be mapped as distinct members.

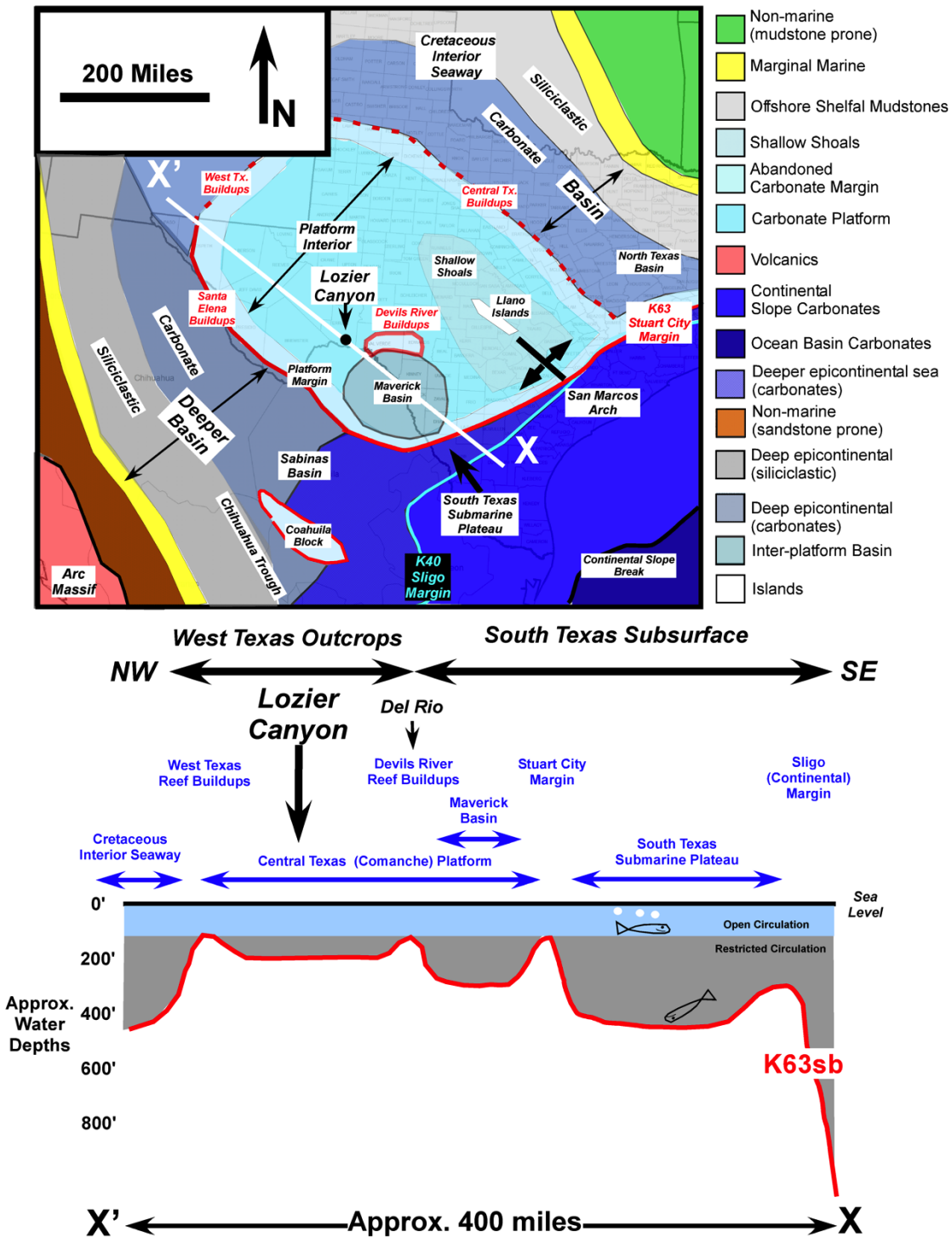

Figure 3. Map and Cross Section of the Late Cenomanian Comanche Platform. Modified after Donovan and Staerker 2010; Donovan et al., 2012.

4. METHODS

This study of the Eagle Ford Group strata in Lozier Canyon and Antonio Creek involved both field work and petrographic analysis. A composite stratigraphic section was measured and described in each canyon in 2012. Carbonate rocks were classified using Dunham's classification (1962), and sedimentary structures were described following Campbell's classification (1967). Measured sections include descriptions of bed lithology, color, thickness, fossils, ichnofabric index (BI) after Droser and Bottjer (1986), and sedimentary structures. Hand samples were collected every 2-3 ft (60-90 cm) at the Lozier Canyon section and every foot (30 cm) in the Antonio Creek section. A Gigapan™ system was used to photograph Eagle Ford Group outcrops and create photomosaics to document the variation of individual beds across thousands of feet of outcrop. A hand-held gamma-ray scintillometer, (Radiation Solutions RS230), collected spectral gamma-ray (SGR) values at 1-ft (30-cm) intervals from each measured section. Slabbed and polished hand samples from the outcrop were described with a hand lens and a binocular microscope. Sixty-seven 2x3 inch (5x7.5 cm) thin sections were described with plain light and cathodoluminescent microscopy.

The five basic lithostratigraphic units (A-E), and 16 sub-units defined by Donovan and others (2012) were identified on the sections measured in this study (Figure 4). The Lozier Canyon measured section in this study (Fig. 1) is located about 3,000 ft (1 km) from the section measured in Lozier Canyon by Donovan and others (2012) along the same cut-bank outcrop. Wave ripples and current ripples share many

characteristics and can look very similar, the criteria used to distinguish between these sedimentary structures are listed in Table 1.

4.1 Sources of Error

There are several variables that may have affected the SGR readings collected during this study. Portions of the SGR data in each section were collected on different trips and during different climatic conditions, which affect the amount of background radiation detected by the RS230. Abrupt changes in temperature can also affect the stability of the instrument. A 1-ft (30-cm) sampling interval was used in both outcrops; beds less than a foot thick that were sampled in one canyon may not have been sampled at the other locality. Different portions of the outcrops have varying degrees of weathering on the surface of the exposure. Effort was made to scrape away the outermost weathered surface before SGR data was collected.

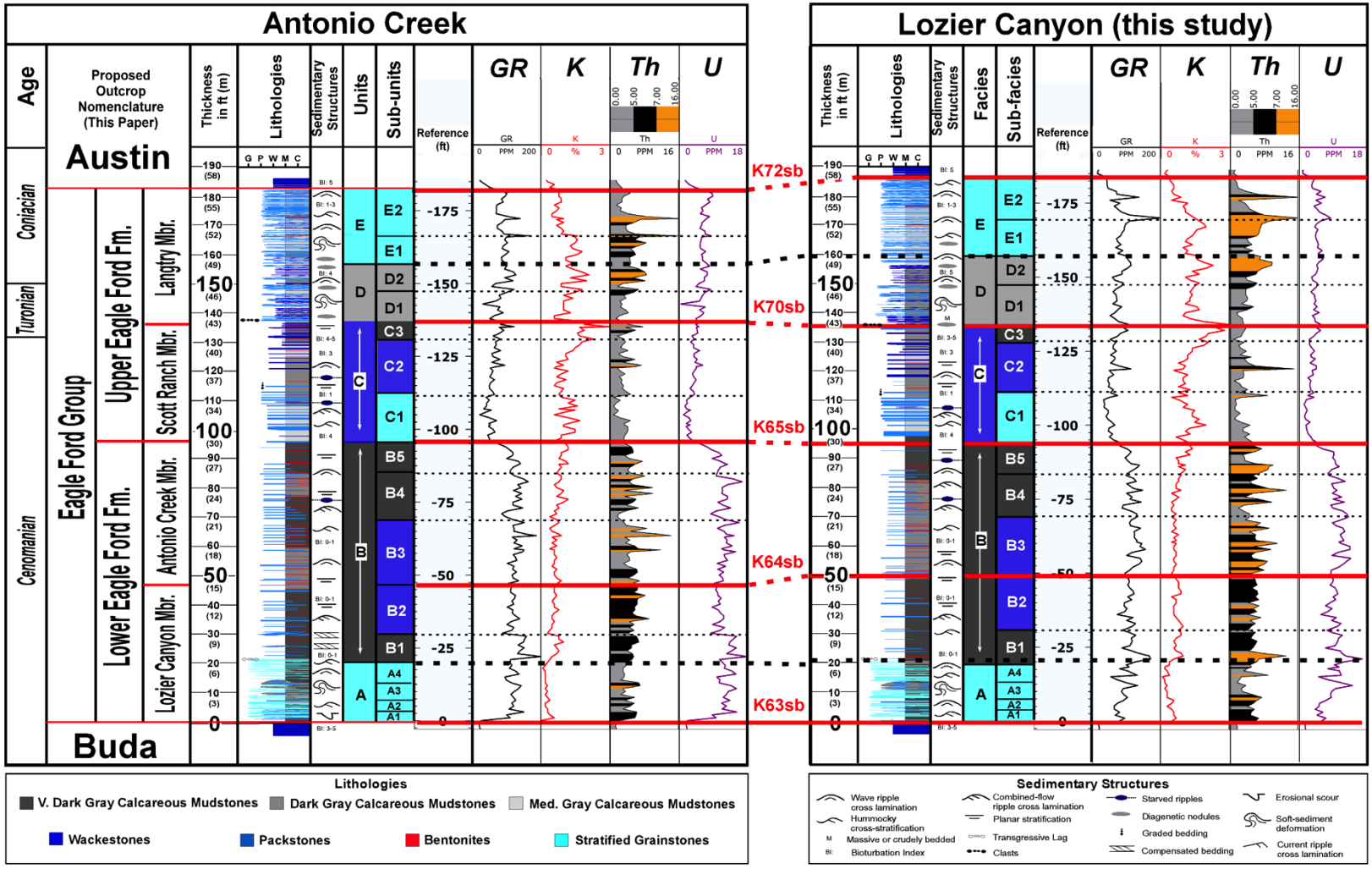

Figure 4. Measured Section Correlations. Antonio Creek is on the left and Lozier Canyon on the right.

Table 1. Caracteristics of Wave and Current Related Structures Used as Guides for Identification Used in This Study. After Harms and others (1975), Reineck and Singh (1975), Campbell (1967).

Wave	Current
Symmetrical and asymmetrical	Asymmetrical
Convex up with bi directional downlap	Rarely Convex up, usually onlap on one side
Hummocks	Trough cross stratification
Swales	Starved ripples
Laminae flatten upwards	Laminae flatten downwards

Table 2. Significant Chronostratigraphic Surfaces

Unit Boundaries				Marker Bentonites	
Boundary	Lozier Canyon	Antonio Creek	ΔThickness	Lozier Canyon	Antonio Creek
A-B	20.5 ft (6.2 m)	22.0 ft (6.7 m)	7.3%	172.5 ft (53 m)	176.6 ft (53.8 m)
B-C	95.0 ft (28.9 m)	96.0 ft (29.3 m)	0.7%	166.5 ft (51.3 m)	170.0 ft (51.8 m)
C-D	135.5 ft (41.3 m)	136.5 ft (41.6 m)	0.0%	77.8 ft (23.7 m)	78.0 ft (23.8 m)
D-E	156.5 ft (47.7 m)	156.5 ft (47.7 m)	4.8%	63.5 ft (19.4 m)	65.3 ft (19.9 m)
E-Austin	183.5.0 ft (55.9 m)	182.5 ft (55.6 m)	3.7%	58.5 ft (17.8 m)	59.8 ft (18.2 m)

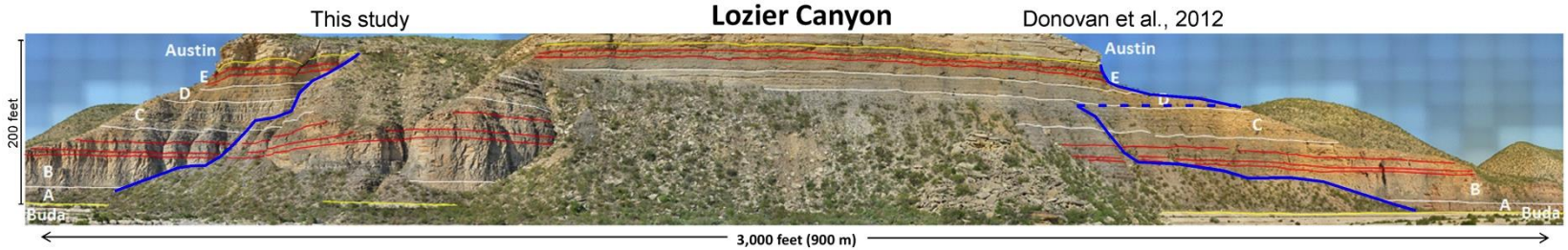

Figure 5. Annotated Photomosaic: Lozier Canyon #1. This is an Eagle Ford Group outcrop in Lozier Canyon. The blue lines show the locations of measured sections. Red lines mark major bentonite beds. White lines are unit boundaries and yellow lines mark the boundaries between the underlying Buda Limestone and the overlying Austin Chalk.

5. RESULTS

As defined by Donovan and others (2012), the Eagle Ford Group in this study area is unconformably bounded succession between the Buda Formation below and the Austin Chalk above (Fig. 2). Erosional surfaces, as well as bentonite beds, provide a chronostratigraphic framework for correlating individual beds between Lozier Canyon and Antonio Creek with a high degree of confidence (Fig. 4; Table 2). This framework also facilitates the location of unit boundaries and beds on Gigapan™ photomosaics (Fig. 5).

5.1 Lithologic Units

The five informal lithostratigraphic units (A-E) of the Eagle Ford Group are outlined below and described in detail in Table 3. Unit A consists of about 20 ft (6.5 m) of hummocky and swaley cross-stratified skeletal grainstone (Fig. 6A) interbedded with very dark gray calcareous mudstone. Few bentonites occur in this unit. Unit B consists of approximately 75 ft (24 m) of very dark gray calcareous mudstone (Fig. 6B) interbedded with thin beds of skeletal packstone (Fig. 6C). Multiple bentonite beds occur within unit B, especially in its upper part. Unit C consists of about 40 ft (13 m) of skeletal wackestone-packstone interbedded with dark gray calcareous mudstone. Thicker bentonite beds are conspicuously absent in unit C. Unit D contains approximately 20 ft (6 m) of nodular skeletal packstone (Fig. 6D) interbedded with

Table 3. Facies Descriptions of the Eagle Ford Group (Lozier Canyon and Antonio Creek, west Texas)

	A	B	C	D	E
Thickness					
Lozier Canyon	20.5 ft (6.2 m)	74.5 ft (22.7 m)	40.5 ft (12.3 m)	21 ft (6.4 m)	27.0 ft (8.2 m)
Antonio Creek	22.0 ft (6.7 m)	74.0 ft (22.6 m)	40.5 ft (12.3 m)	20.0 ft (6.0 m)	26.0 ft (7.9 m)
Lithology	1-12 in-thick (3-30 cm) beds sets of skeletal packstone-grainstone interbedded with calcareous mudstone; thin <1-in - thick (3 cm) bentonite beds; abundant foraminifera; pellets; bivalves; echinoderm fragments, fish bones; locally common <.5 in (1 cm) ammonites, shark teeth, oysters, phosphatic grains, *planolites, chondrites* ; rare gastropods, 3-20-in (8-50 cm) wood fragments; plesiosaur skeleton, framboidal pyrite; rare quartz silt	Very dark gray calcareous mudstone interbedded with skeletal packstone; <1-6 in-thick (3-15 cm) bentonite beds; abundant planktonic foraminifera, micrite clasts; common bivalves, fish bones; locally common *Planolites* ; rare 5-10 in (13-25 cm) ammonites, <6 in (15 cm) bony fish, unidentified large vertebrate skeleton, framboidal pyrite	Medium gray calcareous mudstone interbedded with 2-12 in-thick (6-30 cm) beds sets of skeletal wackestone-packstone; thin <1-in-thick (3 cm) bentonite beds; abundant forams, bivalves, pellets, *Thalassinoides, Teichichnus, Taenidium, Planolites, Chondrite,* frambroidal pyrite	1-8 in-thick (3-20 cm) irregular layers and nodules of skeletal wackestone& packstone; bedding is burrow homogenized; interbedded calcareous mudstone; thin <1 in (3 cm) thick bentonite beds; abundant foraminifera, pellets, bivalves, brachiopods, fish bones, echinoid *Hemiaster jacksonii,* unidentified ichnofossils; locally common 10-25 in (25-64 cm) ammonites, frambroidal pyrite	1-12 in-thick (3-30 cm) skeletal packstone & wackestone; interbedded calcareous mudstone; 1-8 in-thick bentonite beds; abundant foraminifera, pellets, bivalves, brachiopods, fish bones, echinoid *Hemiaster jacksoni, Chondrites, Taenidium,* unidentified ichnofossils, frambroidal pyrite
Sedimentary Structures	Abundant hummocky cross-stratification, wave ripples, combined flow ripples, fluid escape structures; soft sediment deformation; horizontal burrows	Abundant horizontal laminations, low-angle inclined laminations, cross stratification, horizontal burrows, locally common fluid escape structures	Abundant burrows, cross laminations; low-angle inclined laminations, ripple laminations,	Abundant burrows; rare preserved cross stratified laminations in nodules	Abundant burrows; ripple laminations; cross stratification
Environment	Restricted shelf, above storm wave base; anoxic	Restricted shelf, episodically above storm wave base; anoxic	Open shelf, above storm wave base, oxic	Open shelf, above storm wave base, oxic	Open shelf, above storm wave base, oxic

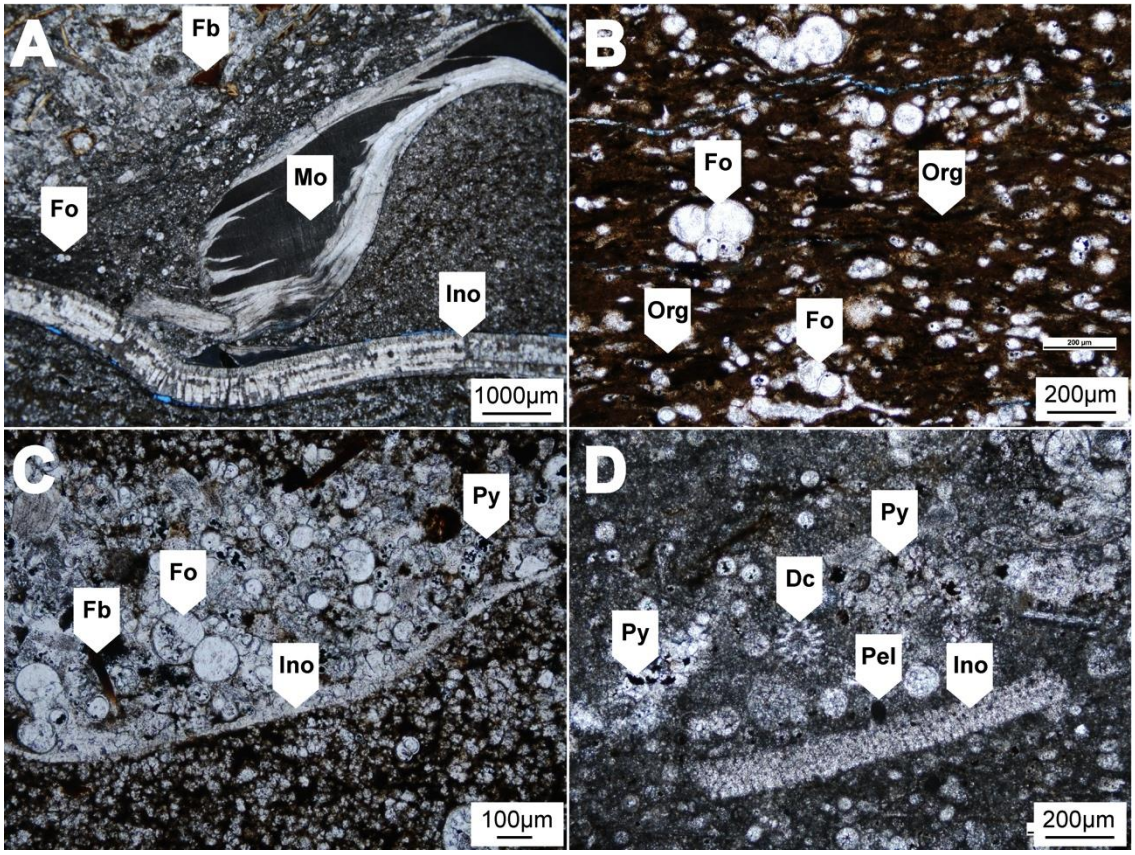

Figure 6. Photomicrographs. These photomicrographs contain planktonic foraminifera (Fo), fish bones (Fb), oysters (Mo), Inoceramid bivalves (Ino), organic matter (Org), pyrite (Py), Dasycladacean algae (Dc), and peloids (Pel). (A) Skeletal grainstone in subunit A4. (B) Calcareous mudstone in unit B. (C) Skeletal packstone in unit B. (D) Skeletal packstone in unit D.

medium gray calcareous mudstone. There are several thin bentonites in unit D and one deformed zone. Unit E consists of about 25 ft (8 m) of wave-rippled skeletal packstone interbedded with medium gray calcareous mudstone. Two bentonite marker beds and at least two deformed zones also occur in unit E.

5.2 Lateral Correlations

Key surfaces and individual beds of the Eagle Ford Group were traced across each outcrop and correlated between the two composite sections (Fig. 7). The thickness of subunits typically varies by less than a few feet across the study area (Table 4). Thicker bentonites are the most correlative beds; however, some resistant grainstone beds and bedsets are also correlative. The lateral continuity of several of these beds is described below. All footage notes in the proceeding sections and figures are in height above the Buda Formation–Eagle Ford Group contact.

5.2.1 Lower Eagle Ford Formation

In Unit A, four thin (<2 inch or 3 cm thick) bentonite beds and four thicker, laterally continuous skeletal grainstone bedsets are laterally continuous across the study area (Fig. 8). These grainstone bedsets mark the boundaries of the four subunits. Most beds in unit A are laterally discontinuous and pinch out or are scoured out over tens of feet (several meters), but the beds within each subunit have similar thickness and

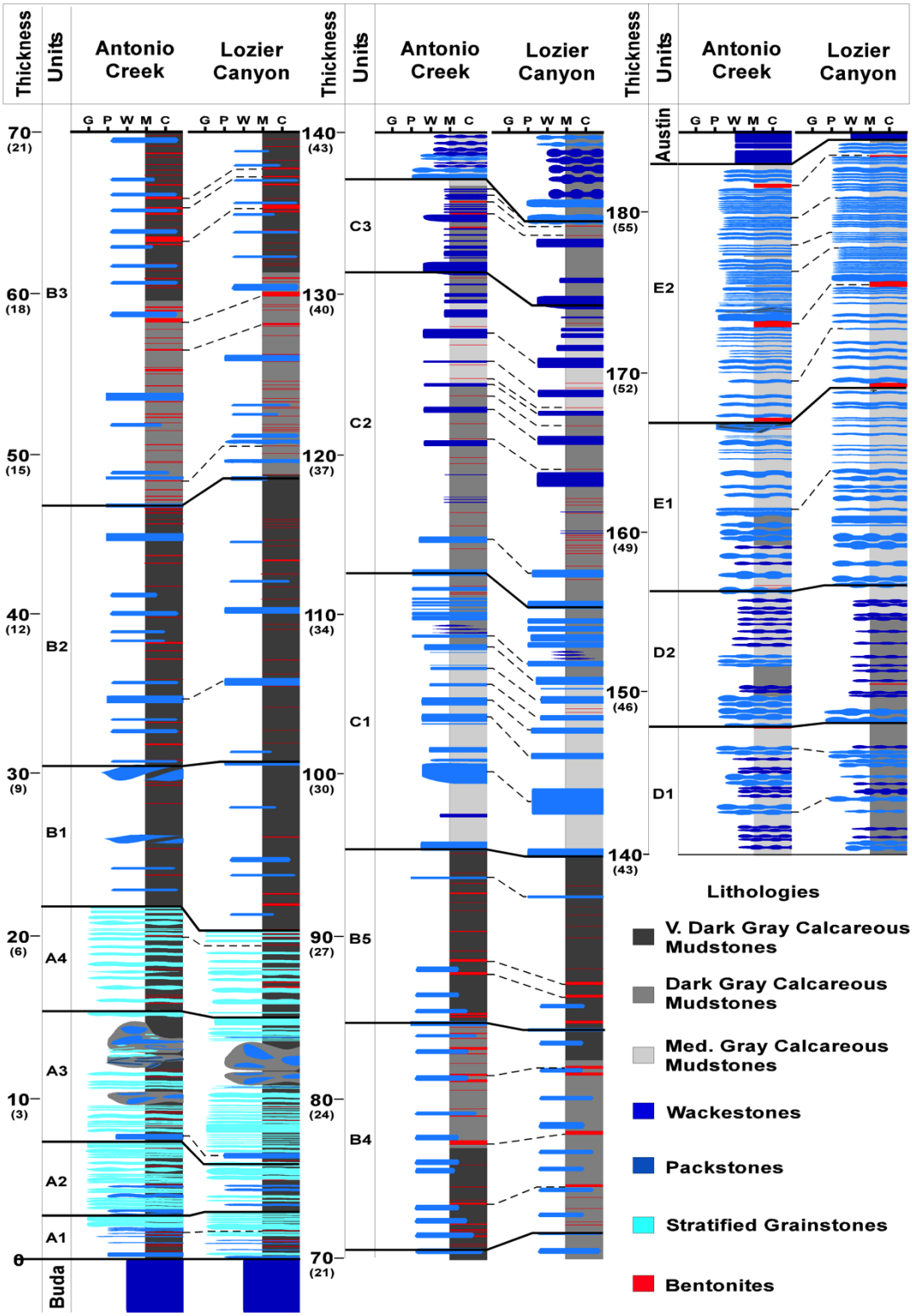

Figure 7. Detailed Lithologic Correlations. Solid black lines are unit boundaries. Dashed lines are high-confidence correlations.

Table 4. Thickness of Subunits in Feet (Meters)

Subunit	Lozier Canyon	Antonio Creek	Subunit	Lozier Canyon	Antonio Creek	Subunit	Lozier Canyon	Antonio Creek
E2	16.0 (4.9)	13.5 (4.1)	C2	21.0 (6.4)	20.5 (6.2)	B2	18.0 (5.5)	16.0 (4.9)
E1	10.0 (3.0)	13.5 (4.1)	C1	14.0 (4.3)	16.0 (4.9)	B1	10.0 (3.0)	8.0 (2.4)
D2	8.5 (2.6)	9.0 (2.7)	B5	9.0 (2.7)	10.0 (3.0)	A4	7.0 (2.1)	6.5 (2.0)
D1	12.5 (3.8)	11.0 (3.4)	B4	11.5 (3.5)	13.5 (4.1)	A3	7.0 (2.1)	8.0 (2.4)
C3	5.5 (1.7)	3.5 (1.1)	B3	26.0 (7.9)	26.5 (8.1)	A2	3.5 (1.1)	4.5 (1.4)
						A1	3.0 (0.9)	3.0 (0.9)

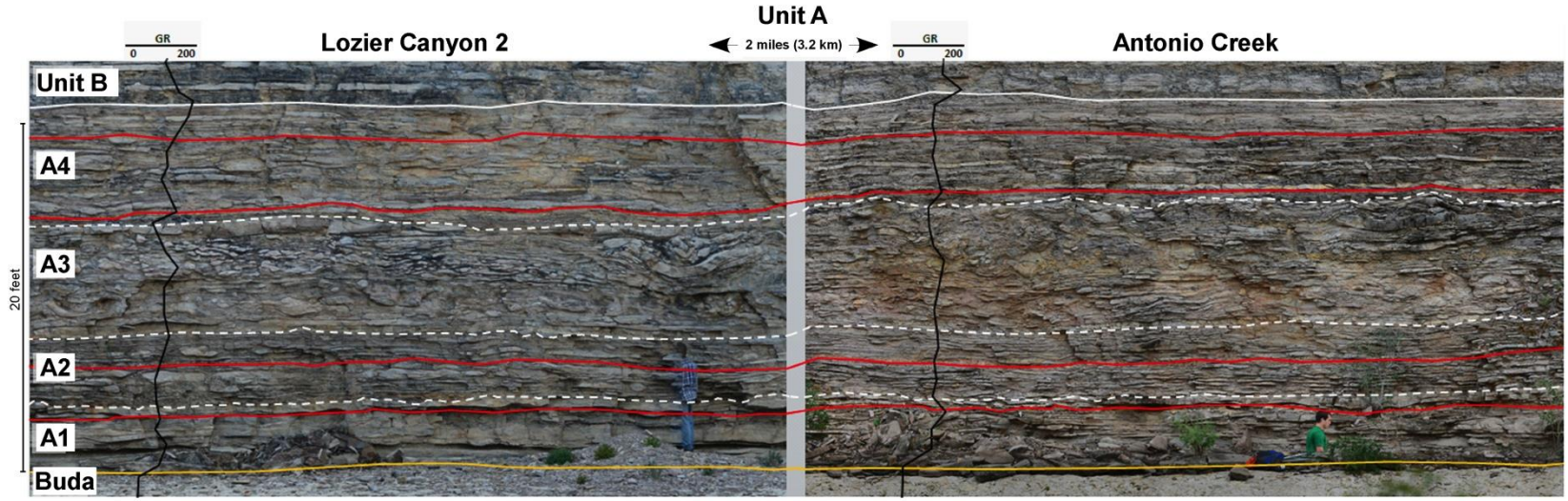

Figure 8. Annotated Photomosaic: Lozier Canyon #2 and Antonio Creek. The yellow line marks the contact with the underlying Buda Limestone. Red lines mark laterally continuous bentonite beds. White dotted lines are sub unit boundaries and the solid white line is a unit boundary.

sedimentary structures across the study area. A zone of laterally continuous deformed bedding in subunit A3 ranges in thickness from 2–5 ft (0.6-1.5 m). Soft-sediment deformation in the form of load casts, convolute bedding, and fluid-escape structures are common. Portions of the skeletal grainstone beds are internally homogenized and lack primary sedimentary structures. In Antonio Creek at 9 ft (2.7 m), an additional, separate zone of deformed bedding occurs locally. This contorted zone is discontinuous, less than 1 ft (30 centimeters) thick and commonly less than 10 ft (3 m) wide in several locations across a 1,000-ft (300-m) unit A in Antonio Creek and is not visible elsewhere. In subunit A4, a zone of shell lags containing oysters, bivalves, shark teeth, fish bones, and phosphatic grains occurs across the study area.

Unit B is characterized by organic-rich calcareous mudstone interbedded with about 15% skeletal packstone beds and 5% bentonite beds by volume. Thicker bentonite and skeletal packstone beds within unit B are laterally continuous across the study area. Erosional surfaces are common within the calcareous mudstone facies, and thinner bentonites are locally scoured out. Intervals of closely spaced thinner bentonite beds can be correlated across the study area, but individual beds cannot. Thinner skeletal packstone beds commonly are lensoidal and pinch out completely over hundreds of feet (tens of meters). In 2-D outcrops, skeletal packstone beds form a continuum of morphologies from isolated lenses to continuous pinch and swell beds (Fig. 9). Two skeletal packstone beds (26 and 30) change significantly across the study area (Fig. 10). Bed 30 in Antonio Creek consists of stacked, laterally discontinuous skeletal packstone lamina sets of 5 to-10 ft- (2-3 m-) thick hummocks and swales. Over thousands of feet

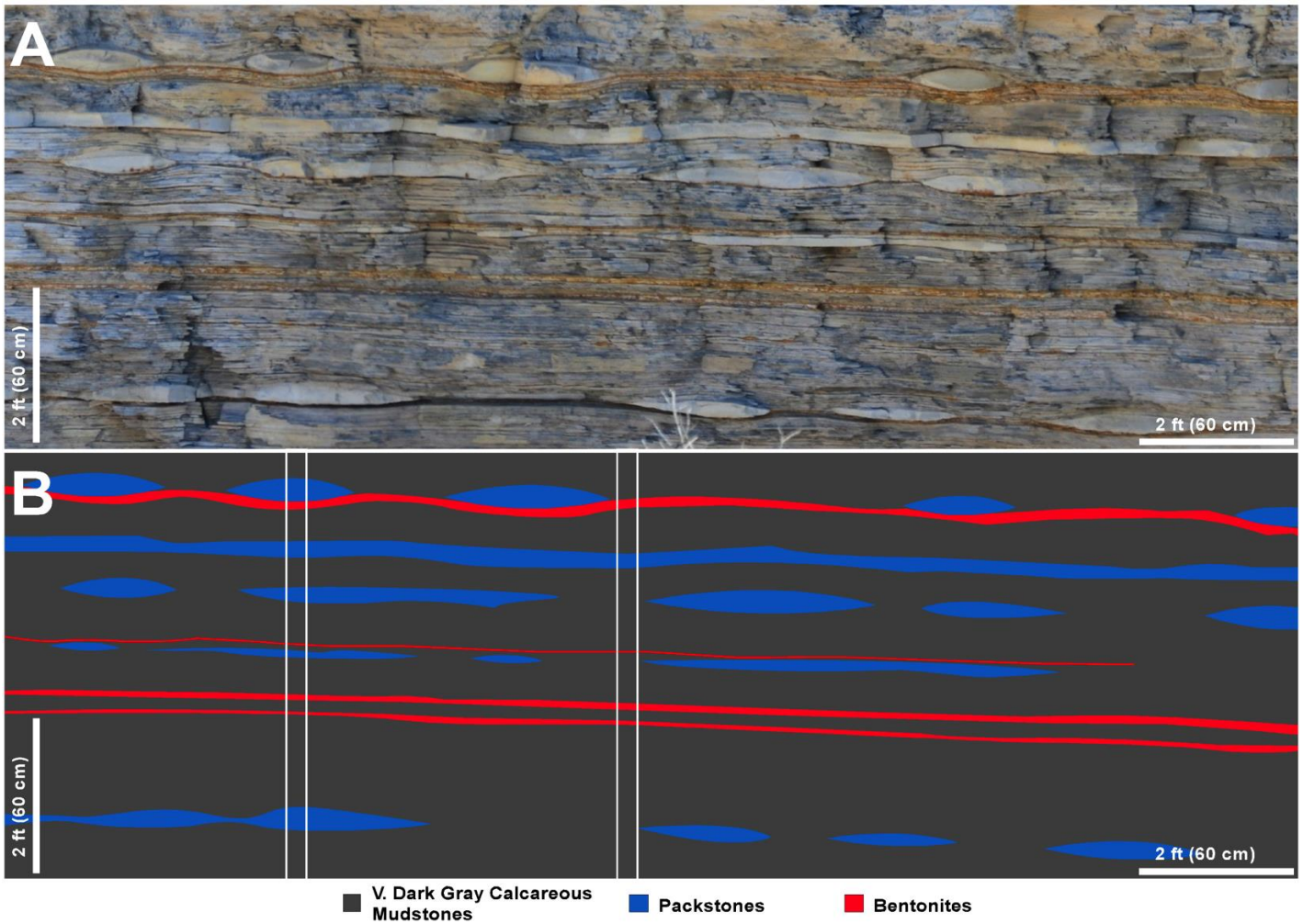

Figure 9. Lensoidal Skeletal Packstone Beds in Unit B. (A) Uninterpreted and (B) interpreted skeletal packstone beds in unit B show a continuum of isolated lenses to continuous beds. The white lines represent hypothetical vertical cores. Note how different the two cores would be over just a few feet.

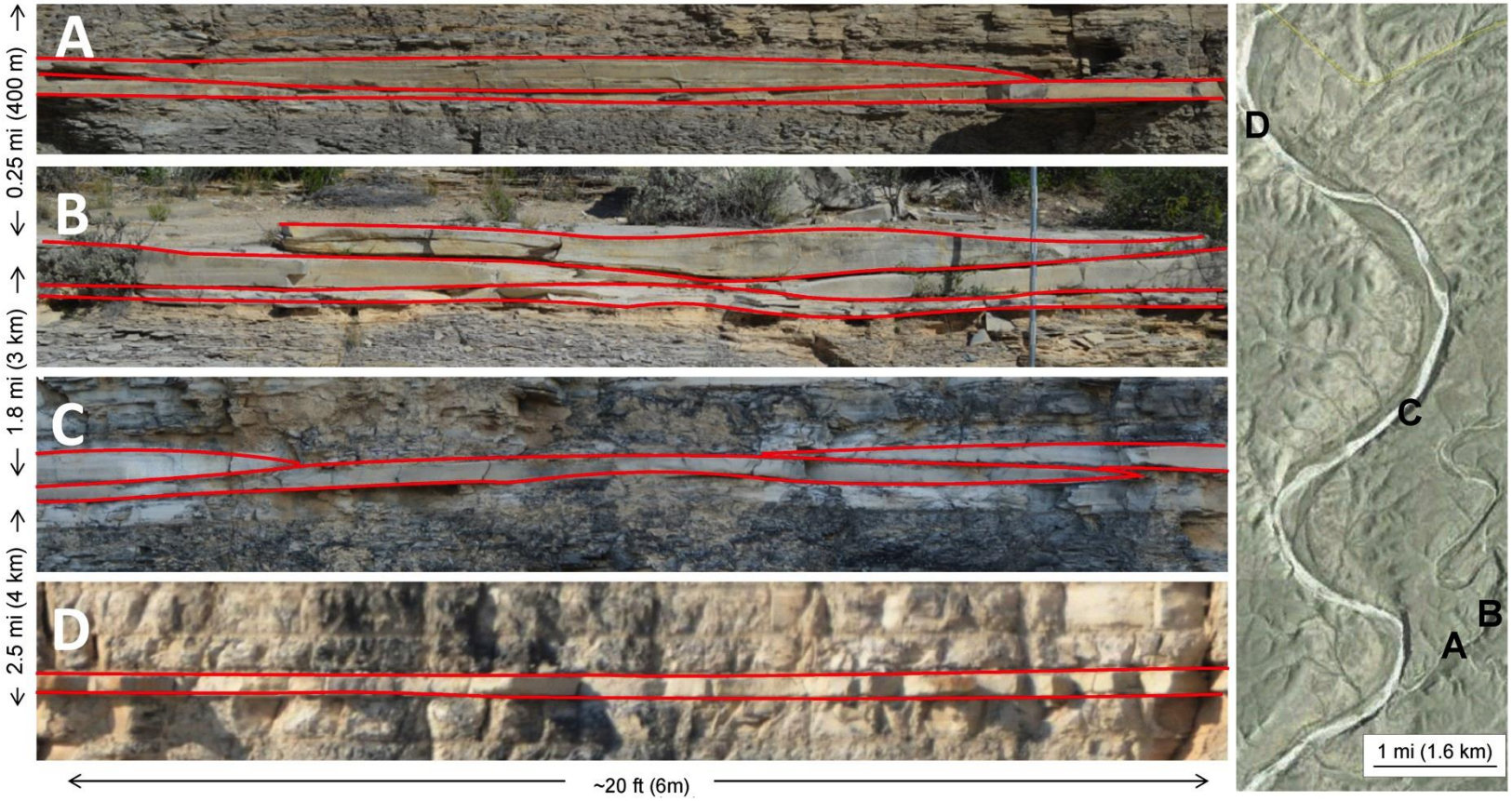

Figure 10. Comparison of Bed 30. (A, B) Bed 30 in Antonio Creek. (C) Bed 30 at Lozier Canyon 2. (D) Bed 30 at the Lozier Canyon 1 outcrop. Note that this bed transitions from a multiple, stacked lamina sets to a single lamina set over about 4 miles.

(hundreds of meters), several of these lamina sets pinch out completely and the bed consists of a single lamina set at the Lozier Canyon 1 site (Fig. 9). Bed 26 is similar to bed 30, but bed 26 is thinner and pinches out completely over about 1,000 ft (300 m).

Skeletal packstone beds have consistent internal bedding features (low-angle inclined laminations, horizontal laminations, wave ripples, small-scale hummocky cross stratification, current ripples) across the study area. Laterally continuous skeletal packstone beds tend to have horizontal to lower angle laminations that transition to higher angles concomitant with the lateral change to discontinuous isolated lenses.

5.2.2 Upper Eagle Ford Group

Lateral continuity of individual beds is more consistent within the Upper Eagle Ford Group across the study area (Fig. 10). There is significant variation in subunit C3 in Antonio Creek, which contains an additional 2.5 ft (0.8 m) of dark gray calcareous mudstone below the contact with the overlying unit D in one location. However, the contact between units C and D is marked by rip-up clasts and is interpreted as the K70 sequence boundary (Fig. 4). The nodular bedding of unit D is heavily bioturbated (BI:4-6) and lacks any preferred orientation in 3-D exposures. Mudstone-prone intervals contain discontinuous isolated nodules. Several thicker, laterally continuous correlative bedsets in unit D are correlative in all outcrops (Fig. 11). A discontinuous contorted zone occurs in subunit D1, with a lateral recurrence interval of hundreds of feet (tens of meters). Two major bentonites occurring in subunit E2 are visible on all the outcrops in

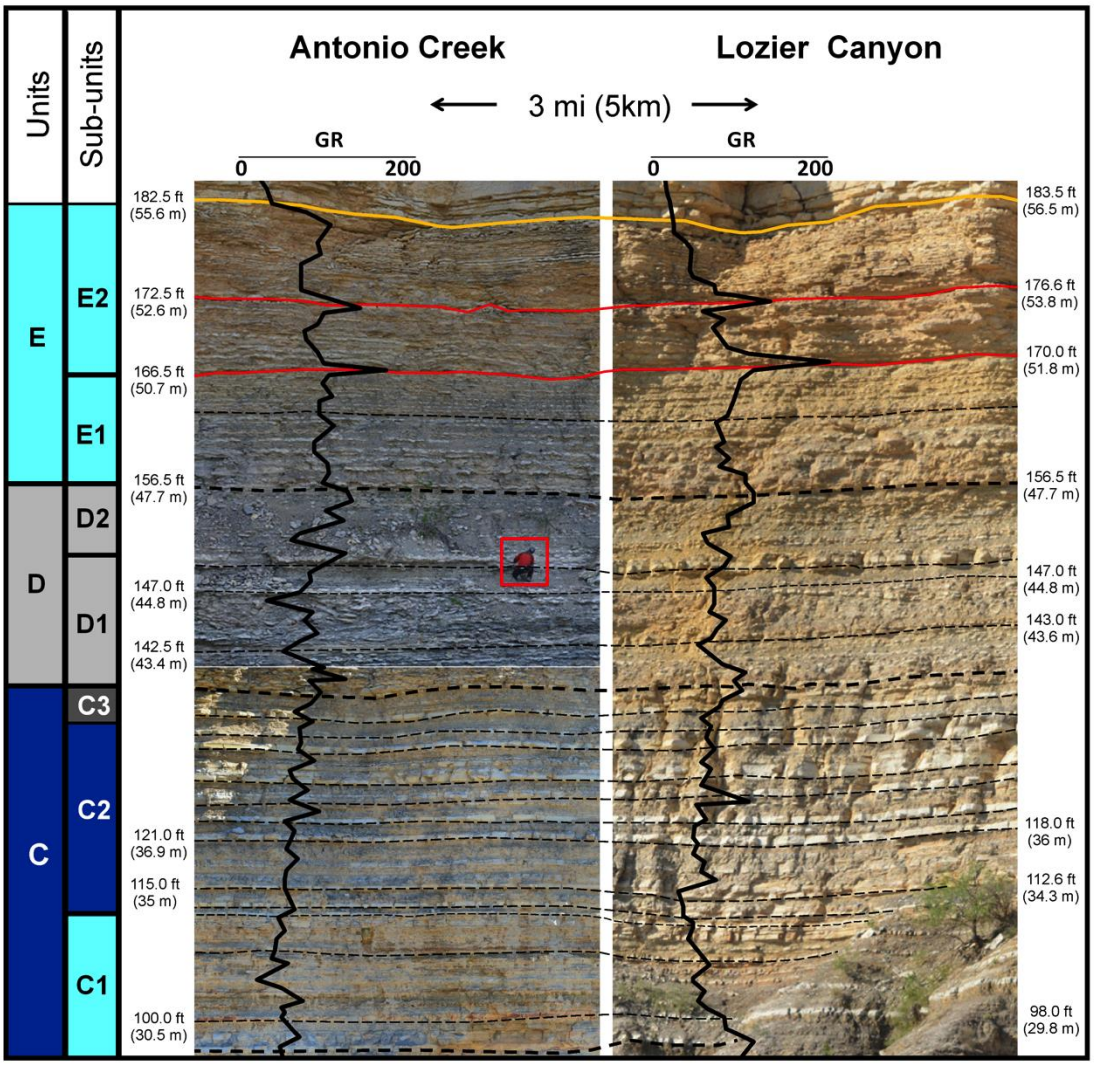

Figure 11. Lithologic Correlation: Upper Eagle Ford. Correlation is between resistant wackestone to packstone beds in the Upper Eagle Ford Group about 3 miles apart. The orange line marks the Eagle Ford Group-Austin Chalk boundary, red lines represent thick bentonites, black dashed lines represent unit boundaries and thin black lines trace individual bedsets. The red box indicates a person on the outcrop for scale. The high-gamma-ray peaks created by bentonite beds could be mistaken for condensed sections in the subsurface.

the study area. In subunit E2 several well-defined upward-thickening packages of ripple-laminated packestone-grainstone beds are laterally continuous in the study area. Also in this unit are two discontinuous contorted zones with horizontal recurrence intervals of tens of feet (3-10 m). The contact with the Austin Chalk is abrupt and marked by rip up clasts and is interpreted as the K72 sequence boundary (Donovan and others, 2012).

5.3 Spectral Gamma Ray Logs

SGR logs provide insight into the vertical changes in clay (K), bentonite (Th), and organic matter (U) enrichment in stratigraphic sections. K, Th, and U are lower within skeletal packstone and grainstone units and higher in mudstone and much higher in bentonites. The Upper Eagle Ford Group is noticeably richer in K and poorer in U than the Lower Eagle Ford succession. The SGR logs from each measured section have the same overall trends (Fig. 4), but not all peaks are correlative. The more notable differences are presented here. An increase in Th and U occurs at the top of subunit E2 just below the Austin Chalk contact in Antonio Creek and not in the Lozier Canyon log. There is an increase in K at the base of subunit B1 in Antonio Creek that does not occur in the other section. Th spikes appear to correspond directly with bentonite beds. There is a large Th spike at the base of subunit B1 in Lozier Canyon that does not occur in Antonio Creek. Many other Th spikes are correlative, but have higher values in Lozier Canyon than Antonio Creek, most notably in the Antonio Creek and Langtry Members.

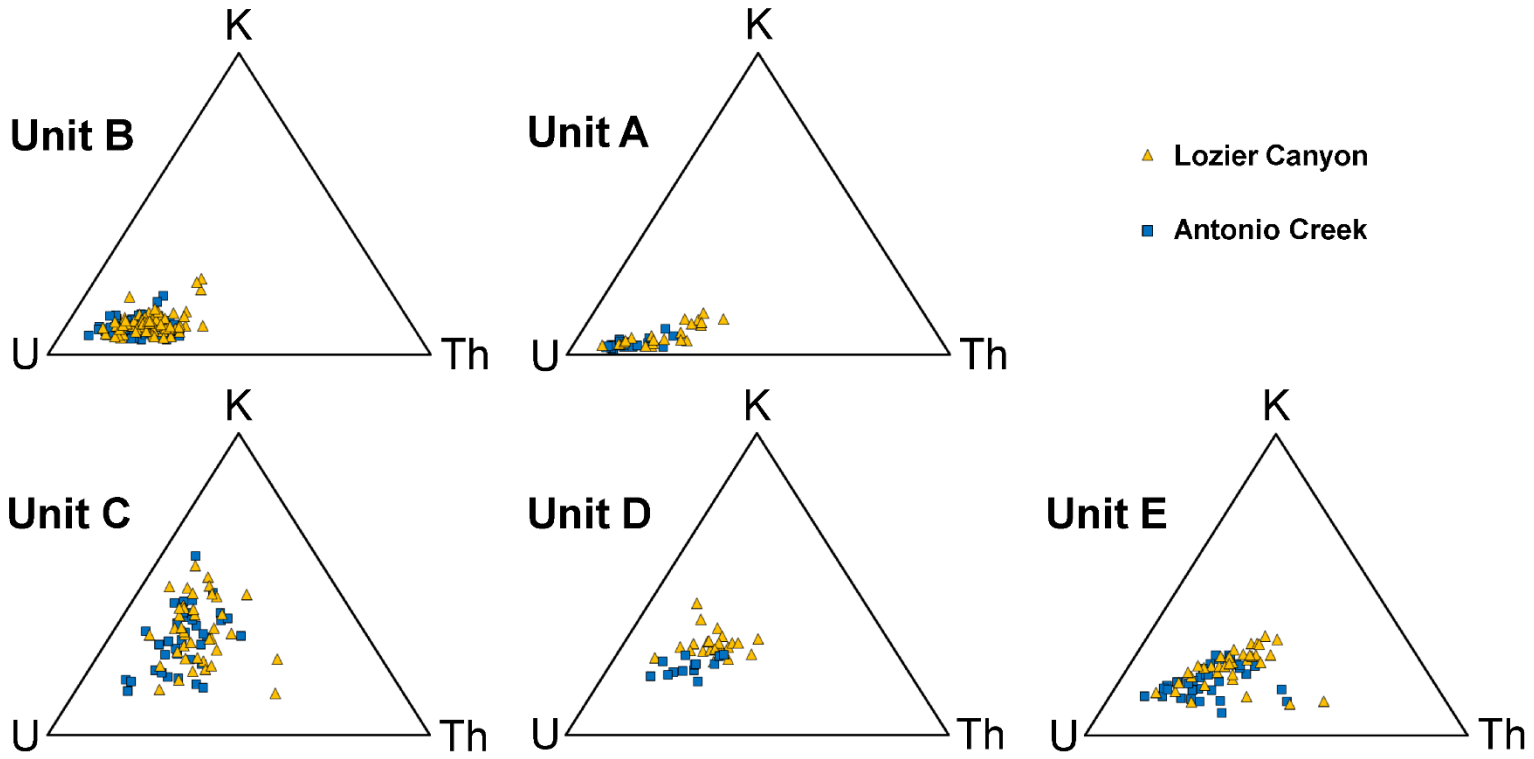

Figure 12. Ternary Diagrams. These are comparing the gamma ray values of equivalent units from Lozier Canyon (orange triangles) and Antonio Creek (blue squares). Each diagram displays the gamma ray readings of equivalent units in different locations. Note the minor differences between clusters of the same unit in each canyon. These differences could be caused by errors in sampling or calibration. These minor differences aside, there are clearly unique gamma ray responses to each unit, especially comparing the lower Eagle Ford (unit A and B) to the upper Eagle Ford (units C,D, and E). These diagrams highlight the better ability of SGR data to distinguish between units.

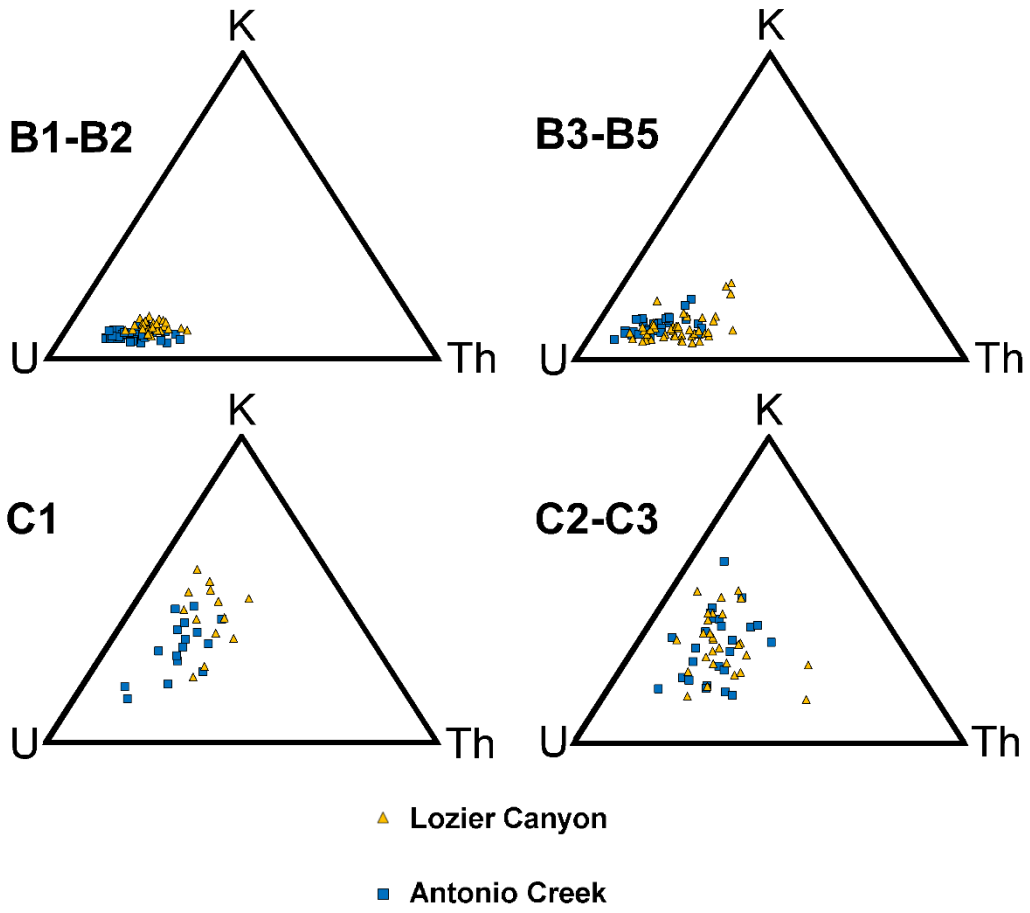

Figure 13. Subunits B1-B2, Antonio Creek, and Scott Ranch Members. Ternary diagrams comparing the gamma ray readings of equivalent units from Lozier Canyon (orange triangles) and Antonio Creek (blue squares). Subunits B1-B2 definitely more tightly clustered than B3-B5. This could be a result of the presence of bentonites in B3-B5. C1 and C2-C3 are very similar. The author expected a more pronounced difference between these two intervals because C2-C3 marks the onset of ocean anoxic event 2 (OAE2) as described by Donovan and others, 2012.

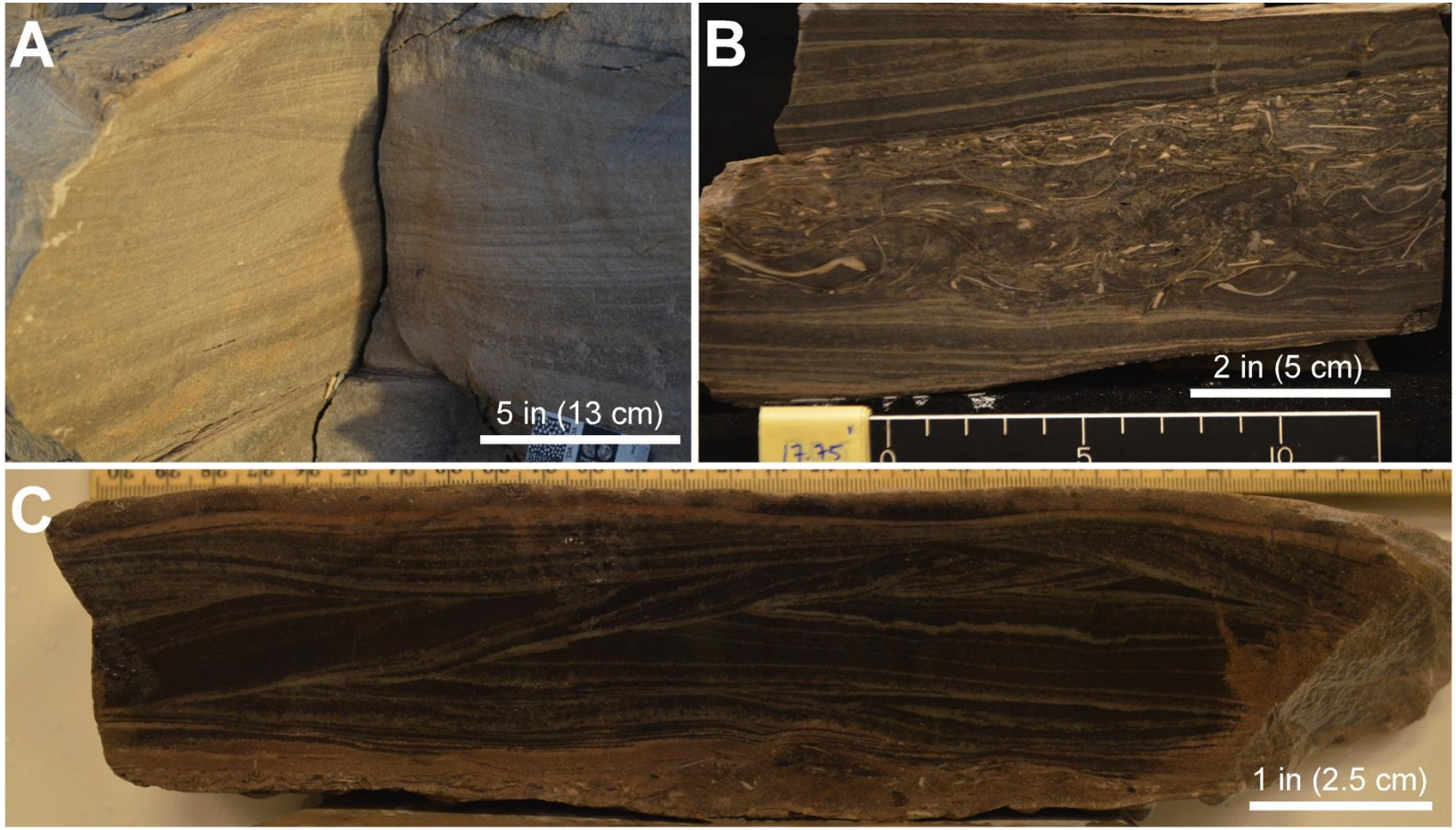

Figure 14. Hummocky Cross Stratification. (A) HCS bed in subunit A1. (B) Shell lag in subunit A3. (C) A thin skeletal grainstone bed from subunit B3. Note the shell lag at the base, typical of shallow-water storm deposits.

Viewing the data in ternary diagrams (Fig. 12) highlights differences that are less noticeable on the logs. These diagrams plot the ratios of K, U, and Th. All of the units have similar ratios of U and Th, however they differ in K values and how closely grouped or spread out the data is. The SGR data for unit A plots as a tight group very close to the zero K line. Unit B is less tightly grouped and contains higher values for K. K values in unit C are much higher, but data points group poorly. Unit D and E contain moderate K values and are more closely clustered than C. Data plot of Unit E is not disimilar to that of unit A, which is unsuprising given the similar lithologies of these two units. When subunits B1-B2 are compared with the Antonio Creek member(B3-B5) there is a clear difference (Fig. 13) which reflects differences in lithology within unit B. Subunits B1-B2 are more homogeneous than the overyling Antonio Creek member, and the SGR data plots in a close group. On the other hand, the SGR data from the Antonio Creek member has more spread. This could be due to the presence of ubiquitous bentonites which are the defining characteristic of the Antonio Creek member.

6. DISCUSSION

6.1 Correlation of Units and Beds

Measured sections in Lozier Canyon and Antonio Creek correlate very well. Similar thickness, sedimentary structures, and SGR response occurs in most correlative beds. These strata correlate so well because the study area is relatively small and there was little or no depositional slope. The units correlated in this study correspond to four depositional sequences that were correlated into the subsurface of south Texas using biostratigraphic, electric log, geochemical, and core data (Donovan et al., 2012). The lack of lateral facies transition across the study area between these sequences supports their interpretation as unique chronostratigraphic units (e.g., unit C does not transition laterally into unit D, unit E does not transition laterally into the Austin Chalk) at the scale of this study area.

The principal lateral variation of these strata on the scale of a horizontal well amounts to the distribution of skeletal packstone beds in unit B. These beds transition from continuous beds to isolated lenses to completely pinching out over thousands of feet. However, the skeletal packstone beds in unit B represent a small percentage of the volume of the rock, which primarily consists of foraminiferal mudstone.

6.2 Correlating Spectral Wireline Logs

Excellent correlation between most trends and major peaks in gamma ray values between each section is not surprising given the similar lithology and proximity of the measured sections. The differences in minor peaks between the two logs could be the result of the SGR sampling error described in the methods section of this paper. This may also be the case with the increase in uranium and thorium values in E2 just below the Austin Chalk contact in Antonio Creek. However, this difference could also represent bentonites that were eroded before deposition of the overlying Austin Chalk (K72 sequence) in Lozier Canyon. The variation in intensity of Th peaks between the two logs can also be attributed to sources of error issues previously described. Many of these differences might not occur if the same rocks were logged using a conventional logging tool in a vertical well that would take measurements continuously instead of at 1-ft (30-cm) intervals like the handheld device.

Th peaks increase significantly in subunit B3 concomitant with an abrupt increase in bentonite beds. U also increases in this interval; however, the total gamma ray curve changes little. The underlying subunit B2 has the highest total organic carbon (TOC) and is the primary completion target of some operators in the subsurface (Donovan et al, 2012) where it thickens stratigraphically. Greater accuracy in geosteering a well into this unit can be achieved by using MWD (measurement while drilling) systems that provide SGR data to distinguish between sub units B2 and B3. This distinction would be problematic with only a total gamma ray curve. Another

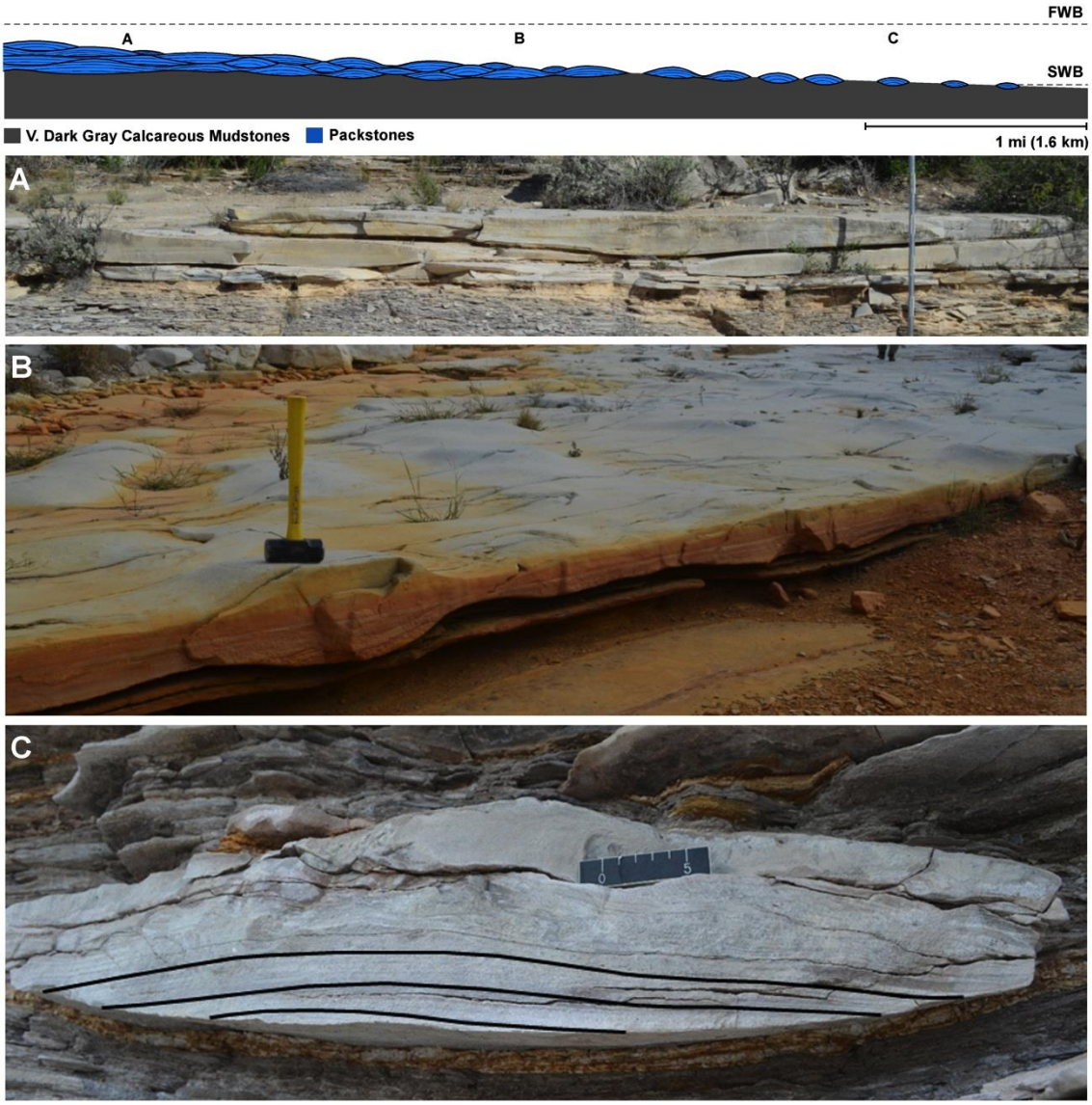

Figure 15. Bed Morphology in Unit B. (A) Bed of stacked lamina sets. (B) Laterally continuous skeletal packstone pinch-and-swell bed. (C) Black lines added to highlight lamina. Skeletal packstone lenses are disk-shaped in 3-d. On the depositional profile, the vertical scale is exaggerated and the size of the bedforms is not to scale. The horizontal scale and lateral transition of bedforms is accurate and based on field observations.

reason to use SGR data is that Th spikes from bentonites could be confused with condensed sections on a total gamma ray curve of a well.

6.3 Depositional Slope and Water Depth on Platform

The depth of water covering the platform during carbonate deposition of unit A in the study area hinges on the interpretation of hummocky cross stratification. HCS structures (Fig. 14) of unit A along the Texas highway 90 and Lozier Canyon outcrops were interpreted as either storm-related structures (Treviño, 1988; Miller, 1990; Treviño and Smith, 2002; Donovan and Staerker, 2010; Donovan et al., 2012) or products of deeper water bottom currents, contourites, or turbidites (Lock and Peschier, 2006; Lock et al., 2010; Ruppel et al., 2012). The sedimentary structures (skeletal lags at the bases of beds, hummocky and swaley cross-stratification, wave ripples) in Lozier Canyon and Antonio Creek outcrops are consistent with carbonate tempestites (e.g., Kreisa, 1981; Aigner, 1982; Tucker and Wright, 1990; Molina et al., 1997; Liu et al., 2012) and indicate shallow-water deposition, likely within 100 feet (30 meters). The skeletal packstone beds in Unit B also contain these sedimentary structures that suggest shallow-water deposition. Deposition of this unit probably periodically occurred above storm wave base (SWB). The prevalence of wave-related structures in the skeletal grainstone to packstone beds throughout the rest Eagle Ford Group in the study area suggest repeated deposition above SWB.

Unit A is 7% thicker in Antonio Creek than in Lozier Canyon, which could be the result of a higher sediment supply at the former locale. Variation in the thickness and lateral continuity of individual beds in unit A are likely a result of deposition well above SWB. The lateral variation of skeletal packstone beds in unit B suggests differences in sediment supply or paleobathymetry during deposition (Fig. 15). The dominance of wave-related structures within these beds suggests they were deposited above SWB. The carbonaceous mudstone facies contains primarily current related structures and may represent the background sedimentation that was periodically interrupted by large storm events during which the skeletal packstone beds were deposited. Any preexisting accommodation (Fig. 3) on the Comanche platform may have been partially filled during deposition of unit A and B creating a flatter platform surface for subsequent deposition. This may explain the higher incidence of correlative, laterally continuous beds in the Upper Eagle Ford Group and the greater similarity in thickness and sedimentary structures of these beds across the study area.

6.4 Oxygenation of Bottom Waters

It may be possible to infer chemical conditions during the deposition of sedimentary rocks based on Th and U concentrations in ash beds (Adams and Weaver, 1958). The Th and U concentrations within the ash bed indicate the chemical conditions of the sediment into which they were deposited. In reducing conditions, the Th/U levels of ash beds would remain roughly constant because the U would not be scavenged or

oxidized. If the ash had settled into oxidized waters, the U would have been oxidized and leached, and thus the Th/U ratio would have increased. They also noted that if Th and U were in zircons of the ash, the Th/U would be relatively impervious to leaching. In the study area, the bentonites in the Lower Eagle Ford Group have Th/U ratios of ≤1. In contrast, the bentonites in the Upper Eagle Ford Group have Th/U ratios between two and four, suggesting more reducing conditions during deposition of the Lower Eagle Ford Group.

The value of U concentration as a proxy for reducing conditions is based on the findings of Hassan et al. (1976) that higher concentrations of U tend to correlate with organic matter (TOC). However, U also is susceptible to both pre-depositional and post-depositional weathering (e.g., Adams and Weaver, 1958; Tribovillard et al., 2006). To ensure that an interpretation of U for reducing conditions is valid, it can be compared with Mo. Molybdenum has the distinction of being an element that does not readily precipitate from the water column, but its incorporation into sediments can be mediated by the presence of HS^- and scavenging by organics and Fe (McManus et al., 2006; Helz et al., 1996). This makes Mo a better proxy for inferring reducing conditions, and thus if U and Mo data are in agreement, the concern of U leaching or mobilization is removed. Preliminary X-ray fluorescence (XRF) data collected at 6-in (15-cm) intervals in Antonio Creek reveal that U and Mo values strongly correlate (Matthew Wehner, personal communication, 2013). In this context, the higher U concentrations in the Lower Eagle Ford Group suggest greater preservation of organic matter and more

reducing conditions than in the Upper Eagle Ford Group, which contains significantly lower U concentrations.

Bioturbation in the mudstone facies of the Lower Eagle Ford Group is rare, but locally abundant *Chondrites* and *Planolites* occur in some skeletal packstone and grainstone beds. Bioturbation (including large vertical traces) is common throughout all facies of the Upper Eagle Ford Group. The BI of the Lower Eagle Ford Group is between 0 and 1 and between 3 and 6 for the Upper Eagle Ford Group. The BI alone is not a reliable proxy for oxygen conditions. However, in conjunction with the geochemical data previously discussed, BI values recorded here reinforce the interpretation of primarily anoxic and oxic conditions during deposition of the Lower and Upper Eagle Ford Groups, respectively. The locally abundant ichnofossils in the skeletal packstone and grainstone facies in the Lower Eagle Ford Group could represent colonization by opportunistic organisms during periods of oxygenation following large storm events.

The pre-existing topography from the Comanchean buildups (Fig. 3) may have initially restricted circulation on the inner platform (Donovan et al., 2012), resulting in the anoxic depositional conditions that were prevalent during deposition of units A and B (Lower Eagle Ford Group). Once the accommodation from pre-existing topography was filled, bottom circulation would have increased, explaining the upward increase in oxygen levels interpreted from the overall increase in widespread bioturbation and decrease in U beginning in unit C and prevalent throughout the remainder of the Upper Eagle Ford Group. Despite the upper Lozier Canyon member (units A-B2) containing

the highest TOC (Donovan et al., 2012), the Lozier Canyon member (B3-B5) has higher U values overall. This apparent paradox is reconciled by the observation that the Antonio Creek member contains many bentonite beds. As previously discussed, the Th/U ratios of bentonites in the Lower Eagle Ford are approximately 1. This not only indicates more reducing conditions, but also that the higher U values in the Antonio Creek member can be attributed to the ubiquitous bentonites in this interval. Additionally, with the help of UV light which causes the smectite clays from the bentonite horizons to glow, it was recently observed in a core taken at the Lozier Canyon #1 site that the strata directly above a bentonite bed contains a significant amount of reworked bentonite. The widespread presence of bentonitic material throughout this interval may explain the higher U values in the Antonio Creek Member despite lower TOC values.

6.5 Deformed Beds

Five zones of deformed bedding occur in Eagle Ford Group outcrops in Antonio Creek (two in unit A, subunit D1, E1, and E2) and three in Lozier Canyon (unit A, subunit D1, E2). These contorted zones show three similar styles of deformation. One type, typically near the base of a contorted zone, consists of clasts of laminated skeletal packstone-grainstone in a matrix of clast-supported breccia (Fig. 16A). These beds were already semi-consolidated when the deformation occurred. Another style of deformation includes folded to overturned beds (Fig. 16B) and soft-sediment deformation (Fig. 16C).

The third style of deformation is represented by homogenized facies that bear no trace of the original depositional fabric (Fig. 16D). This facies commonly occur near the tops of the deformed beds.

These deformation styles likely correspond to the degree of lithification of the strata when deformation occurred. The folded zones described in unit A along Texas highway 90 were attributed to debris flows (Lock and Peschier, 2006, Lock et al., 2010; Ruppel et al., 2012). The widespread, but laterally discontinuous nature of the deformed beds (Fig. 17) suggests a more powerful, discontinuous mechanism produced them. The range of bed-deformation facies suggests that during deformation underlying beds became thixotropic, overlying beds sank into the underlying substrate, and loose material was ejected into the water column and deposited as massive bedding. Cyclic storm loading (e.g., Seilacher, 1984; Molina et al., 1998; Chen et al., 2009; Alfaro et al., 2002) and seismic shaking (e.g., Pope et al., 1997; Rosetti, 1999) were hypothesized to form similar structures. It is currently unclear which of these mechanisms formed the deformed beds in the Eagle Ford Group.

6.6 Application to Industry

Heterogeneities in reservoir properties undoubtedly play a critical part in the exploitation of the Eagle Ford Group. Presently, many Eagle Ford Group operators drill horizontal wells in the minimum horizontal stress direction such that the hydraulic fractures that are created tend to be perpendicular to the wellbore. The basis for

determining the optimal spacing between sets or stages these induced fractures as well as fracture fluid and propping agent volumes tends to be developed based on trial and error results. The anisotropy of bedforms described in skeletal packstone beds in unit B could have an effect on important reservoir properties and play a part in determining the optimal alignment of the wellbore and the spacing of hydraulic fractures placed along a lateral.

A better understanding of the distribution of reservoir properties such as porosity, permeability, and fluid type, mechanical properties (rock moduli, Poisson's ratio, and fracture toughness) should provide a more economical basis for determining optimum well density, lateral direction, and hydraulic fracture spacing. The presence of heterogeneities along the lateral would imply the need for different hydraulic fracturing strategies along the lateral. Obtaining core or other data to obtain these properties is usually prohibitively expensive but it may be possible to correlate the frequency of facies changes observed with this work to develop more economical well placement and fracture spacing scenarios than can be developed purely by trial and error methods. The one-size-fits-al mentality becomes increasingly incorrect within the same horizon on the scale of a field where multiple laterals are often drilled in a row (Fig. 18). Certainly the completion of each well should be considered separately. If observations of unit B in the outcrops correlate into the subsurface, the reservoir properties of a given horizon can change from homogeneous to heterogeneus and back to homogeneous within the same lithology over several miles.

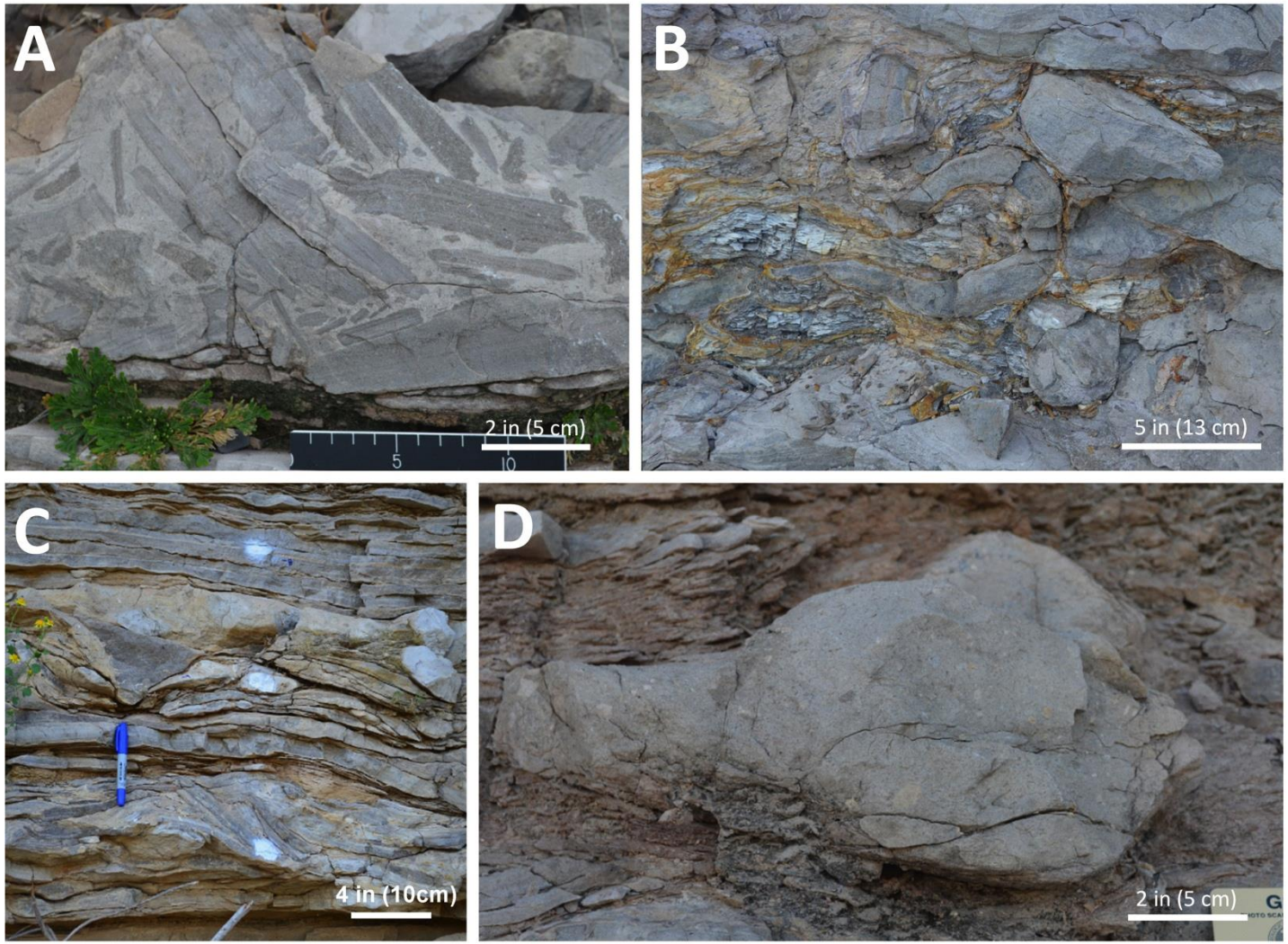

Figure 16. Deformed Bedding. (A) Grainstone breccia in unit A (B) Overturned beds in unit A. (C) Soft-sediment deformation in unit E. (D) Completely homogenized skeletal packstone to grainstone beds in unit A.

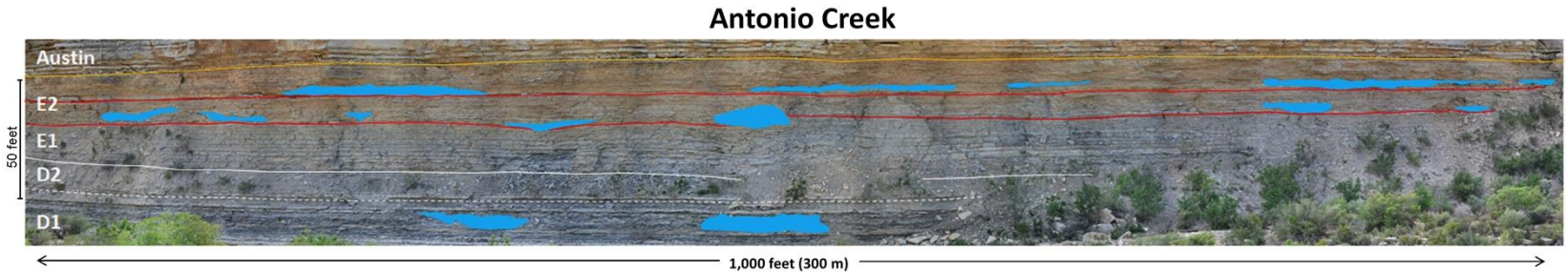

Figure 17. Deformed Bedding: Langtry Member of Antonio Creek. The blue shapes show the area and distribution of deformed beds in this member. The yellow line marks the boundary between the Eagle Ford Group and the Austin Chalk. The red lines are major bentonites. The solid white line is a unit boundary and the dashed white lines are sub unit boundaries. the lateral.

Detection of these heterogeneities in the subsurface is the first step to optimizing completions. Results in this study suggest that SGR data is the key to distinguishing between the high TOC units (B1,B2) and the overlying bentonite-rich Antonio Creek member (B3-B5) in the subsurface. Unfortunately, the SGR response of skeletal packstone and carbonaceous mudstone beds in unit B in this study are very similar, and more sophisticated tools are required to ascertain the horizontal facies changes along laterals landing in this unit. Formation micro-imager (FMI) logs can resolve fractures and sedimentary features in an uncased wellbore. In unit B, skeletal packstone and carbonaceous mudstone beds are dominated by wave and current related structures, respectively. These two lithologies in the field have significantly different natural fracture density and orientation. FMI data could possibly distinguish between the unique sedimentary structures and fracture characteristics of these two adjacent lithologies in the subsurface and completion techniques could be adjusted appropriately. FMI data could also detect deformed beds, although in the study area deformed horizons were not observed to occur in unit B. During drilling, the rate of penetration (ROP) of the drilling unit into the reservoir may give an indication as to horizontal changes in lithology. Additionally, a detailed mudlogger's report may detect the nature and periodicity of any horizontal heterogeneity.

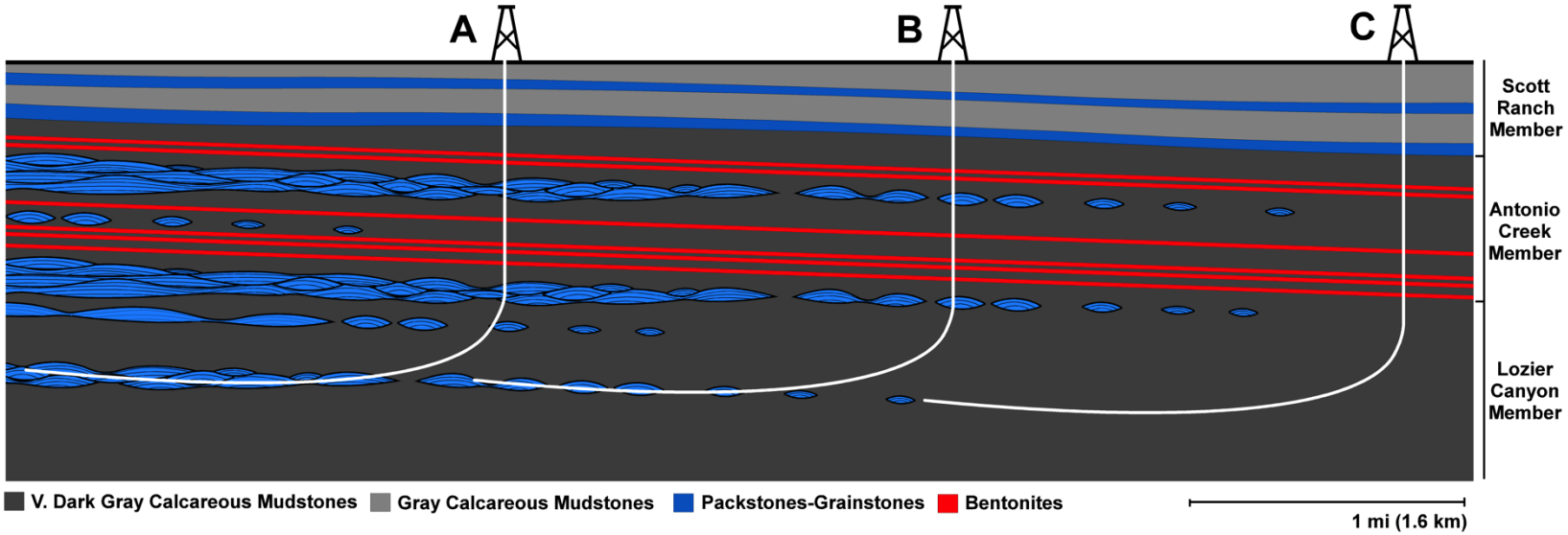

Figure 18. Lateral Facies Change on the Scale of a Lateral. A schematic showing multiple horizontal wells. Vertical scale is exaggerated. The horizontal relationship between bedforms is scaled according to outcrop observations. Note the variation in lithology along the lateral in each well. The reservoir properties of well A would be very different from well C and perhaps warrant a different completion strategy.

7. CONCLUSIONS

The minor variation in thickness and SGR logs of each unit within the Eagle Ford Group across the study area indicates most deposition occurred on a carbonate platform with little or no local depositional slope. Lateral variation of individual beds is greatest in Units A and B. Units within the four interpreted sequences identified by Donovan and others (2012) do not transition laterally into units of overlying or underlying sequences. Geochemical and ichnofossil data suggest that depositional bottom waters were often anoxic during units A and B and oxic during units C, D and E. Sedimentary structures indicate that carbonate deposition throughout the Eagle Ford Group in the study area occurred primarily above storm wave base, probably 100 feet (30 meters). This suggests that deposition of successful unconventional plays like the Eagle Ford Group can occur in relatively shallow water. Widespread deformed zones in the Eagle Ford Group may have been caused by cyclic storm loading or paleoseismicity. SGR data is necessary to accurately land horizontal wells in the most desirable intervals (the Lozier Canyon member) and should be incorporated into MWD systems. The lateral facies changes observed in the primary subsurface reservoir, unit B, may warrant different fracture stage spacing and design along the length of a lateral and between different wells in the same field. FMI logs, muddloger's reports, and ROP data might be used to determine the extent and periodicity of lateral heterogeneities and completions adjusted accordingly.

REFERENCES

Adams, J. A. S., C. E. Weaver 1958, Thorium-to-uranium ratios as indicators of sedimentary processes: examples of concept of geochemical facies. Bulletin of the American Association of Petroleum Geologists, v. 42, no. 2, p. 387-430.

Aigner, T., 1982, Calcareous tempestites: Storm-dominated stratification in Upper Muschelkalk limestones (Middle Trias, SW Germany), in: G. Einsele, and A. Seilacher, eds., Cyclic and Event Stratification: Springer-Verlag, Berlin, p. 180–198.

Alfaro, P., J. Delgado, A. Estevez, J. M. Molina, M. Moretti, and J. M. Soria, 2002, Liquefaction and fluidization structures in Messinian storm deposits (Bajo Segura Basin, Betic Cordillera, southern Spain): International Journal of Earth Sciences, v. 91, p. 505–513.

Campbell, C. V., 1967, Lamina, lamina set, bed and bedset: Sedimentology, v. 8, p. 7-26.

Chen, J., S. K. Chough, S. S. Chun, and Z. Han, 2009, Limestone pseudoconglomerates in the Late Cambrian Gushan and Chaomidian Formations (Shandong Province, China): soft-sediment deformation induced by storm-wave loading: Sedimentology v. 56, p. 1174–1195.

Donovan, A. D., and S. Staerker, 2010, Sequence stratigraphy of the Eagle Ford (Boquillas) Formation in the subsurface of South Texas and the outcrops of West Texas: Gulf Coast Association of Geologic Societies Transactions, v. 60, p. 861-899.

Donovan, A. D., T. S. Staerker, A. Pramudito, W. Li, M. J. Corbett, C. M. Lowery, A. M., Romero, and R. D. Gardner, 2012, The Eagle Ford outcrops of West Texas: a laboratory for understanding heterogeneities within unconventional mudstone reservoirs: GCAGS Journal, v. 1, p. 162-185.

Droser M. L., and D. J. Bottjer, 1986, A semiquantitive field classification of ichnofabrics: Journal of Sedimentary Petrology, v. 56, p. 558–559.

Dunham, R. J., 1962, Classification of carbonate rocks according to depositional texture, in W. E. Ham, ed., Classification of carbonate rocks: American Association of Petroleum Geologists Memoir, p. 108-121.

Freeman, V. L., 1961, Contact of the Boquillas flags and Austin Chalk in Val Verde and Terrell counties, Texas: American Association of Petroleum Geologists Bulletin, v. 45, p. 105–107.

Freeman, V. L., 1968, Geology of the Comstock Indian Wells area Val Verde, Terrell, and Brewster counties, Texas: U.S. Geological Society Professional Paper 594–K, 26 p.

Harms, J. C., J. Southard, D. Spearing, and R. Walker, 1975, Depositional environments as interpreted from primary sedimentary structures and stratification sequences: SEPM Short Course Notes, v. 2, 161 p.

Grabowski, G. J., 1995, Organic rich chalks and calcareous mudstone of the Upper Cretaceous Austin Chalk and Eagleford Formation, south-central Texas, USA, in B. J. Katz, ed., Petroleum Source Rocks: Springer-Verlag, Berlin, p. 209–234.

Hassan, M., A. Hossin, and A. Combaz, 1976, Fundamentals of the differential gamma ray log: interpretation technique, in Society of Professional Well Log Analysts, Transactions of Seventeenth Annual Logging Symposium, paper H,18 p.

Hazzard, R. T., 1959, Measured section, in R. L. Cannon, R. T. Hazard, A. Young, and K. P. Young, eds., Geology of the Val Verde Basin: West Texas Geological Society Guidebook, November 5–8, Midland, 118 p.

Helz, G. R., C. V. Miller, J. M. Charnock, J. F. W. Mosselmans, R. A. D. Pattrick, C. D. Gardner, and D. J. Vaughan, 1996, Mechanism of molybdenum removal from the sea and its concentration in black shales: EXAFS evidence. Geochima et Cosmochimica, v. 60, n. 19, p. 3631-3642.

Hill, R. T. 1887, The Texas section of the American Cretaceous: American Journal of Science, 3rd Series, v. 34, p. 287–309.

Kreisa, R. D., 1981, Storm-generated sedimentary structures in subtidal marine with examples from the Middle and Upper Ordovician of southwestern Virginia. Journal of Sedimentary Petrology, v. 51, p. 823–848.

Liu, X., J. Zhong, R. Grapes, S. Bian, and L. Chen, 2012, Late Cretaceous tempestite in northern Songliao Basin: China Journal of Asian Earth Sciences, v. 56, p. 33-41.

Lock, B. E., and L. Peschier, 2006, Boquillas (Eagle Ford) upper slope sediments, West Texas: Outcrop analogs for potential shale reservoirs: Coast Association of Geological Societies Transactions, v. 56, p. 491-508.

Lock, B. E., L. Peschier, and N. Whitcomb, 2010, The Eagle Ford (Boquillas Formation) of Val Verde County, Texas—A window on the South Texas play: Gulf Coast Association of Geological Societies Transactions, v. 60, p. 419–434.

McManus, J., W. M. Berelson, S. Severmann, R. L. Poulson, D. E. Hammond, G. P. Klinkhammer, and C. Holm, 2006, Molybdenum and uranium geochemistry in

continental margin sediments: Paleoproxy potential: Geochima et Cosmochimica, v. 70, p. 4643-4662.

Miller, R. W., 1990, The stratigraphy and depositional environment of the Boquillas Formation of southwest Texas: M.S. Thesis, University of Texas at Arlington, 156 p.
Molina, J. M., P. A. Ruiz-Ortiz, and J.. Vera, 1997, Calcareous tempestites in pelagic facies (Jurassic, Betic Cordilleras, Southern Spain): Sedimentary Geology, v. 109, p. 95–109.

Molina, J. M., P. Alfaro, M. Moretti, and J. M. Soria, 1998, Soft-sediment deformation structures induced by cyclic stress of storm waves in tempestites (Miocene, Guadalquivir Basin, Spain): Terra Nova, v. 10, p. 145–150.

Pessagno, E. A., 1969, Upper Cretaceous stratigraphy of the western Gulf Coast area of Mexico, Texas, and Arkansas: Geological Society of America Memoir 111, Boulder, Colorado, 139 p.

Pope, M. C., J. F. Read, R. Bambach, H. J. Hofmann, 1997, Late Middle to Late Ordovician seismites of Kentucky, southwest Ohio and Virginia: Sedimentary recorders of earthquakes in the Appalachian basin: Geological Society of America Bulletin, v. 109, p. 489-503.

Reineck, H. E., and I. B. Singh, 1975, Depositional Sedimentary Environments, with Reference to Terrigenous Clastics: New York, Springer Verlag, 439 p.

Ruppel, S., R. Loucks, and G. Fr*é*bourg (leaders), 2012, Guide to Field Exposures of the Eagle Ford-Equivalent Boquillas Formation and Related Upper Cretaceous units in Southwest Texas: The University of Texas at Austin, Bureau of Economic Geology Field Seminar (3/8/2012), 151 p.

Rosetti, D. F., 1999, Soft-sediment deformation structures in late Albian to Cenomanian deposits, Sao Luis Basin, northern Brazil: Evidence for palaeoseismicity: Sedimentology, v. 46, p. 1065-1081.

Seilacher, A., 1984, Sedimentary structures tentatively attributed to seismic events: Marine Geology, v. 55, p. 1-12.

Sloss, L. L., 1963, Sequences in the cratonic interior of North America: Geological Society of America Bulletin, v. 74, p. 93-114.

Smith, C. C., 1981, Calcareous nannoplankton and stratigraphy of late Turonian, Coniacian, and early Santonian age of the Eagle Ford and Austin Groups of Texas: U.S. Geological Society Professional Paper 1075, 96 p.

Treviño, R. H., 1988, Unit and depositional environments of the Boquillas Formation, Upper Cretaceous of southwest Texas: M.S. Thesis, University of Texas at Arlington, 135 p.

Treviño, R. H., and C. I. Smith, 2002, Facies and depositional environments of the Boquillas Formation (abs.): American Association of Petroleum Geologists Annual Convention Program, v. 11, p. A177–A178.

Tribovillard, N., T. J. Algeo, T. Lyons, and A. Riboulleau, 2006, Trace metals as paleoredox and paleoproductivity proxies: An update: Chemical Geology, v. 232, p. 12-32.

Tucker, M. E., and V. P. Wright, 1990, Carbonate Sedimentology: John Wiley & Sons, 482 p.

Winter, J. A., 1961, Stratigraphy of the Lower Cretaceous (subsurface) of South Texas: Gulf Coast Association of Geological Societies Transactions, v. 11, p. 15-24.

APPENDIX A PHOTOMOSAICS

This section contains additional annotated photomosaics

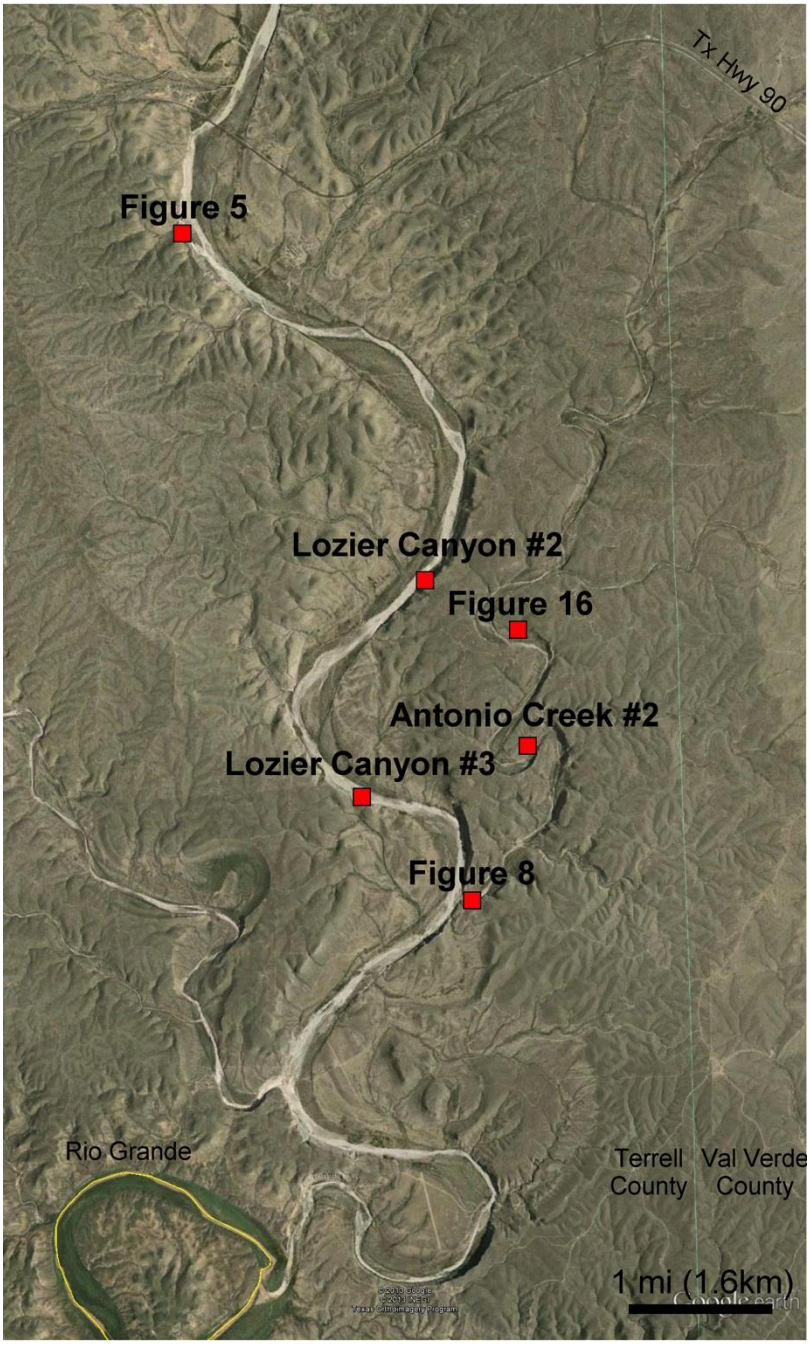

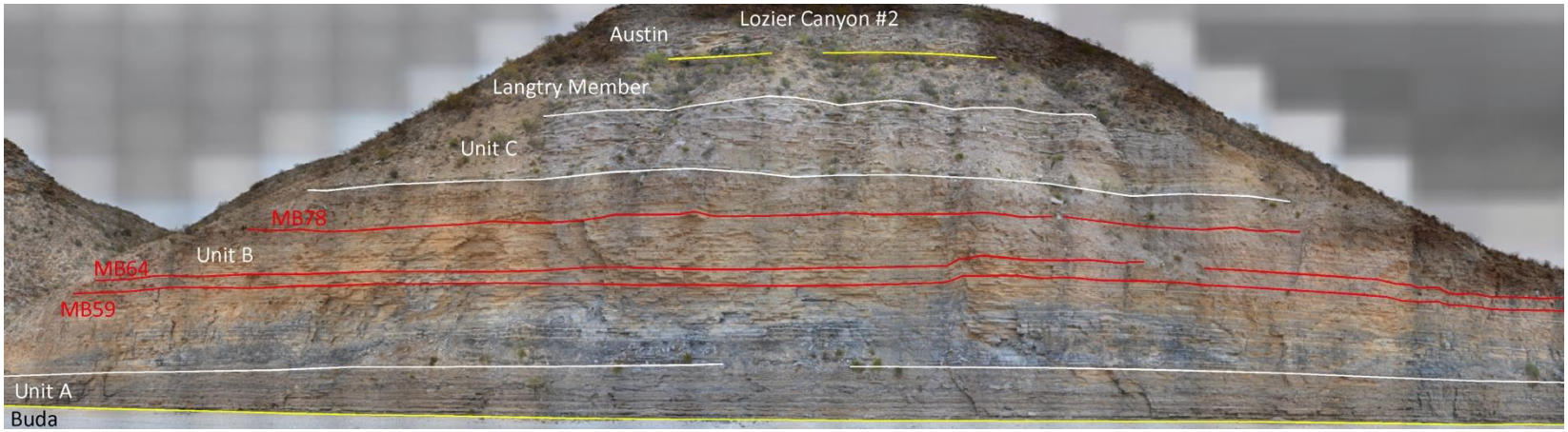
Austin
Lozier Canyon #2
Langtry Member
Unit C
MB78
Unit B
MB64
MB59
Unit A
Buda

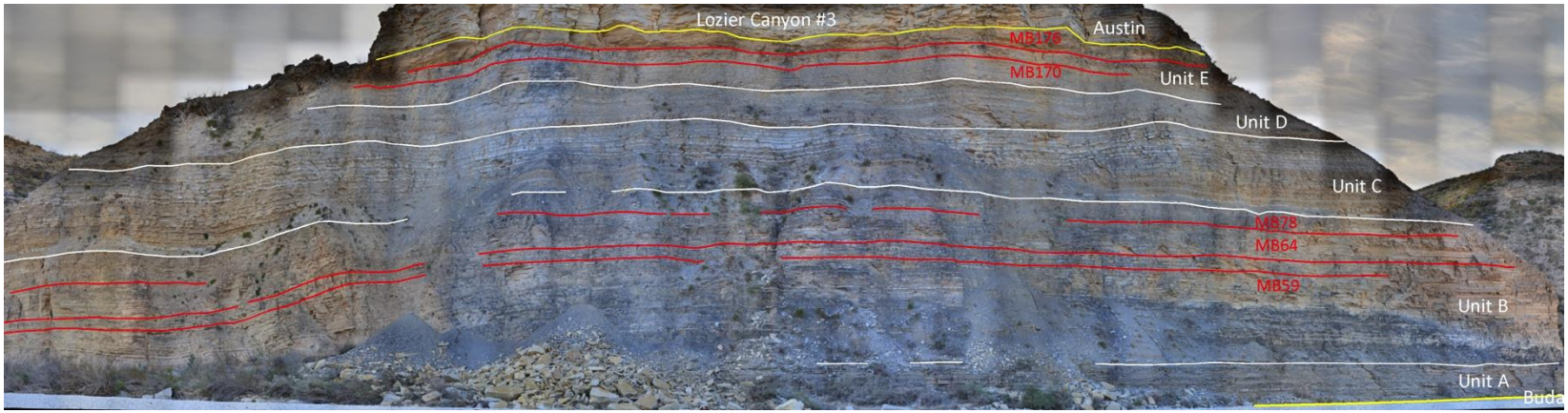
Lozier Canyon #3
Austin
MB176
MB170
Unit E
Unit D
Unit C
MB78
MB64
MB59
Unit B
Unit A
Buda


D1
Antonio Creek #2
C3
C2
C1
B5
B4
MB78

APPENDIX B PHOTOMICROGRAPHS

Thin sections taken from hand samples at Lozier Canyon. All footage is in height above the Buda Limestone.

Unit	Height Above Buda	Unit	Height Above Buda
	1.50		98.00
	2.00		105.90
	2.50		108.50
	2.95		112.60
	3.50		115.50
	4.30	C	121.00
	6.20		122.00
A	7.90		125.50
	14.90		129.00
	15.50		133.00
	16.00		134.00
	17.30		135.20
	17.75		136.90
	19.50		141.00
	20.50		143.00
	23.80		147.40
	24.80	D	149.20
	25.50		152.30
	28.20		153.70
	30.80		154.40
	36.00		154.70
	40.00		157.30
	42.00		159.30
	44.20		160.00
	49.00		165.00
B	49.50		167.00
	51.00	E	168.60
	63.80		170.50
	67.80		171.30
	68.00		178.50
	71.90		182.90
	77.00		
	82.80		
	83.50		
	85.90		
	95.00		

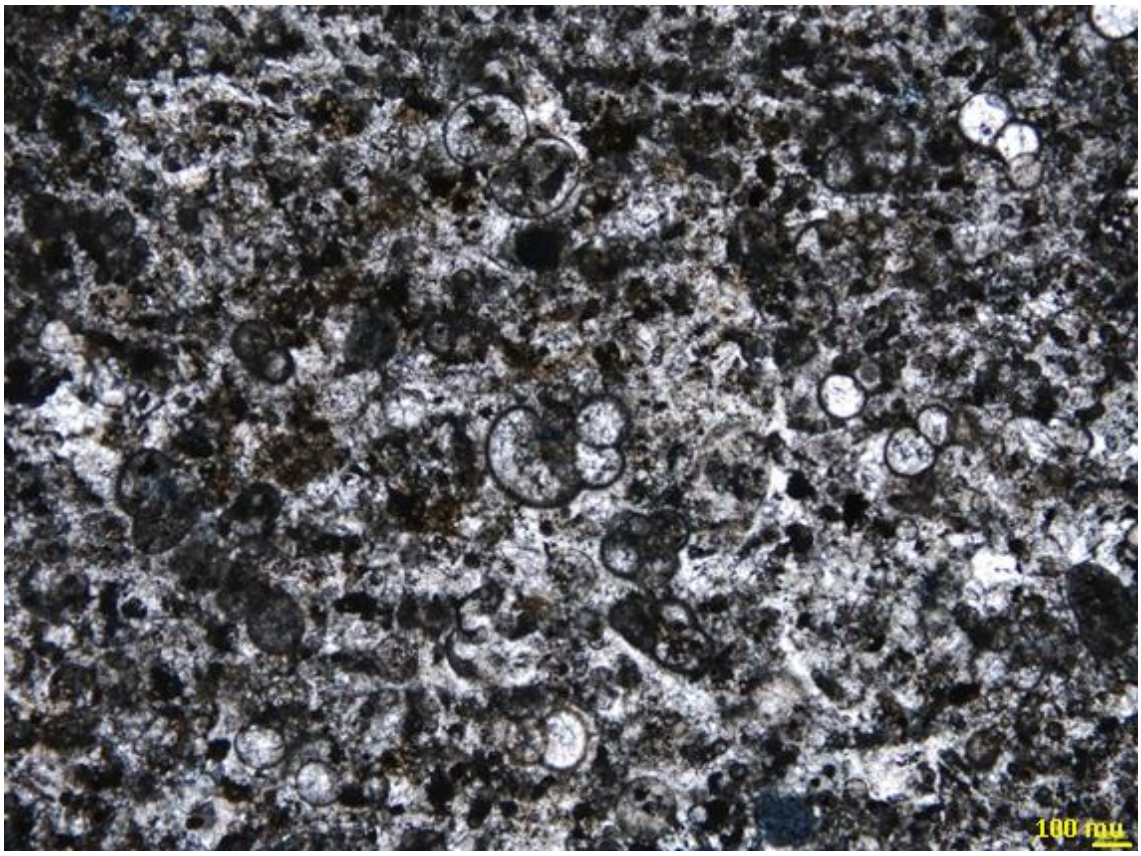

Height Above Buda:	1.5 feet
Skeletal Grain Types	Abundance
Planktonic Foram.	90%
Inoceramid Bivalves	5%
Pyrite	5%
Organics	<1%

Other Diagenetic Features:
Recrystallized skeletal fragments
Some moldic porosity (foraminerifera)

Rock Name:
Foramineriferal Packstone-Grainstone

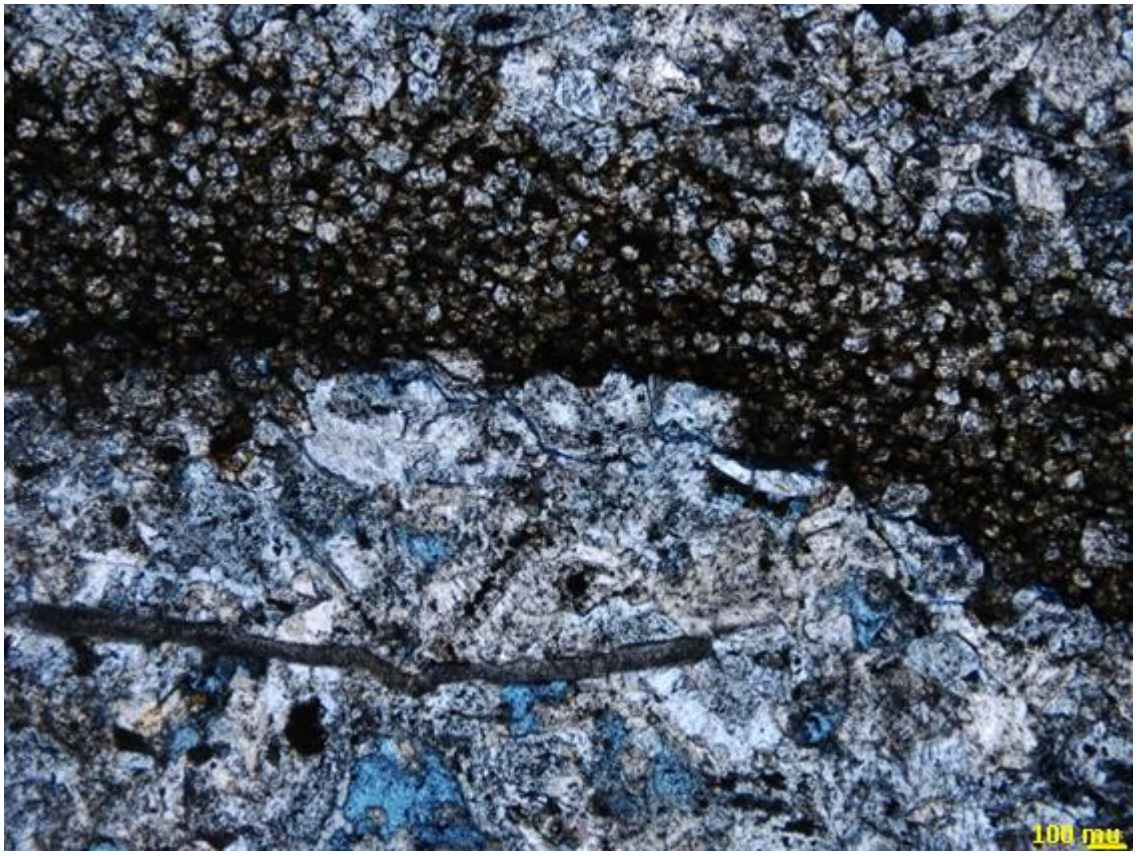

Height Above Buda:	2.0 feet
Skeletal Grain Types	Abundance
Pelagic Crinoid Frag.	60%
Dolomite Rhombs	20%
Inoceramid Bivalves	10%
Unidentified	10%
Organics	<1%

Other Diagenetic Features:

Some intergranular porosity (<5%)
Many grains heavily recrystallized, sutured contacts. Dolomite rhombs are probably reworked from underlying layers.

Rock Name: Skeletal
Crinoidal Packstone-Grainstone

Height Above Buda:	2.5 feet
Skeletal Grain Types	Abundance
Dolomite Rhombs	95%
Pyrite	5%
Organics	<1%
Bivalve Fragments	<1%
Fish Bones	<1%

Other Diagenetic Features:
Phosphatized bone fragments
No visible porosity

Rock Name:
Dolostone

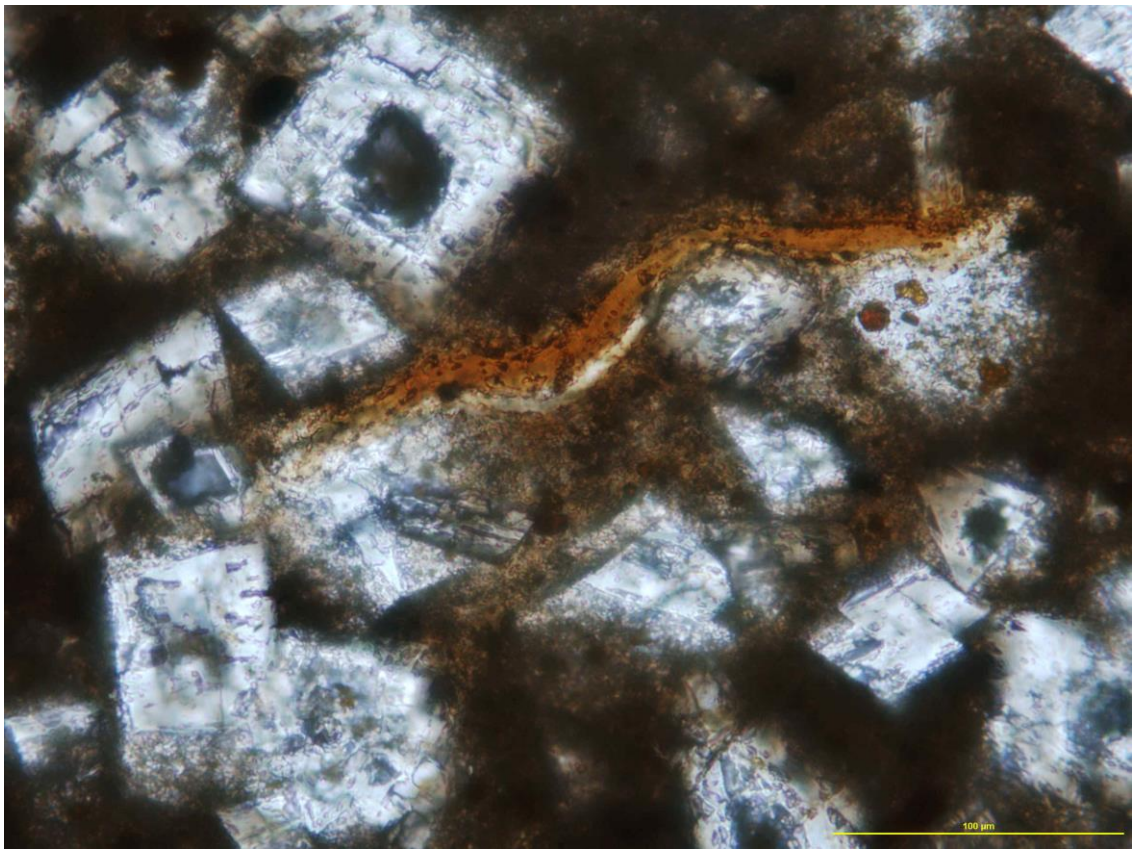

Height Above Buda:	2.95 feet
Skeletal Grain Types	Abundance
Dolomite Rhombs	90%
Pyrite	5%
Organics	5%
Bivalve Fragments	<1%

Other Diagenetic Features:
Many of the rhombs have dark cores. Some organic matter drapes over other grains suggesting some compaction.

Rock Name:
Dolostone

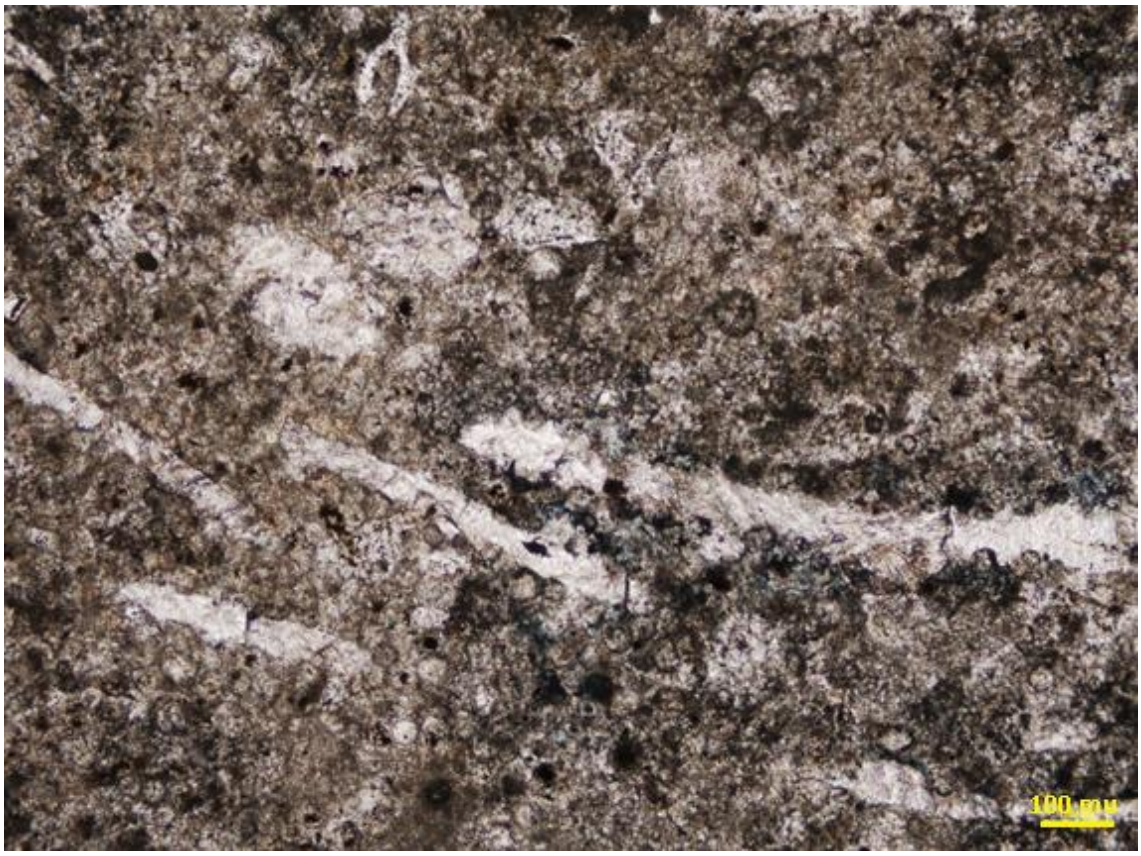

Height Above Buda:	3.5 feet
Skeletal Grain Types	Abundance
Foraminifera	50%
Bivalves Fragments	40%
Pyrite	5%
Unidentified	5%
Fish Bones	<1%

Other Diagenetic Features:
Many skeletal fragments are partially or wholly micritized. Rare moldic porosity. Calcite filled fractures common.

Rock Name:
Skeletal Packstone

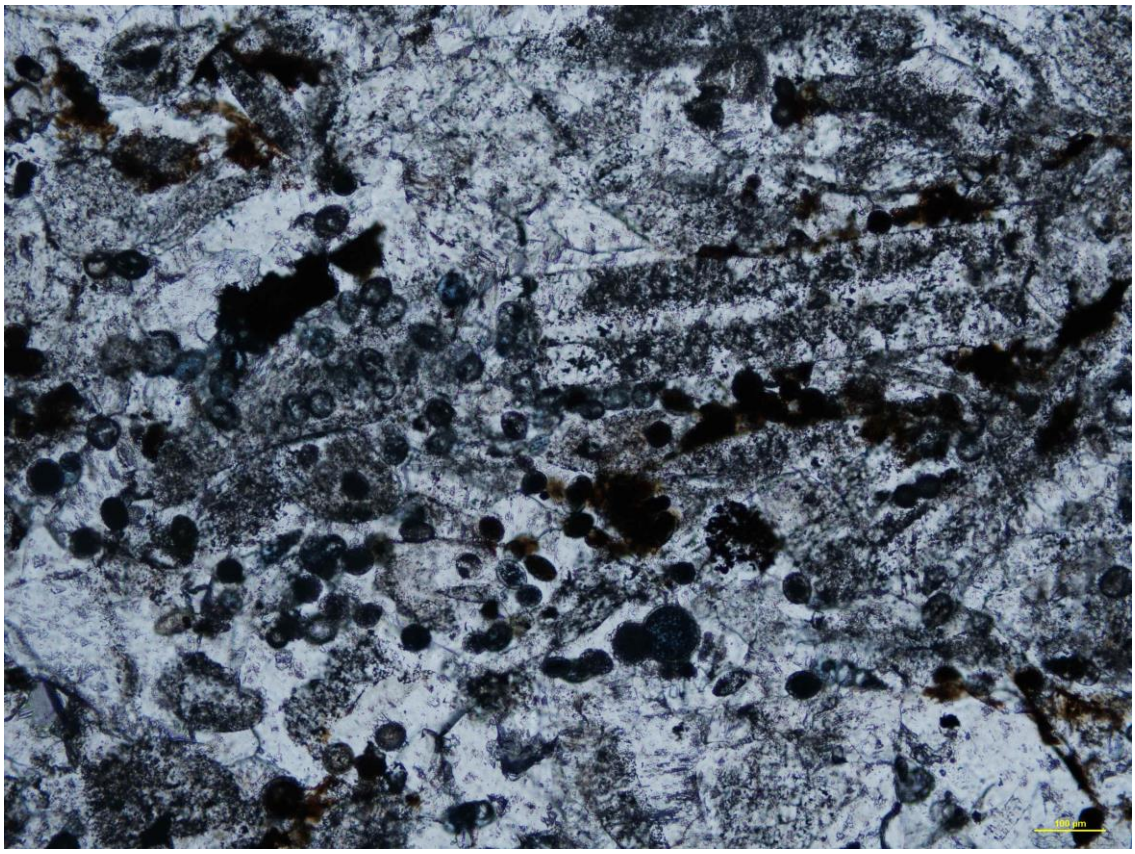

Height Above Buda:	4.3 feet
Skeletal Grain Types	Abundance
Pelagic Crinoid Fragments	50%
Pellets	20%
Brachiopod Fragments	20%
Foraminifera	10%
Pyrite	<1%

Other Diagenetic Features:
Many skeletal fragments are micritized.

Rock Name:
Skeletal Grainstone

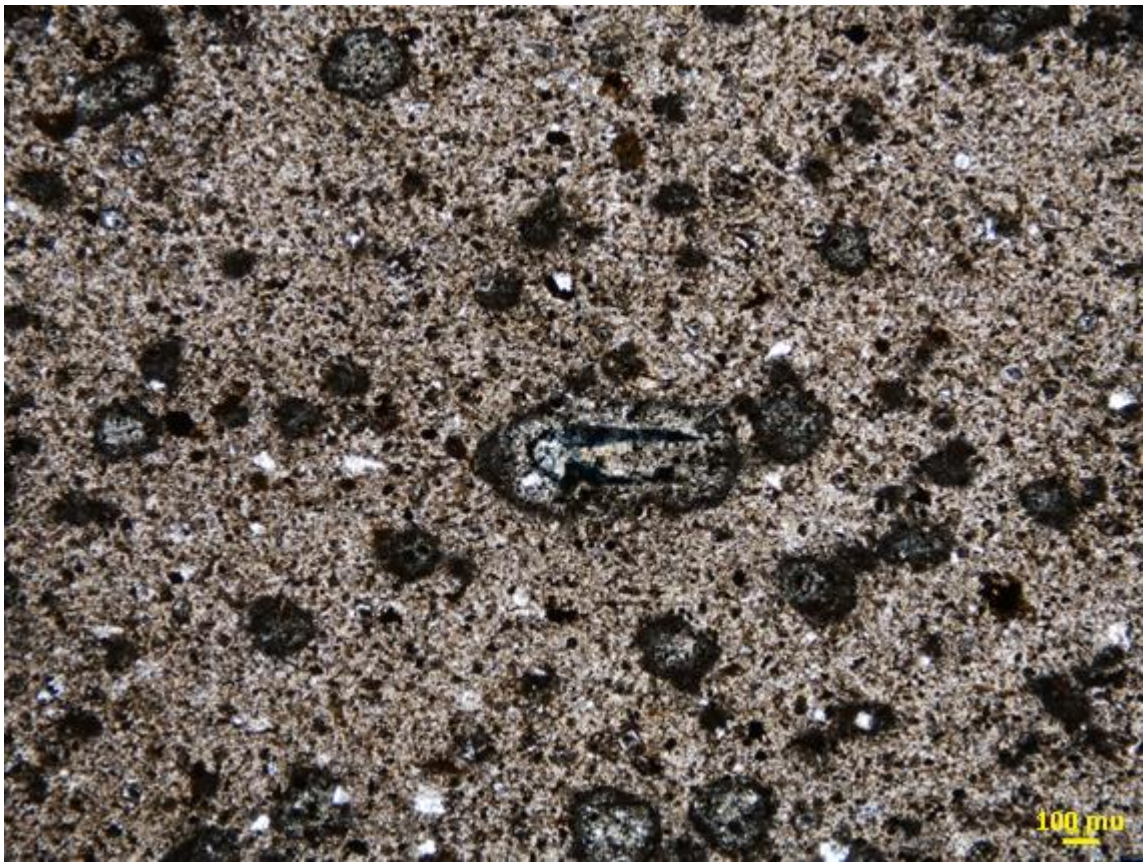

Height Above Buda:	6.2 feet
Skeletal Grain Types	Abundance
Unidentified	90%
Quartz	5%
Planktonic foraminifera	5%
Pyrite	<1%
Fish bones	<1%

Other Diagenetic Features:
This may be a silicified ash layer.

Rock Name:
Silicified Mudstone

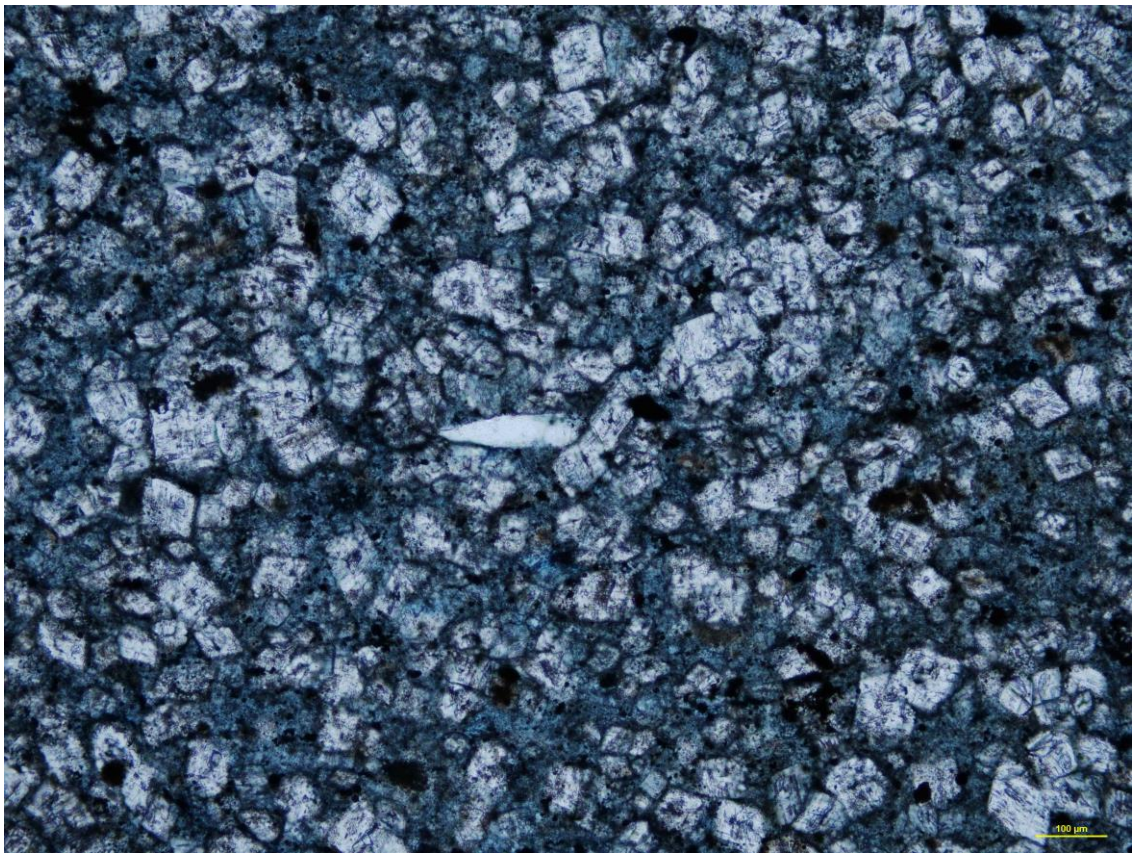

Height Above Buda:	7.9
Skeletal Grain Types	Abundance
Dolomite Rhombs	50%
Unidentified	40%
Pyrite	<5%
Quartz	<1%

Other Diagenetic Features:
This bed is laterally extensive and has a unique pink color that can be picked out all over the study area to the highway outcrops 30 miles to the east. There is some intragranular porosity.

Rock Name:
Dolomitic Packstone

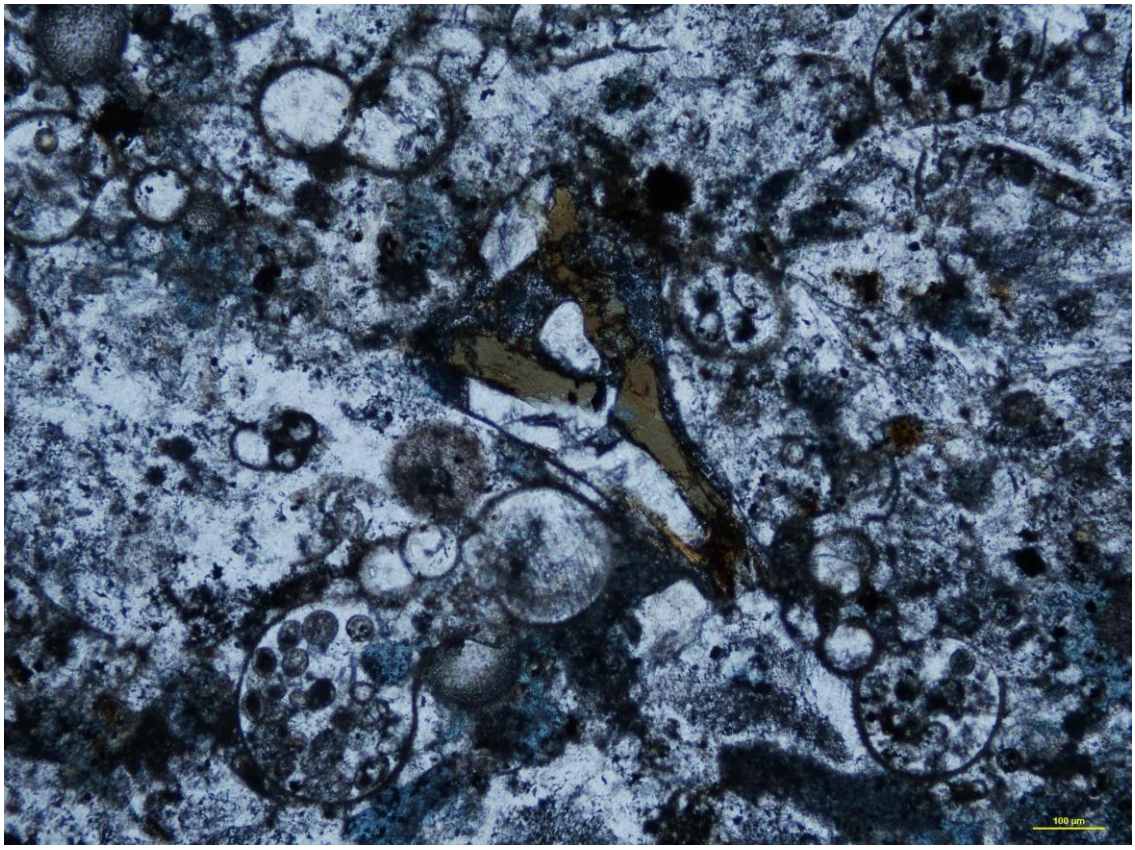

Height Above Buda:	14.9
Skeletal Grain Types	Abundance
Planktonic Foraminifera	90%
Organics	5%
Pellets	5%
Brachiopod Fragments	<1%
Fish Bones	<1%

Other Diagenetic Features:
Micritized and recrystallized grains. Fish bones are phosphatized.

Rock Name:
Foraminiferal Grainstone

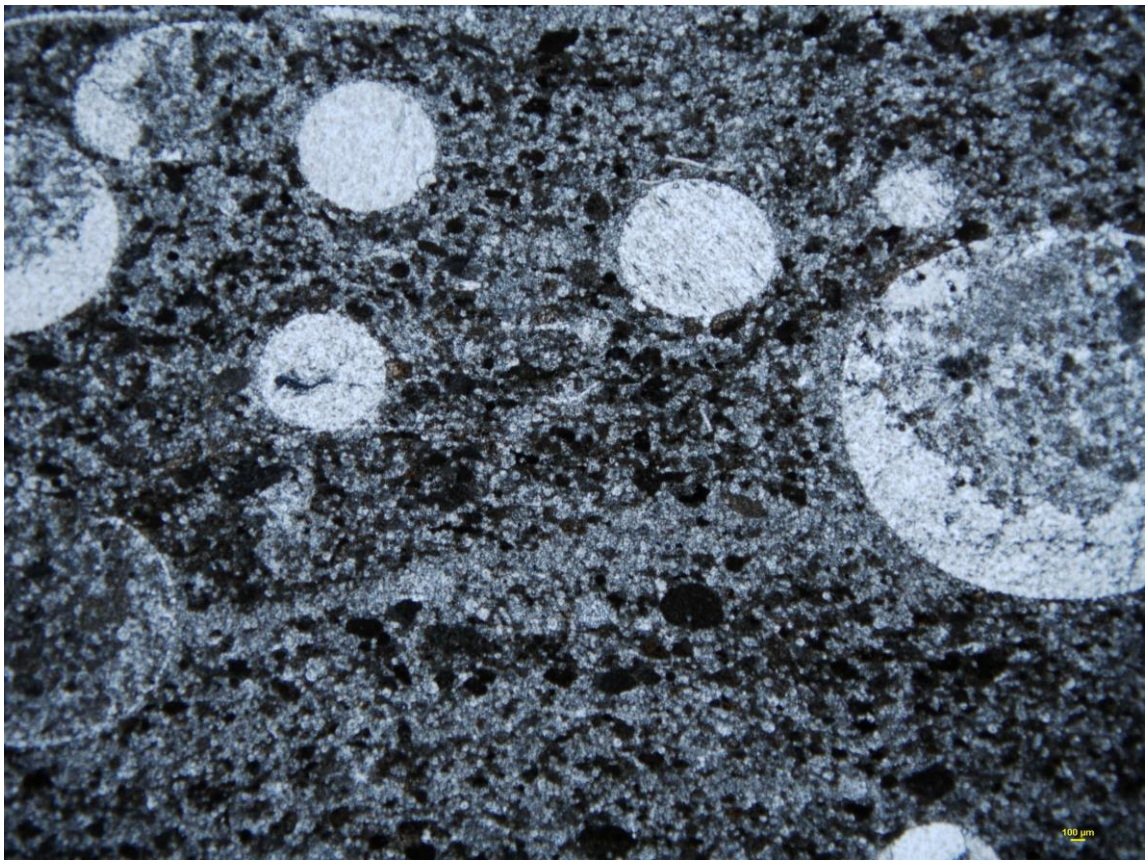

Height Above Buda:	15.5 feet
Skeletal Grain Types	Abundance
Planktonic Foram.	60%
Pellets	20%
Bivalve Fragments	10%
Organics	5%
Ammonites	<5%

Other Diagenetic Features:
Ammonoids replaced with sparry calcite cement. Most forams are completely recrystallized. Some grains appear to be ripped up clasts of mudstone.

Rock Name:
Foraminiferal Grainstone

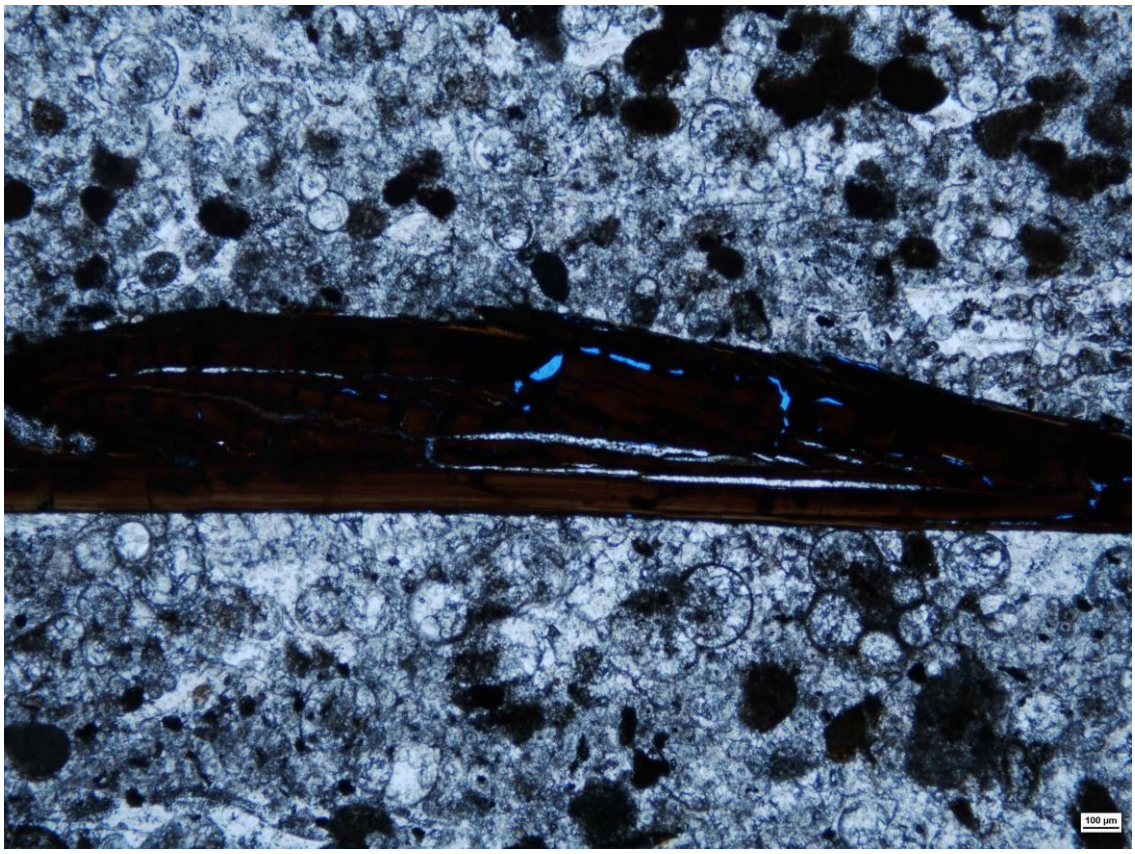

Height Above Buda:	16.0 feet
Skeletal Grain Types	Abundance
Planktonic Foramifera	80%
Pellets	10%
Pelagic Crinoid Fragments	10%
Plant Matter	<5%

Other Diagenetic Features:
Some intragranular porosity. Micritized grains.

Rock Name:

Ripple Laminated Foramineriferal Grainstone

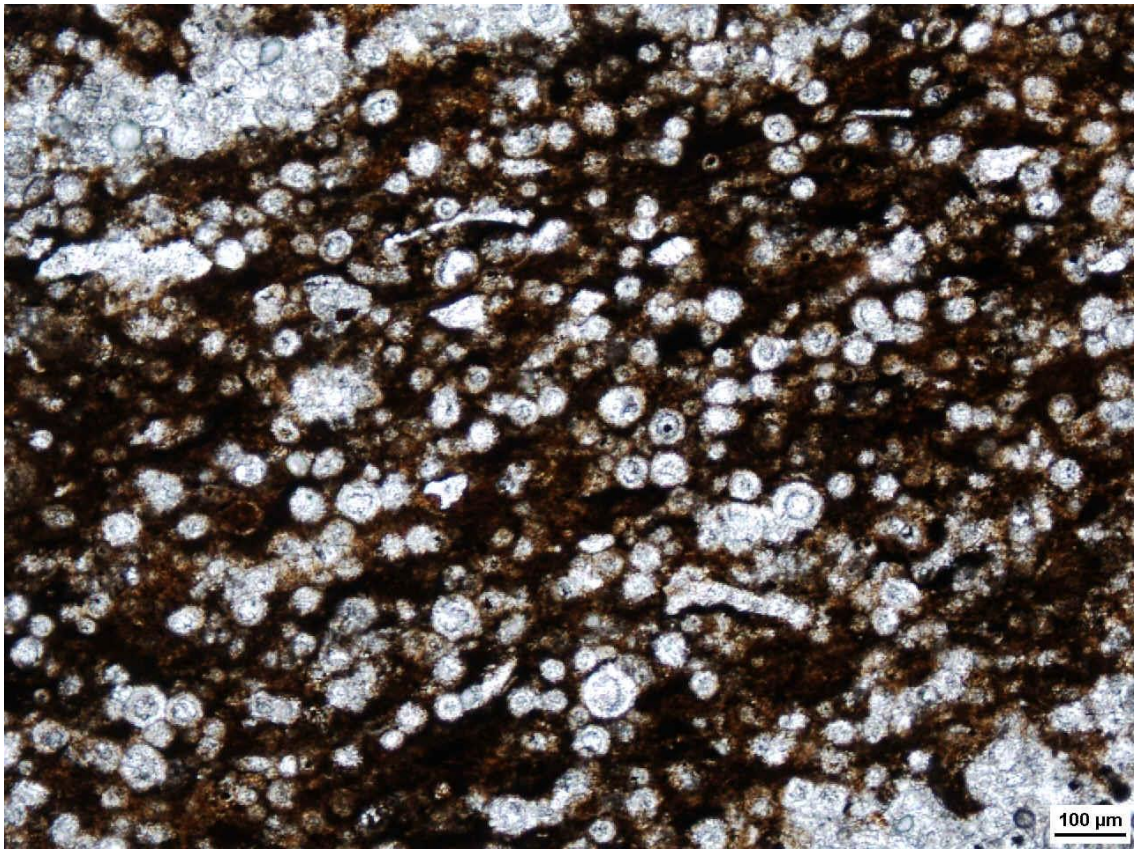

Height Above Buda:	17.3 feet
Skeletal Grain Types	Abundance
Planktonic Foraminerifera	90%
Organics	5%
Bivalve Fragments	<5%
Unidentified	<5%

Other Features:
Ripple laminations. Larger skeletal grains are within individual lamina. The darker grains appear to be mudstone rip-up clasts and are subrounded.

Rock Name:
Ripple Laminated Foraminerifera Packstone

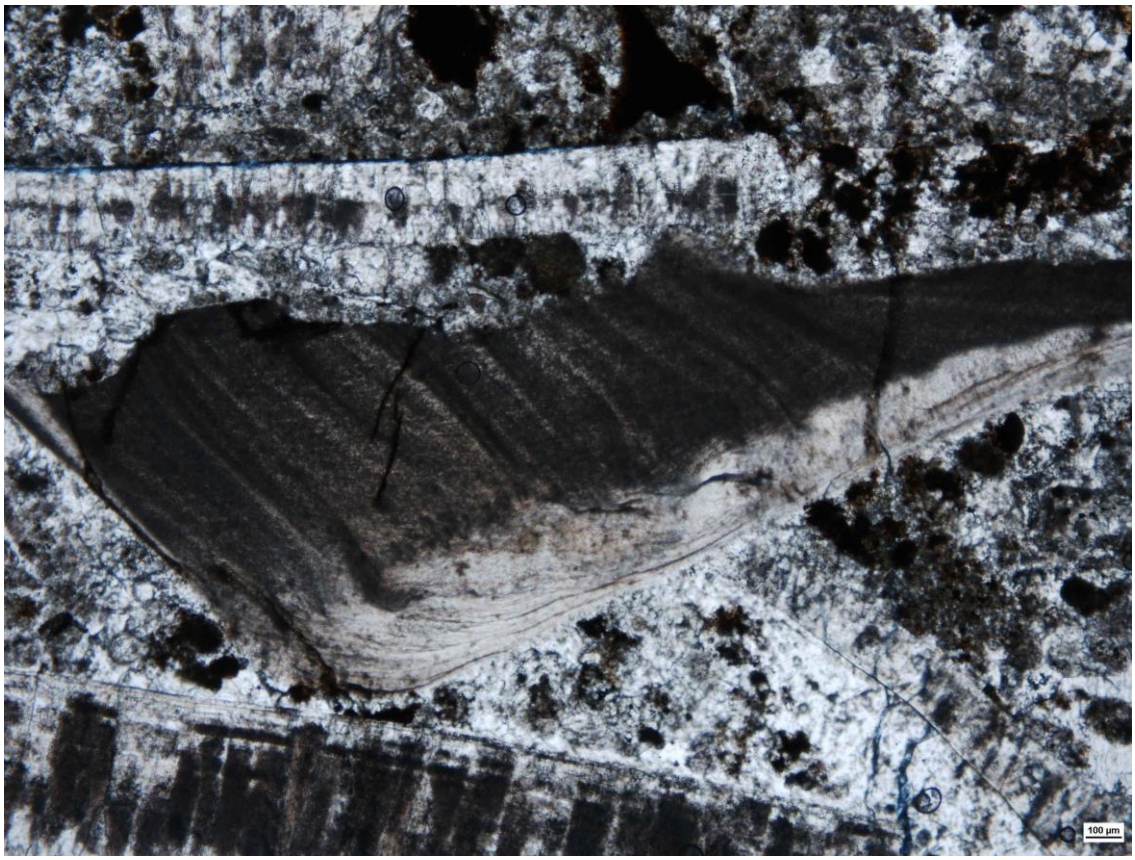

Height Above Buda:	17.75 feet
Skeletal Grain Types	Abundance
Bivalve Shells	75%
Ammonites	20%
Pyrite	5%
Organics	<1%
Pellets	<1%
Fish bones	<1%

Other Diagenetic Features:
About 50% of the bivalve fragments are recrystallized. Fractures are filled with calcite. Phosphatized fish bones

Rock Name:
Bivalve Grainstone

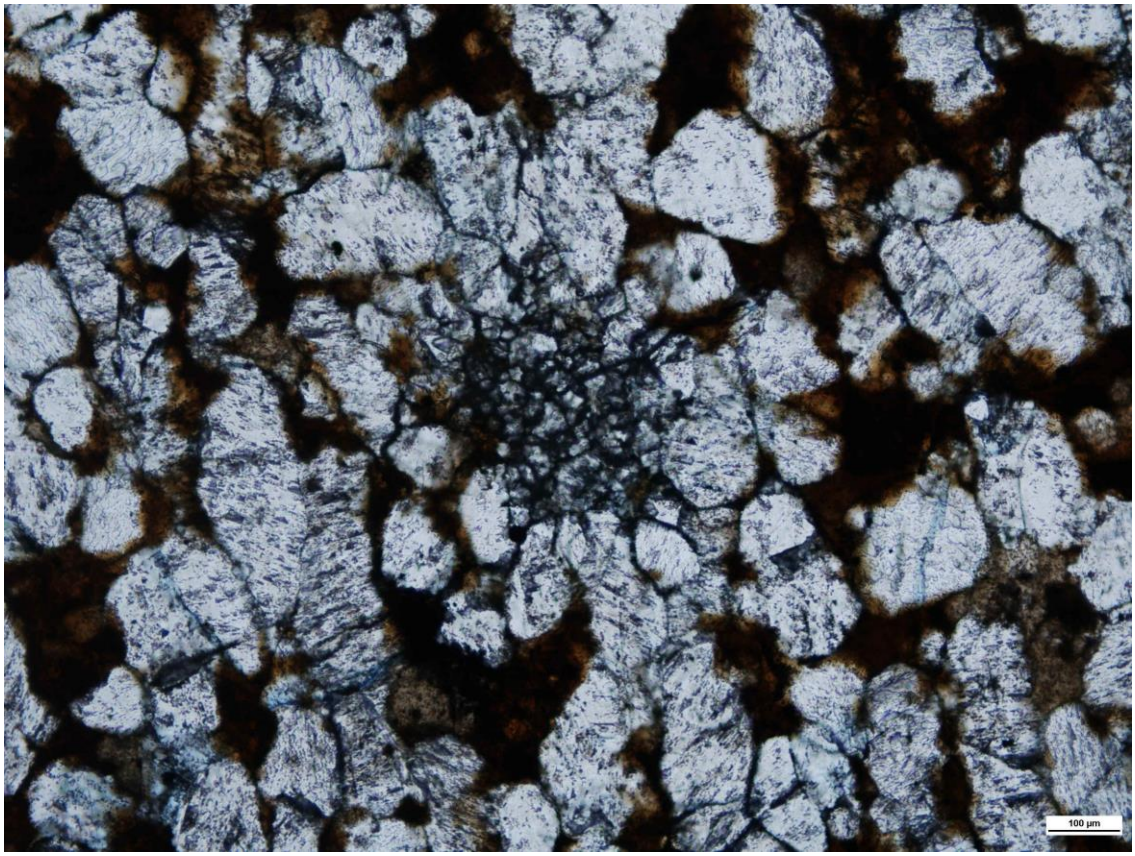

Height Above Buda:	19.5 feet
Skeletal Grain Types	Abundance
Unidentified Calcite Fragments	90%
Organics	10%
Radiolarian	Rare
Pyrite	<1%

Other Diagenetic Features:
Some grains have sutured contacts.

Rock Name:
Skeletal Grainstone

Height Above Buda:	20.5 feet
Skeletal Grain Types	Abundance
Oysters	70%
Fish Bones	20%
Organics	<1%
Bryozoans	Rare
Pyrite	Rare
Foraminifera	Rare

Other Diagenetic Features:
Fish bones and teeth are phosphatized.

Rock Name:
Molluscan Packstone

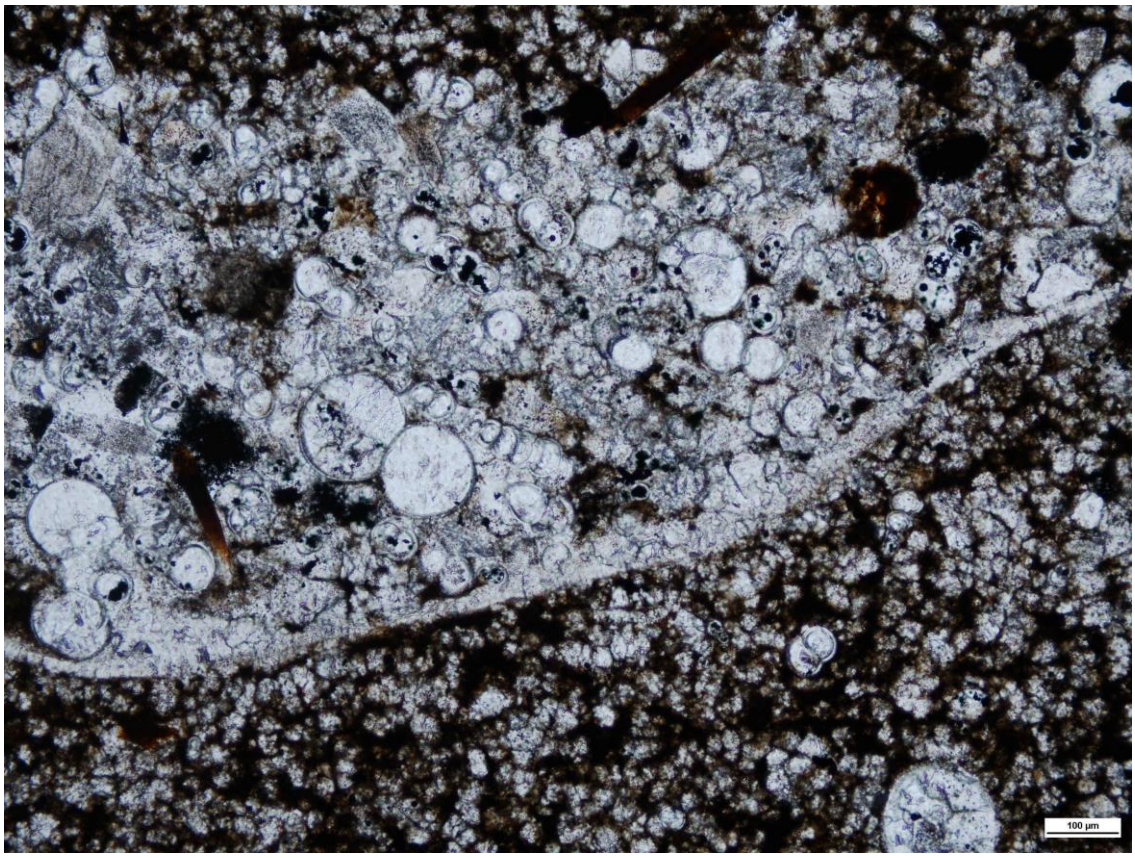

Height Above Buda:	23.8 feet
Skeletal Grain Types	Abundance
Planktonic Foram.	95%
Bivalves	5%
Pyrite	<1%

Other Diagenetic Features:
Calcite cement has formed between larger skeletal grains within the shelter of a large inoceramid bivalve fragment

Rock Name:
Foraminiferal Packstone

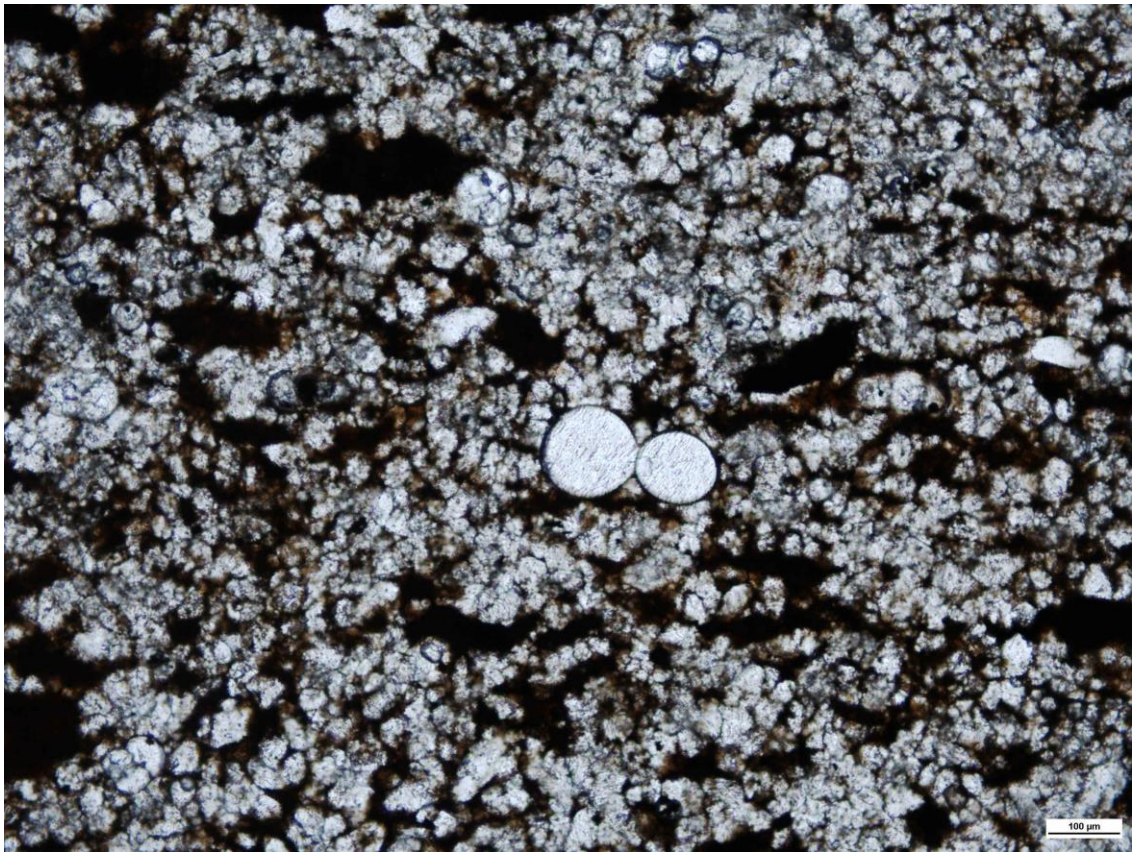

Height Above Buda:	24.8 feet
Skeletal Grain Types	Abundance
Planktonic Foram.	90%
Organics	10%
Bivalves	<1%

Other Diagenetic Features:
Many smaller foraminifera are recrystallized. The organic matter has a fabric that suggests compaction.

Rock Name:
Foraminiferal Packstone

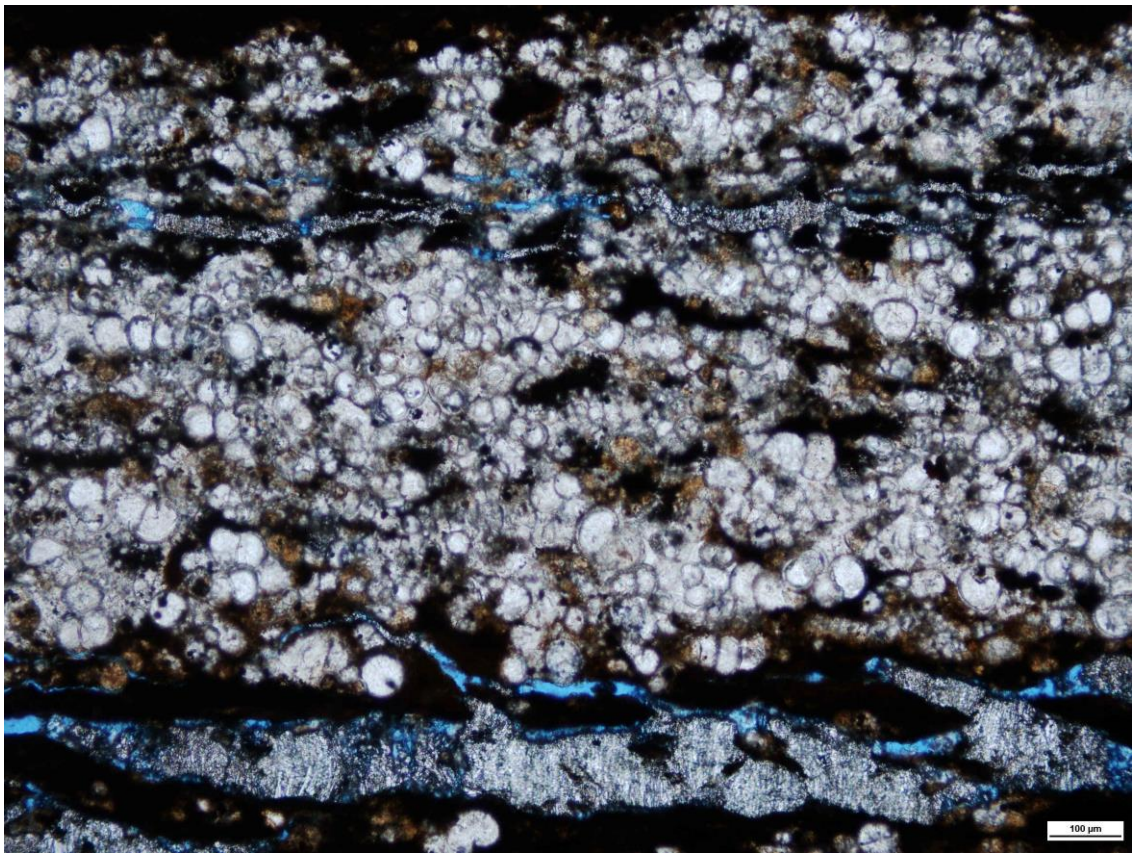

Height Above Buda:	25.5
Skeletal Grain Types	Abundance
Planktonic Foram.	80%
Bivalve Fragments	10%
Organics	10%
Pyrite	<1%

Other Diagenetic Features:
Calcite filled fractures are primarily horizontal. Some foraminifera appear to be filled with organics.

Rock Name:
Foraminiferal Mudstone

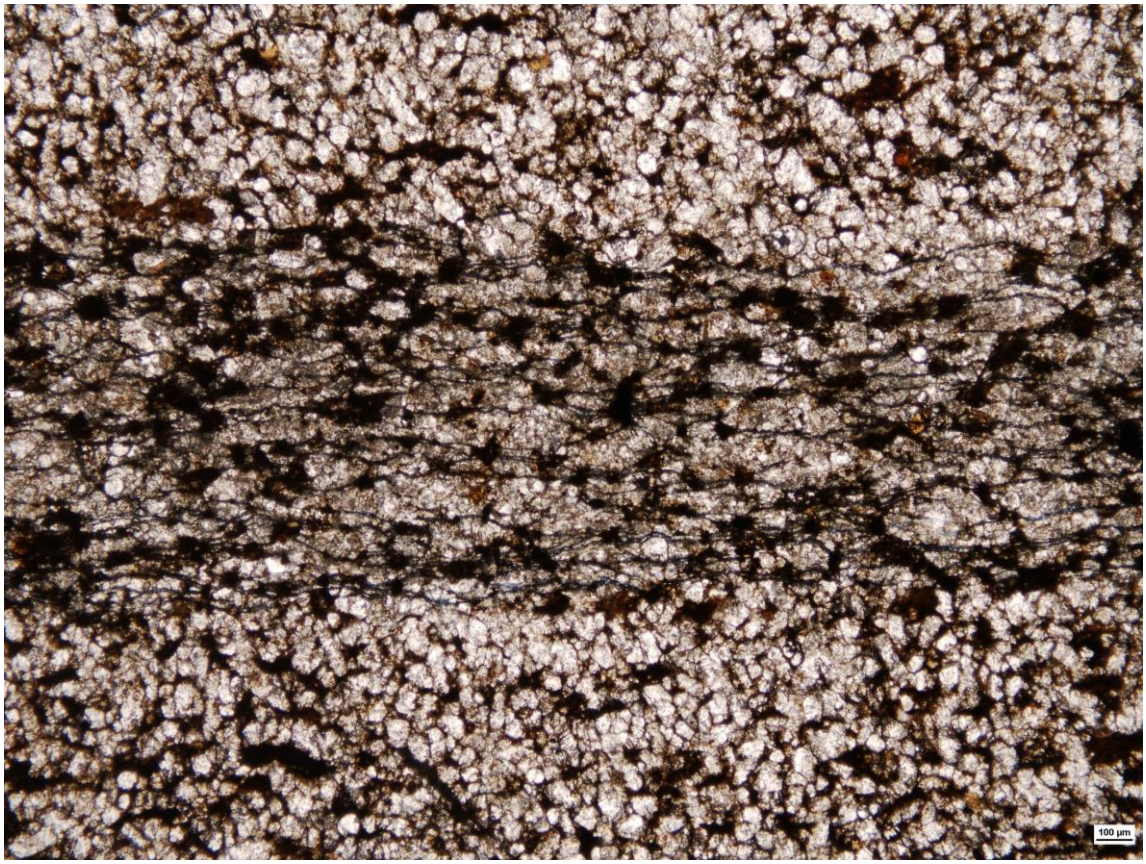

Height Above Buda:	28.2 feet
Skeletal Grain Types	Abundance
Planktonic Foram.	95%
Organics	5%
Bivalves	<1%

Other Diagenetic Features:
Most grains are completely recrystallized. Horizontal fractures connect organic matter in several horizons.

Rock Name:
Foraminiferal Packstone

Height Above Buda:	30.8 feet
Skeletal Grain Types	Abundance
Planktonic Foram.	95%
Organics	5%
Bivalves	Rare

Other Diagenetic Features:
Most grains are completely recrystallized

Rock Name:
Laminated Foraminiferal Packstone

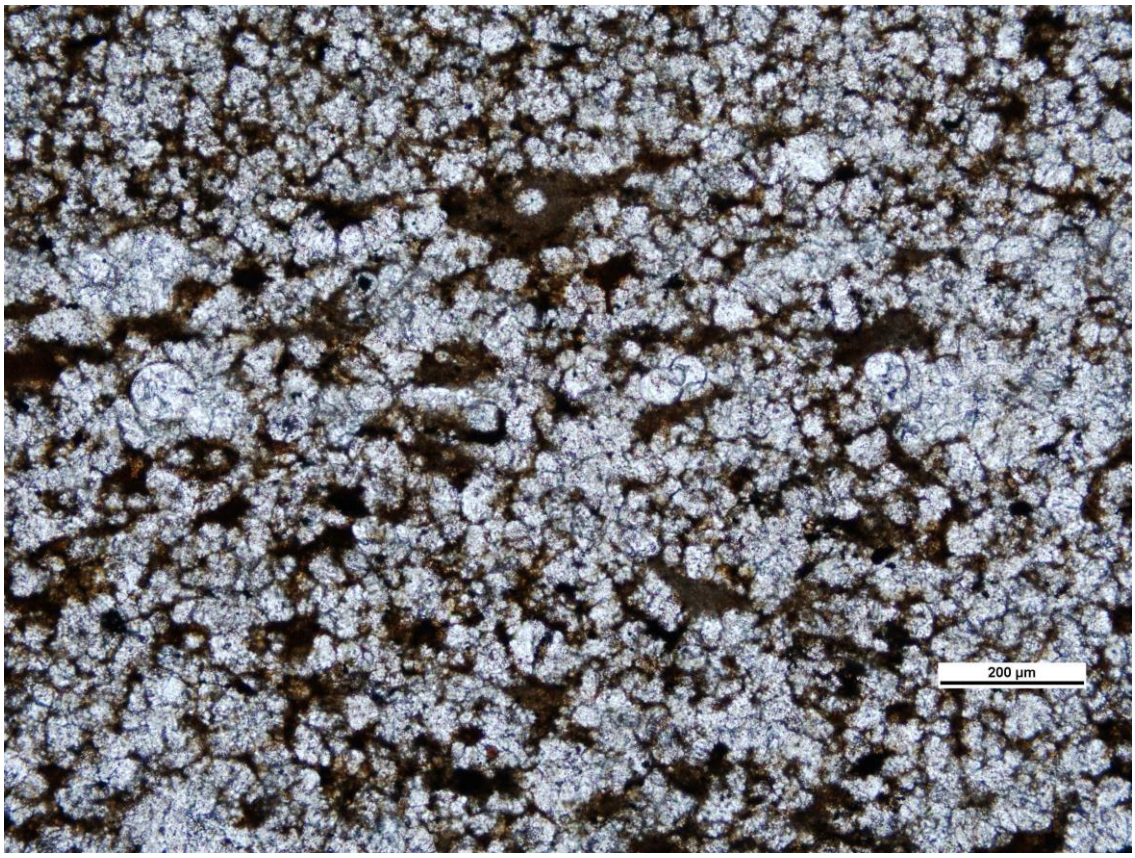

Height Above Buda:	36.0 feet
Skeletal Grain Types	Abundance
Planktonic Foram.	95%
Organics	5%
Bivalves	Rare
Pyrite	Rare

Other Diagenetic Features:
Completely recrystallized forams.
Calcite filled fractures.

Rock Name:
Laminated Foraminiferal Packstone

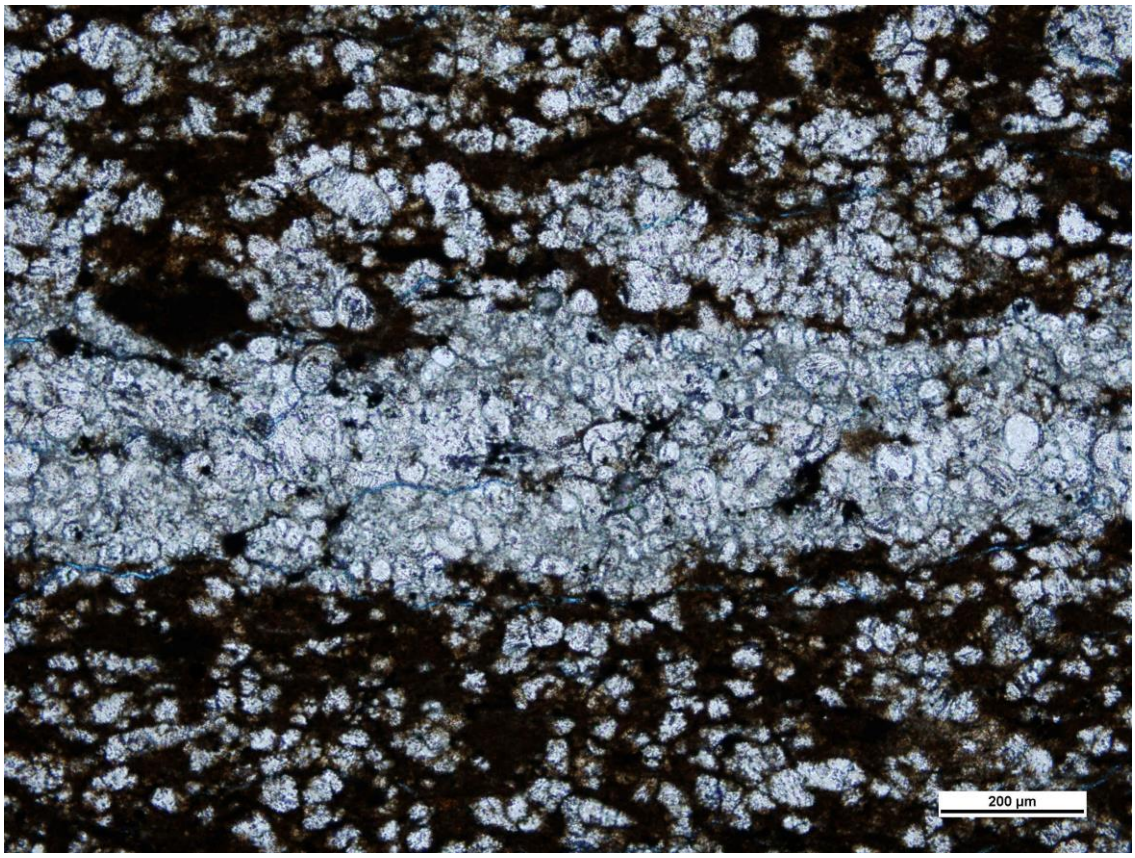

Height Above Buda:	40.0 feet
Skeletal Grain Types	Abundance
Planktonic Foraminiferal	90%
Organics	10%
Bivalves	Rare

Other Features:
Well defined laminations of mud. Foraminifera in mud-lean horizons are more recrystallized than those in mud-rich sections of the sample.

Rock Name:
Laminated Foraminiferal Packstone

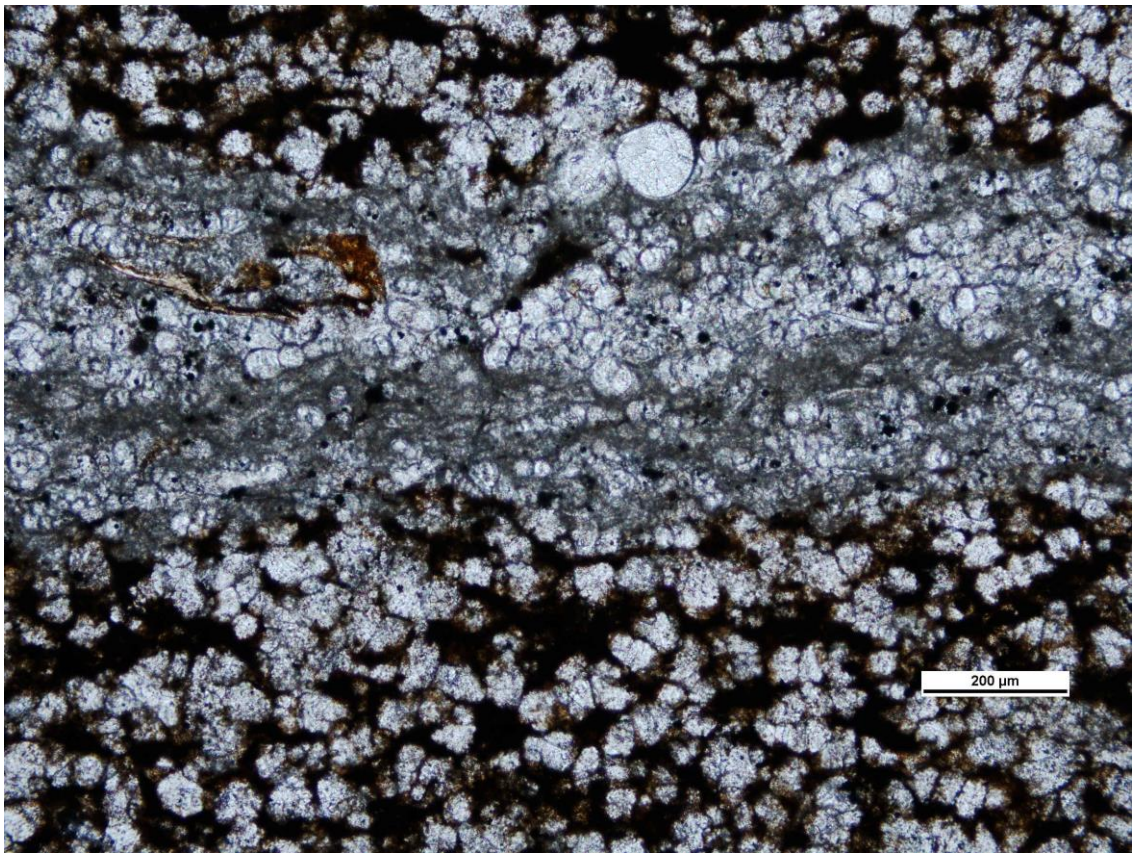

Height Above Buda:	42.0 feet
Skeletal Grain Types	Abundance
Planktonic Foram.	85%
Organics	10%
Fish Bones	5%
Bivalves	<1%

Other Diagenetic Features:
Most forams are completely recrystallized. Fish bones are phosphatized. Certain horizons have lighter colored matrix.

Rock Name:
Foraminiferal Packstone-Wackestone

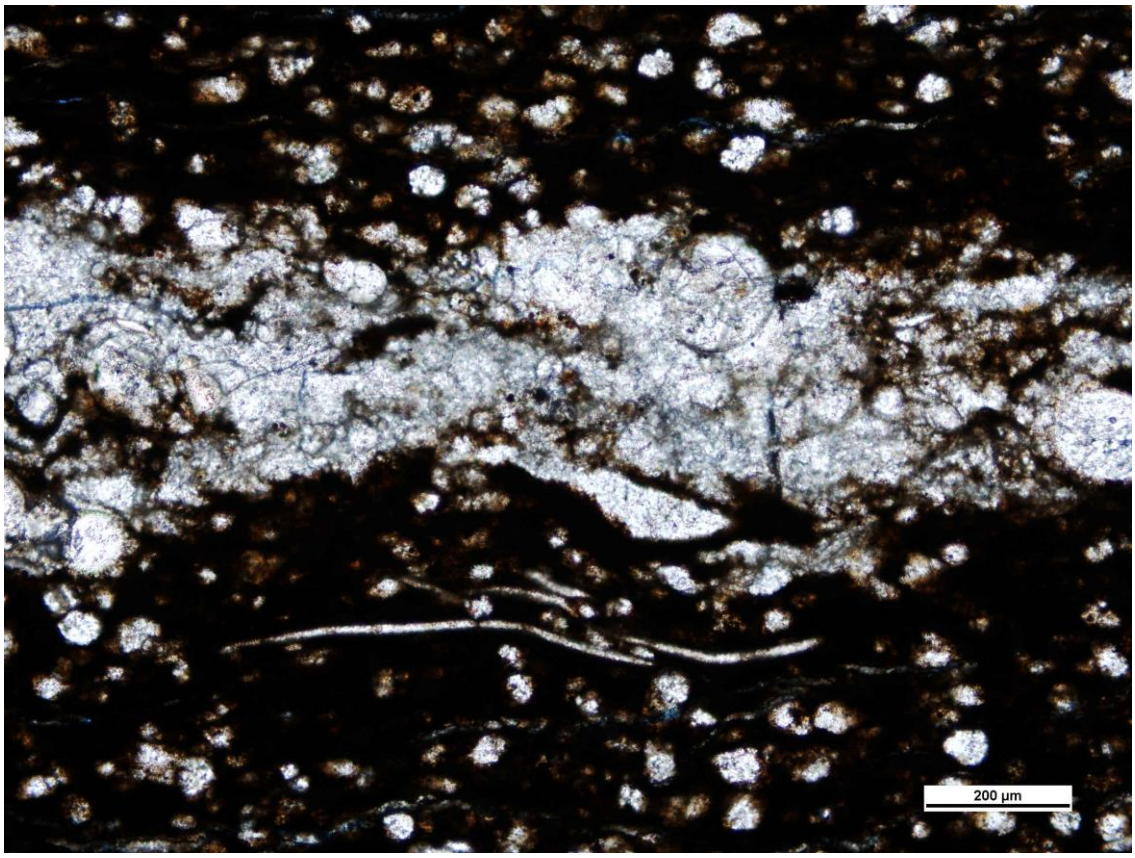

Height Above Buda:	44.2 feet
Skeletal Grain Types	Abundance
Planktonic Foram.	70%
Organics	30%
Bivalves	<1%

Other Diagenetic Features:
Calcite filled fractures are common.
Foram rich laminations are more recrystallized than forams in a mud matrix

Rock Name:
Laminated Foraminiferal Mudstone

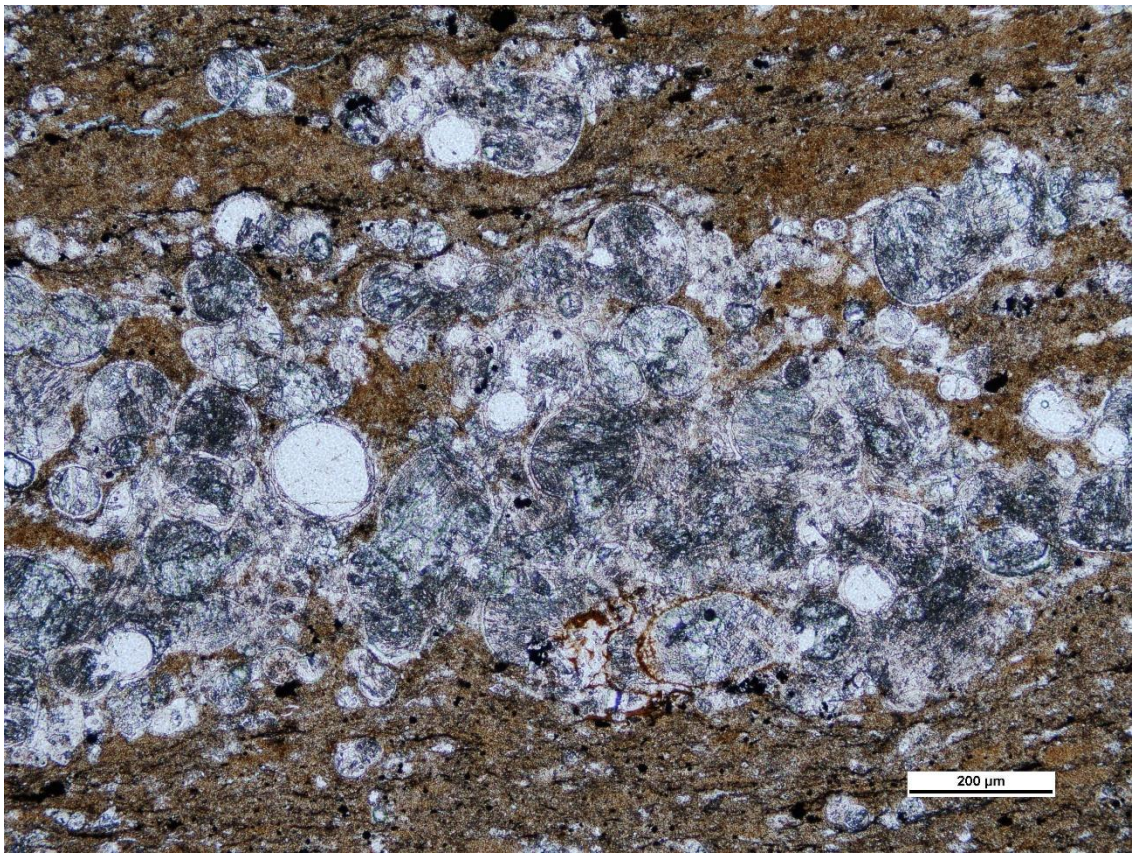

Height Above Buda:	49.0 feet
Skeletal Grain Types	Abundance
Planktonic Foram.	90%
Organics	5%
Pyrite	5%
Bivalves	<1%

Other Diagenetic Features:
Recrystallized grains. Sutured Contacts between some forams.

Rock Name:
Laminated Foraminiferal Mudstone

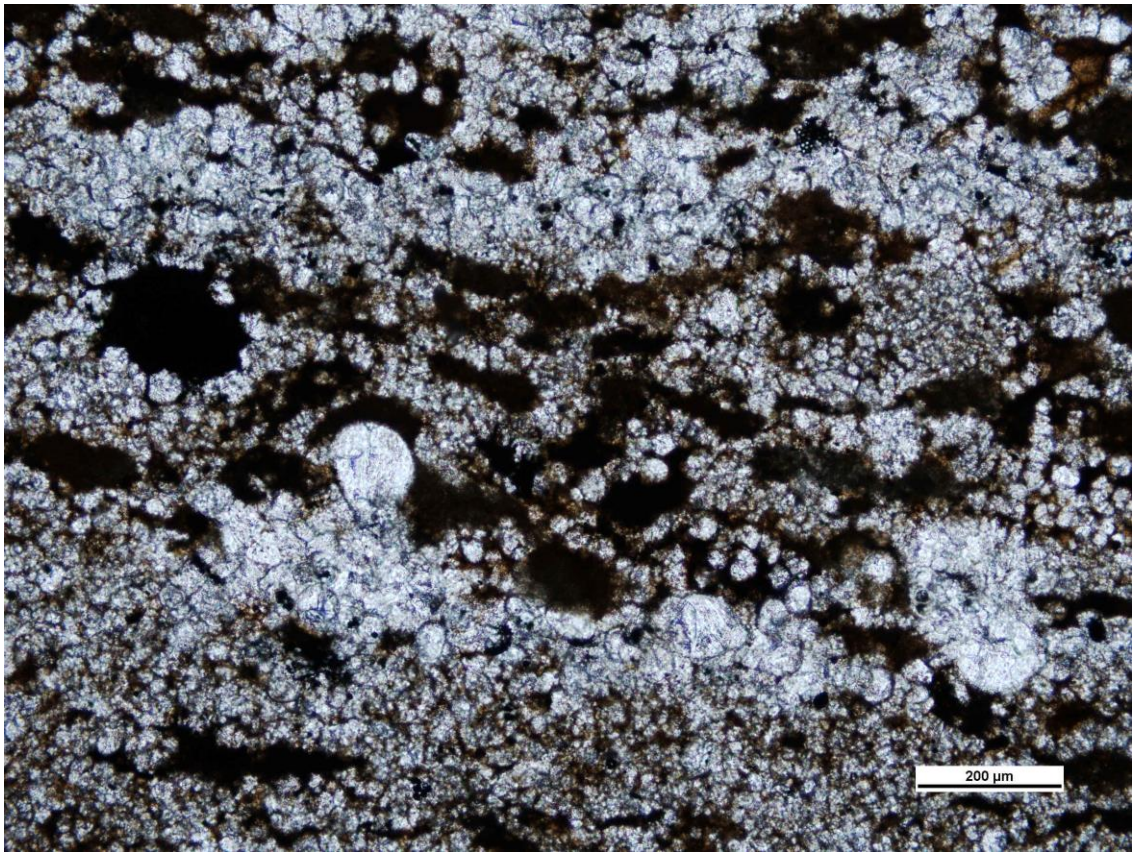

Height Above Buda:	49.5 feet
Skeletal Grain Types	Abundance
Planktonic Foram.	90%
Pellets	5%
Organics	5%
Pyrite	Rare
Bivalves	Rare

Other Diagenetic Features:

Rock Name:
Foraminiferal Packstone

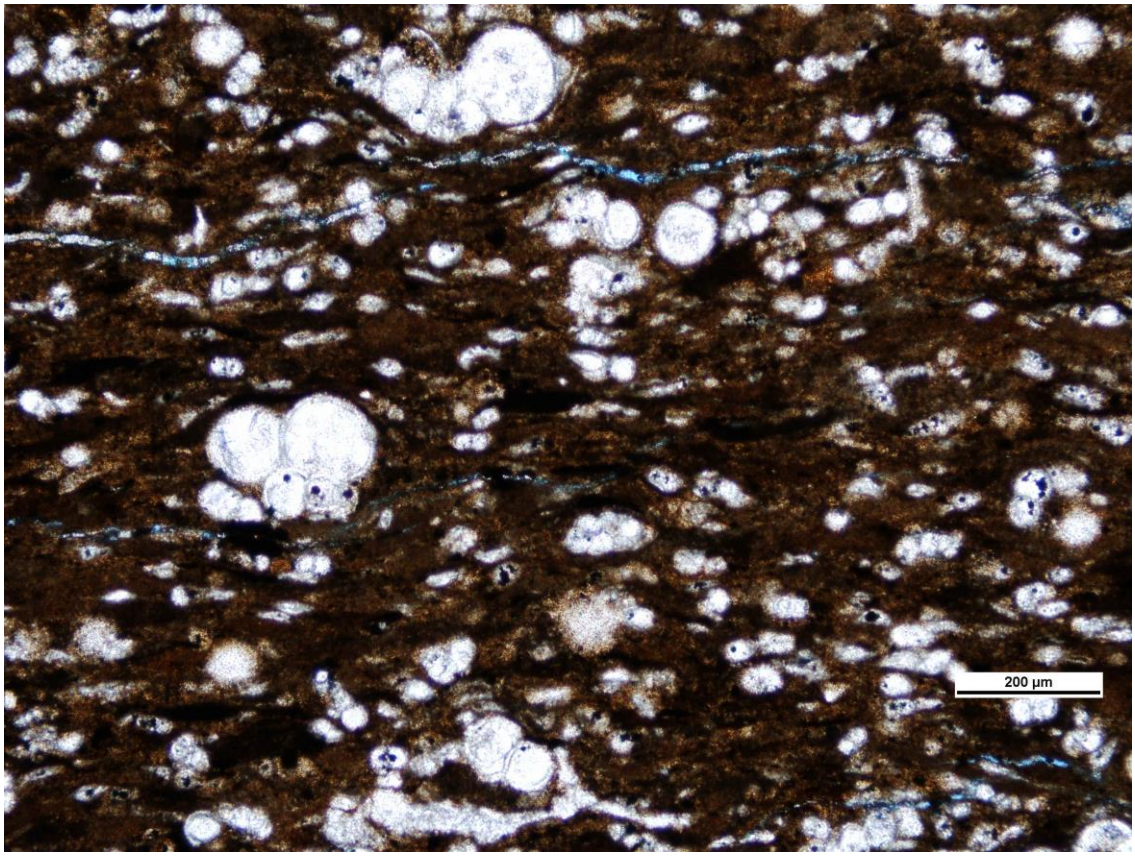

Height Above Buda:	51.0 feet
Skeletal Grain Types	Abundance
Planktonic Foram.	90%
Organics	10%
Bivalves	<1%

Other Diagenetic Features:
Calcite filled fractures. Organic matter is flattened.

Rock Name:
Foraminiferal Mudstone

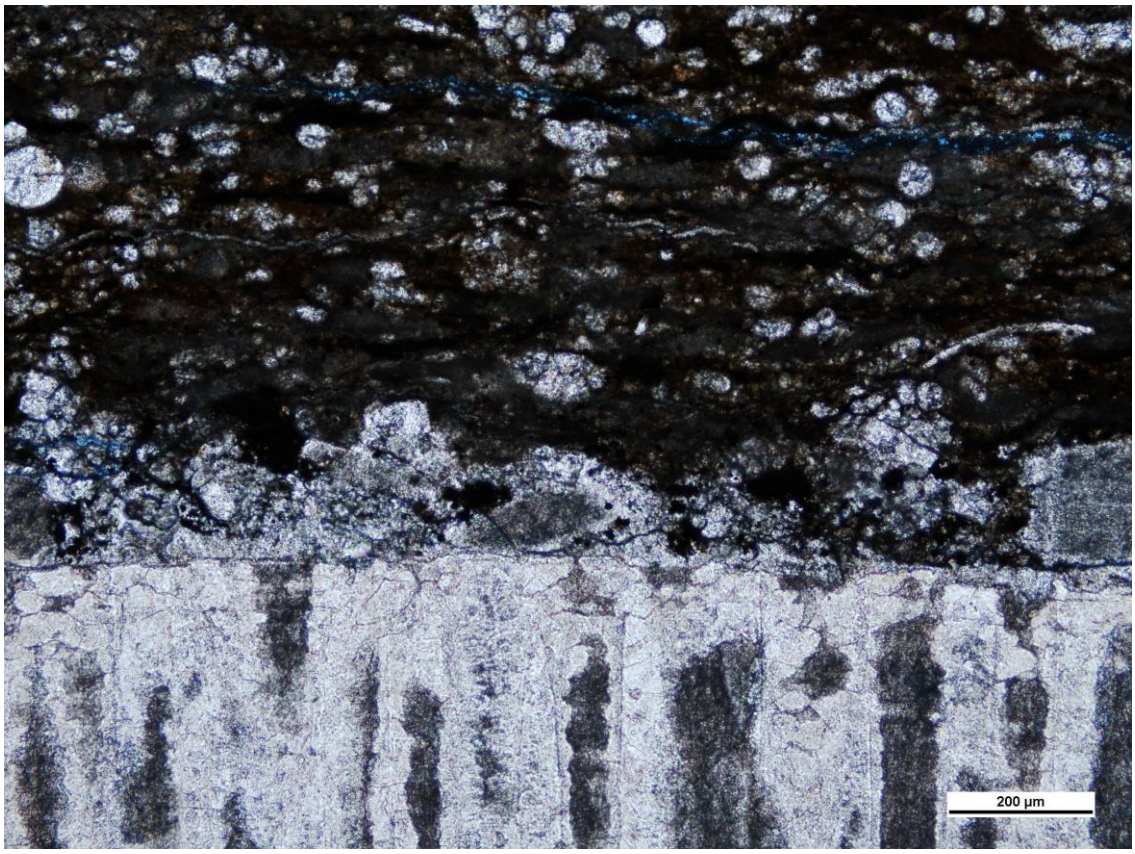

Height Above Buda:	63.8 feet
Skeletal Grain Types	Abundance
Planktonic Foram.	85%
Bivalves	10%
Organics	5%
Pyrite	<1%
Radiolaria	Rare

Other Diagenetic Features:
Flattened Organics. Recrystallization is more complete on the edges of bivalve shells than the center regions. Calcite filled fractures.

Rock Name:
Foraminiferal Packstone-Wackestone

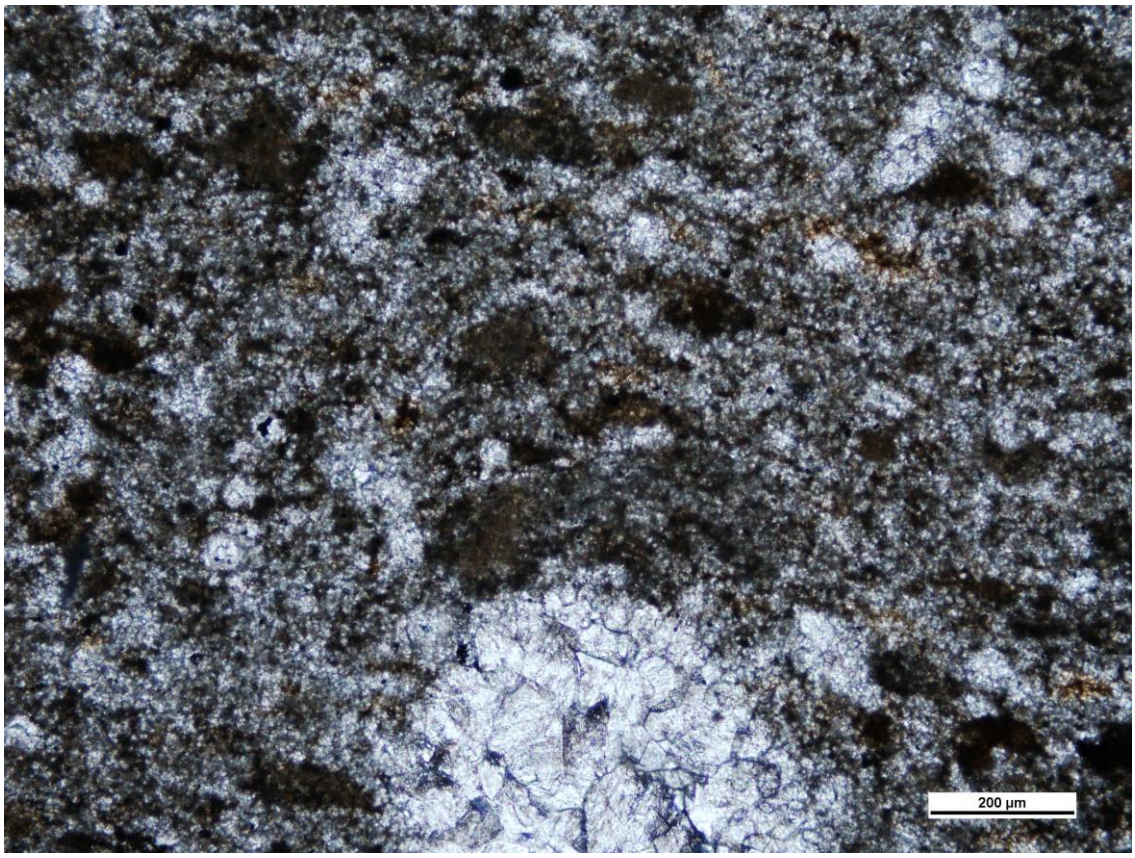

Height Above Buda:	67.8 feet
Skeletal Grain Types	Abundance
Planktonic Foram.	90%
Pellets	10%
Bivalves	<1%
Fish Bones	Rare
Radiolaria	Rare
Other Diagenetic Features:	

Rock Name:
Foraminiferal Packstone

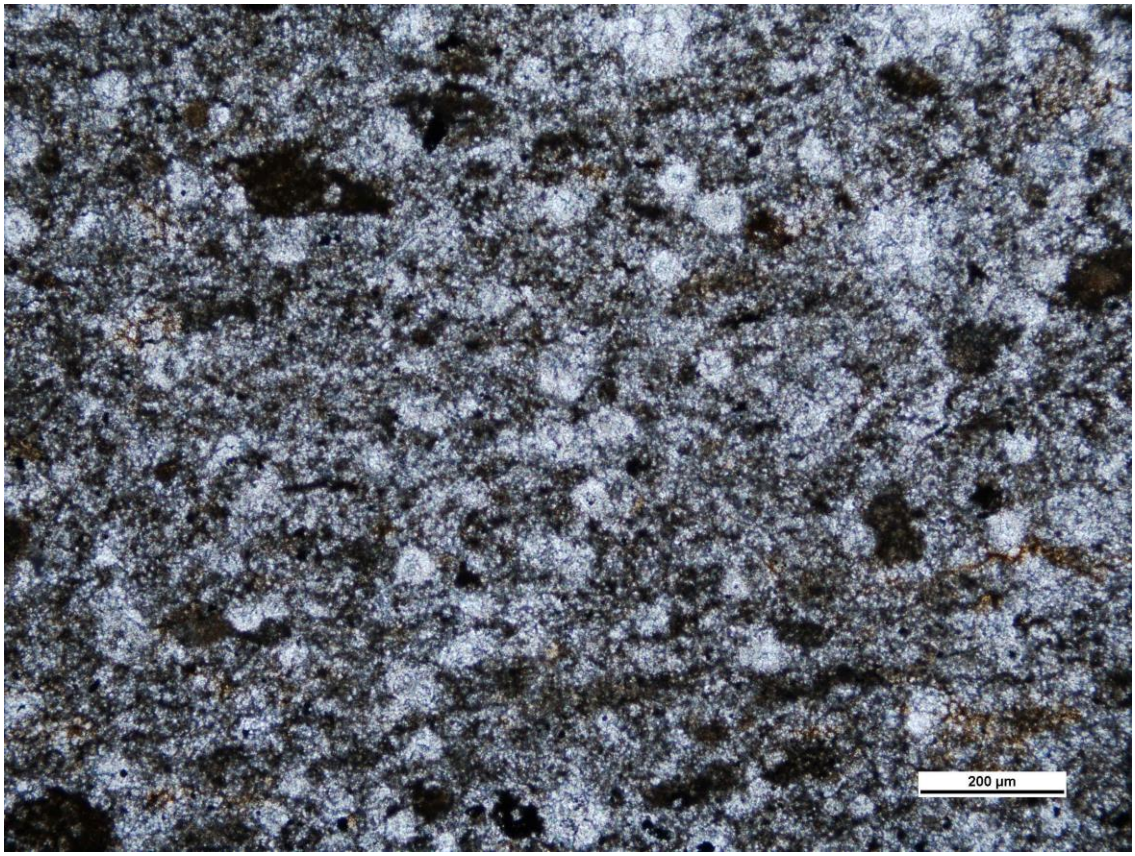

Height Above Buda:	68.0 feet
Skeletal Grain Types	Abundance
Planktonic Foram.	85%
Ammonites	5%
Pellets	5%
Bivalves	5%
Pyrite	<1%

Other Diagenetic Features:
Grains and matrix are recrystallized.

Rock Name:
Foraminiferal Packstone

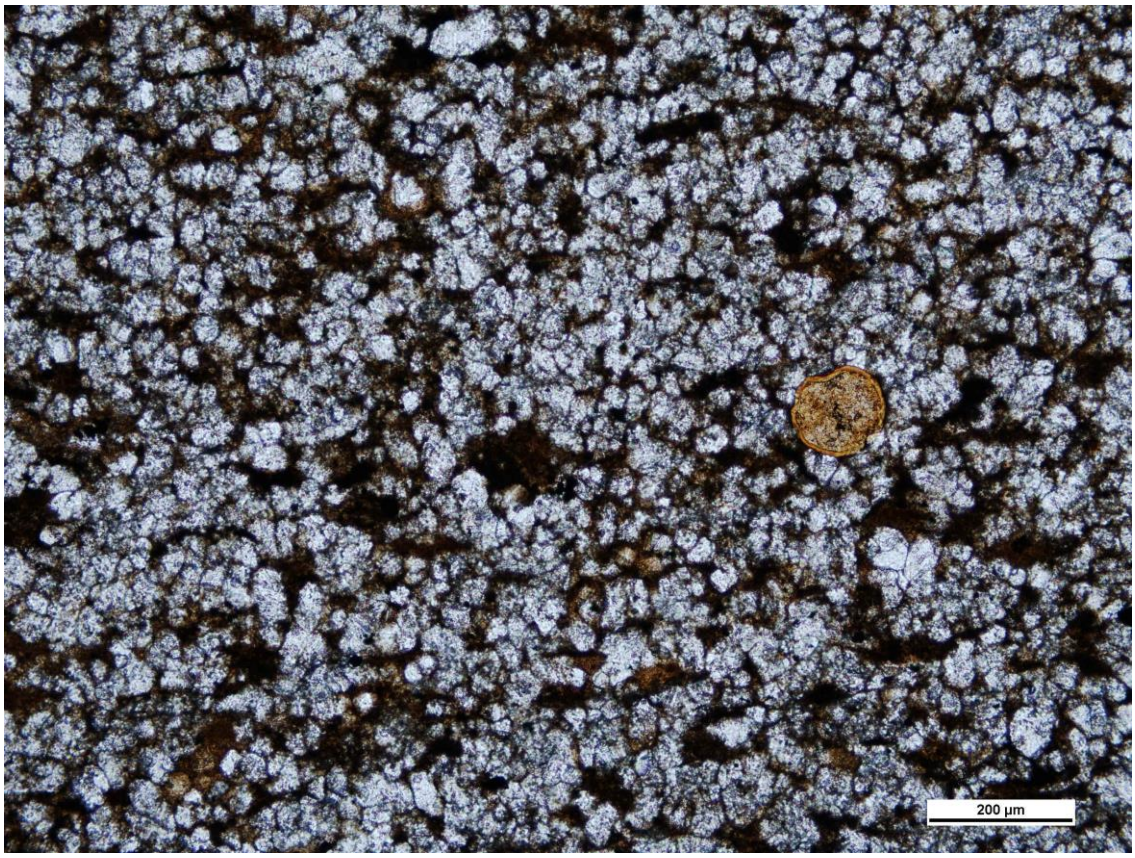

Height Above Buda:	77.0 feet
Skeletal Grain Types	Abundance
Planktonic Foram.	95%
Organics	5%
Pyrite	<1%

Other Diagenetic Features:
Most foram tests are recrystallized

Rock Name:
Laminated Foraminiferal Packstone

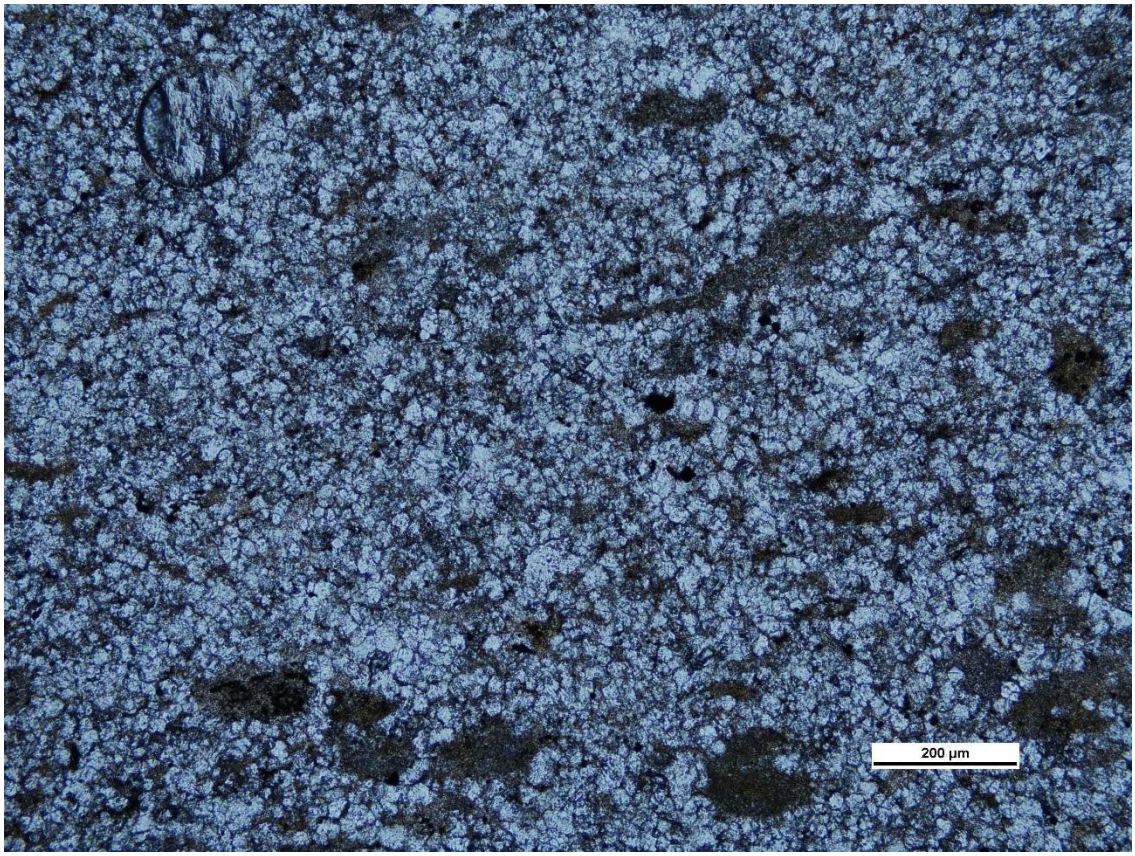

Height Above Buda:	82.8 feet
Skeletal Grain Types	Abundance
Planktonic Foram.	95%
Organics	5%
Pyrite	<1%
Bivalves	<1%

Other Diagenetic Features:
Most grains are completely recrystallized

Rock Name:
Foraminiferal Packstone

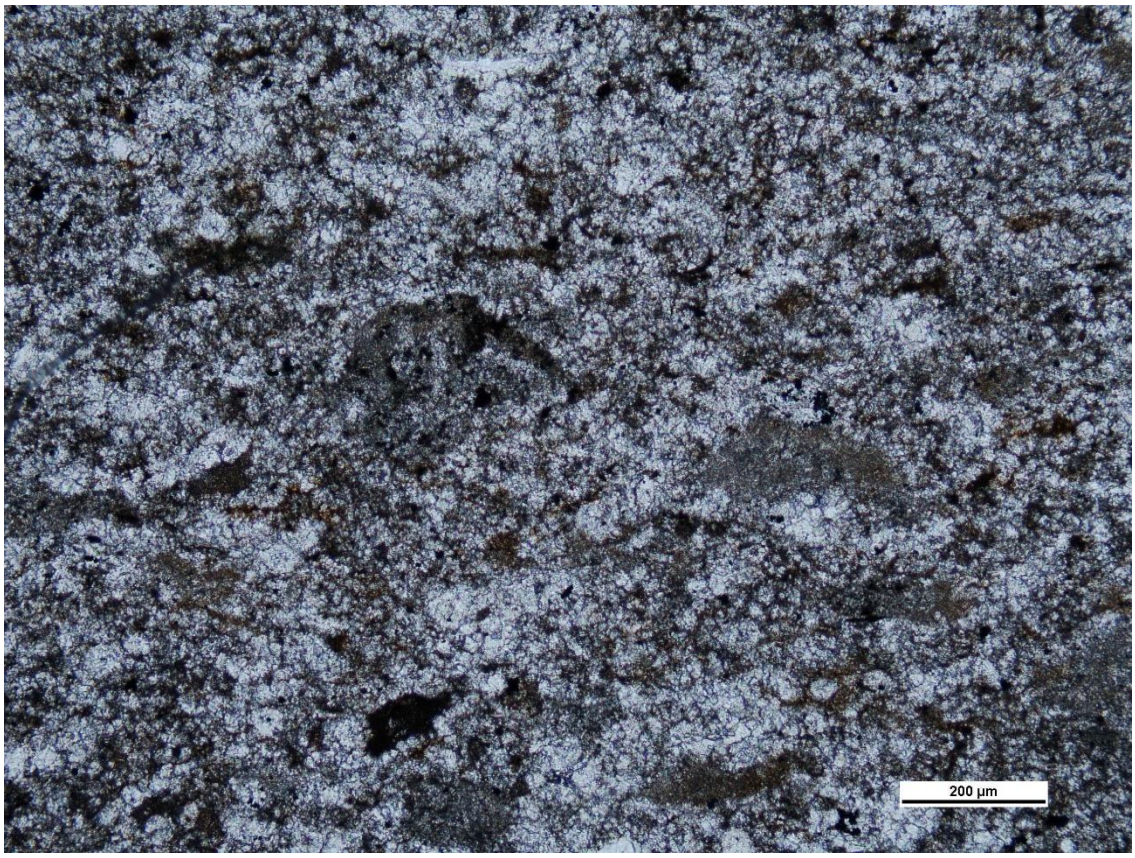

Height Above Buda:	83.5 feet
Skeletal Grain Types	Abundance
Unidentified	80%
Planktonic Foram.	20%
Fish Bones	<1%
Organics	<1%
Bivalves	Rare

Other Diagenetic Features:
Most of the matrix is entirely recrystallized.

Rock Name:
Skeletal Packstone

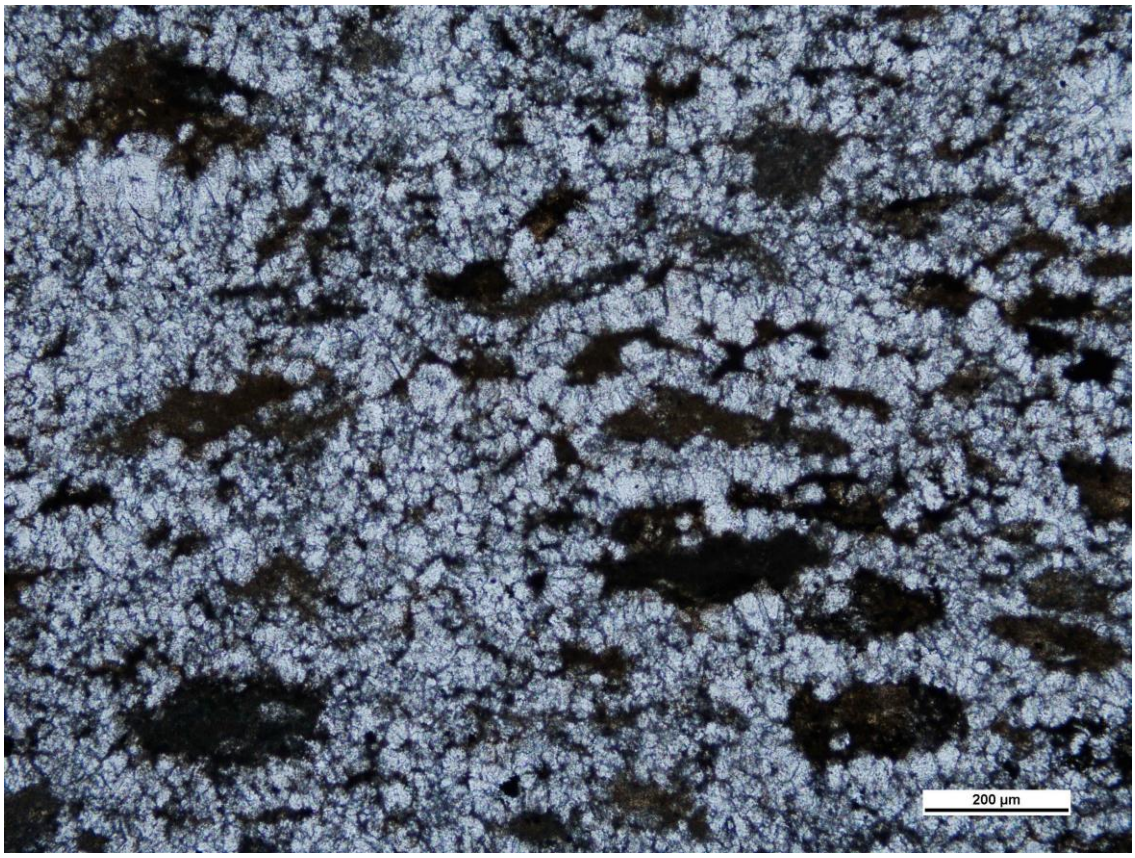

Height Above Buda:	85.9 feet
Skeletal Grain Types	Abundance
Planktonic Foraminifera	90%
Pellets	5%
Organics	5%
Pyrite	<1%

Other Diagenetic Features:
Organics and some micrite clasts are flattened. Most grains are completely recrystallized and assumed to be forams.

Rock Name:
Foraminiferal Packstone-Grainstone

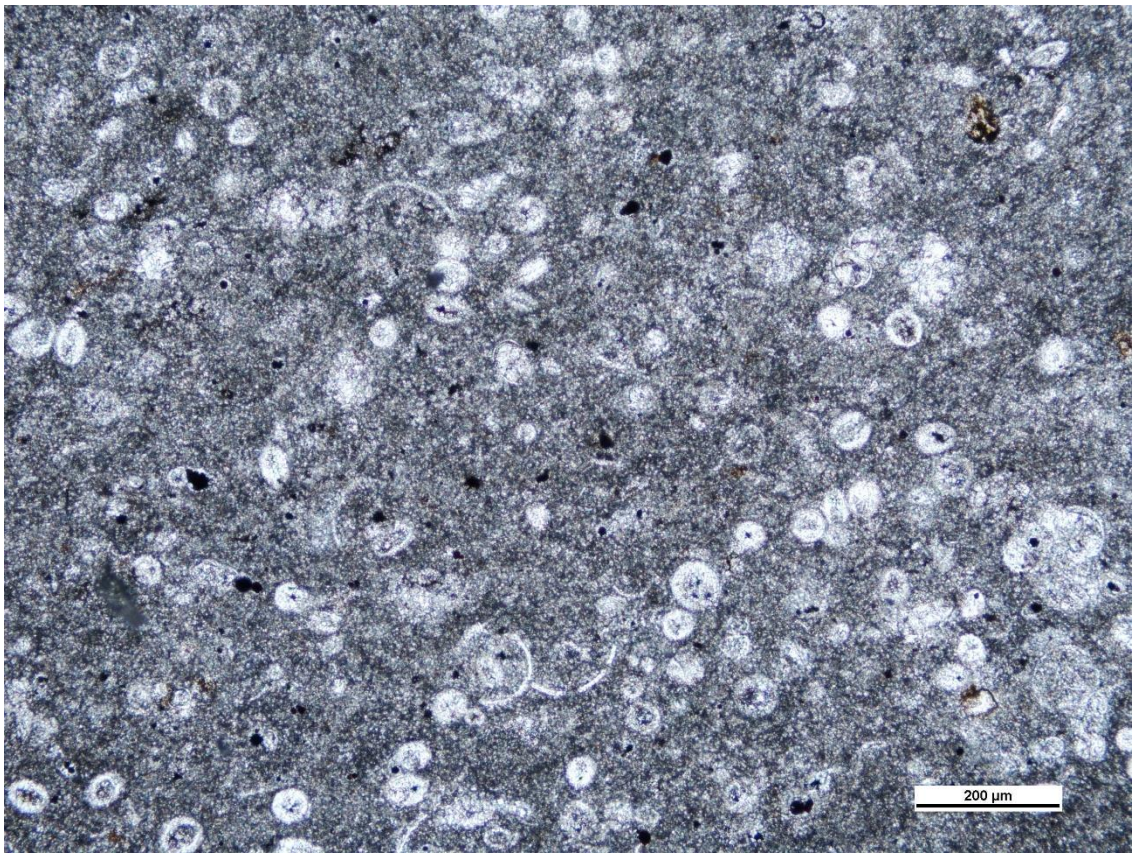

Height Above Buda:	95.0 feet
Skeletal Grain Types	Abundance
Planktonic Foram.	400%
Pellets	30%
Bivalves	20%
Pyrite	5%
Organics	5%
Fish Bones	<1%

Other Diagenetic Features:
Matrix is recrystallized.

Rock Name:
Foraminiferal Wackestone-Packstone.

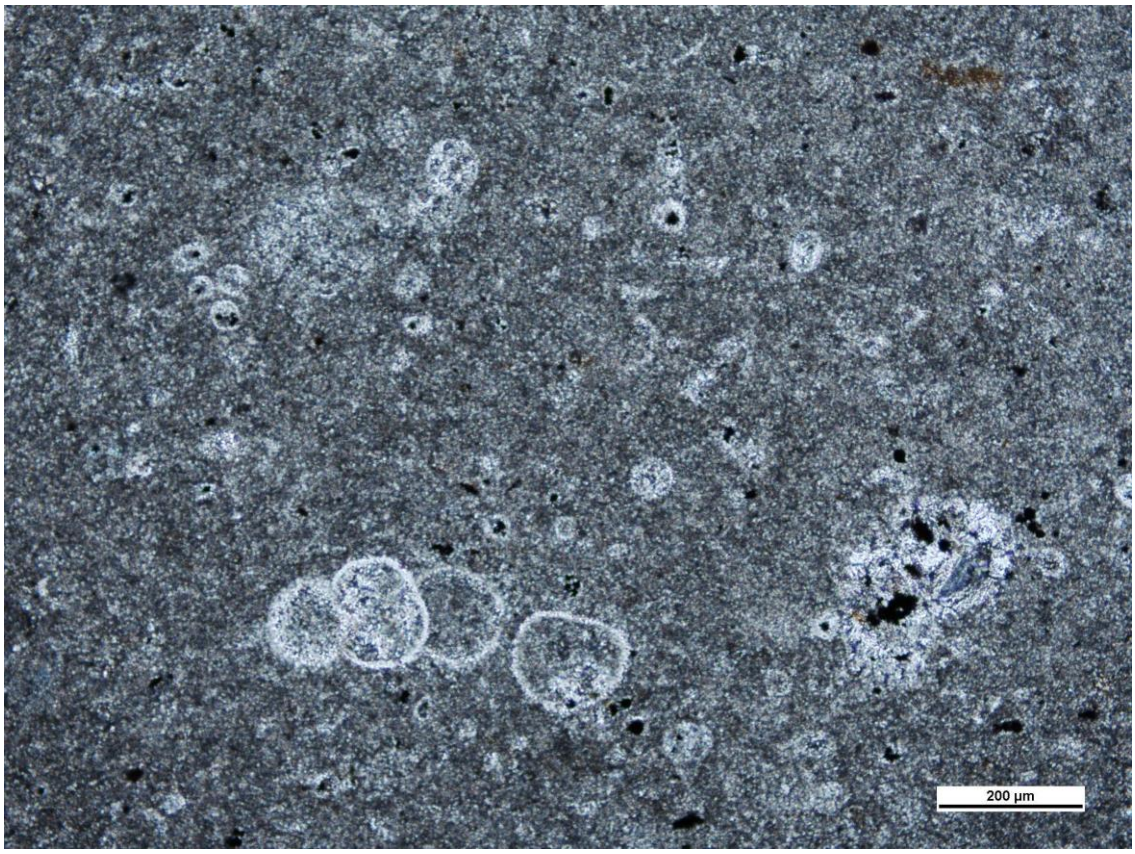

Height Above Buda:	98.0 feet
Skeletal Grain Types	Abundance
Planktonic Foram.	85%
Bivalve Fragments	10%
Pyrite	5%

Other Diagenetic Features:
Calcite filled fractures. Some grains preplaced by pyrite.

Rock Name:
Foraminifera Wackestone-Packstone

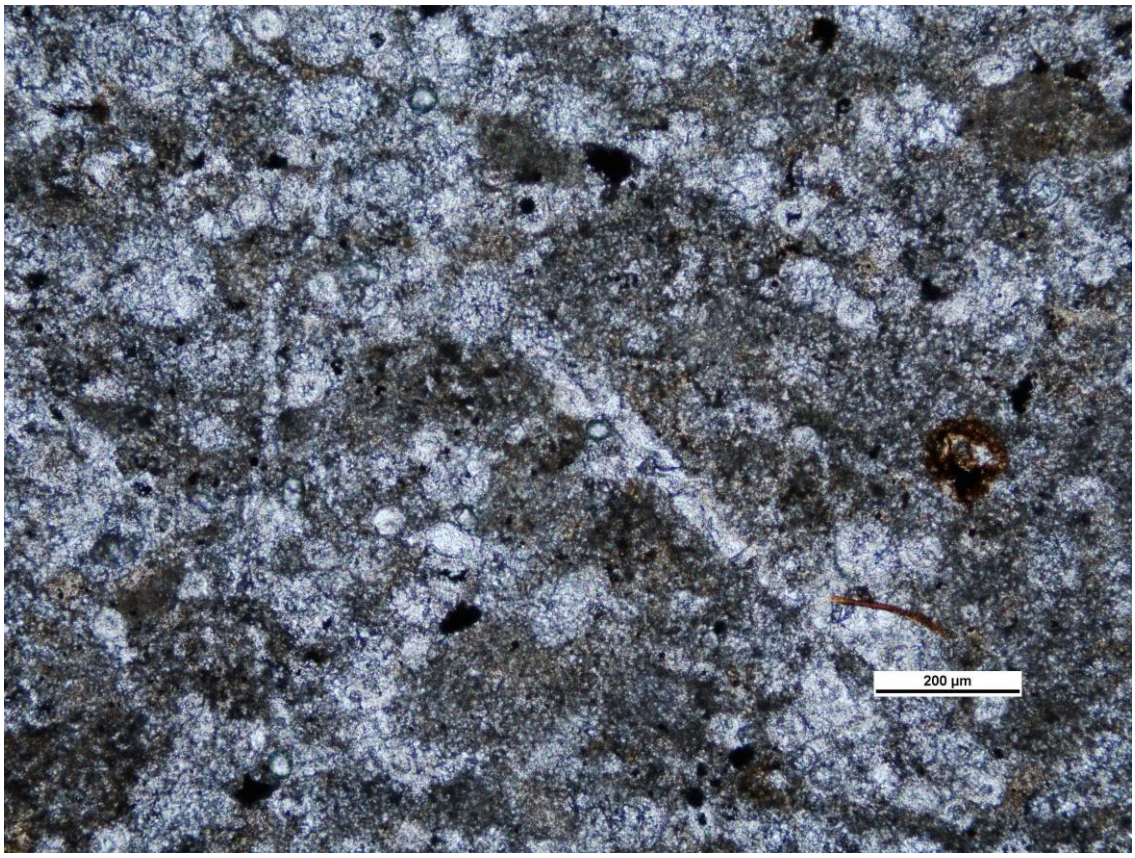

Height Above Buda:	105.9 feet
Skeletal Grain Types	Abundance
Planktonic Foram.	75%
Pellets	10%
Inoceramid Bivalves	10%
Pyrite	5%
Fish Bones	<1%
Other Diagenetic Features:	

Rock Name:
Foraminiferal Wackestone-Packstone

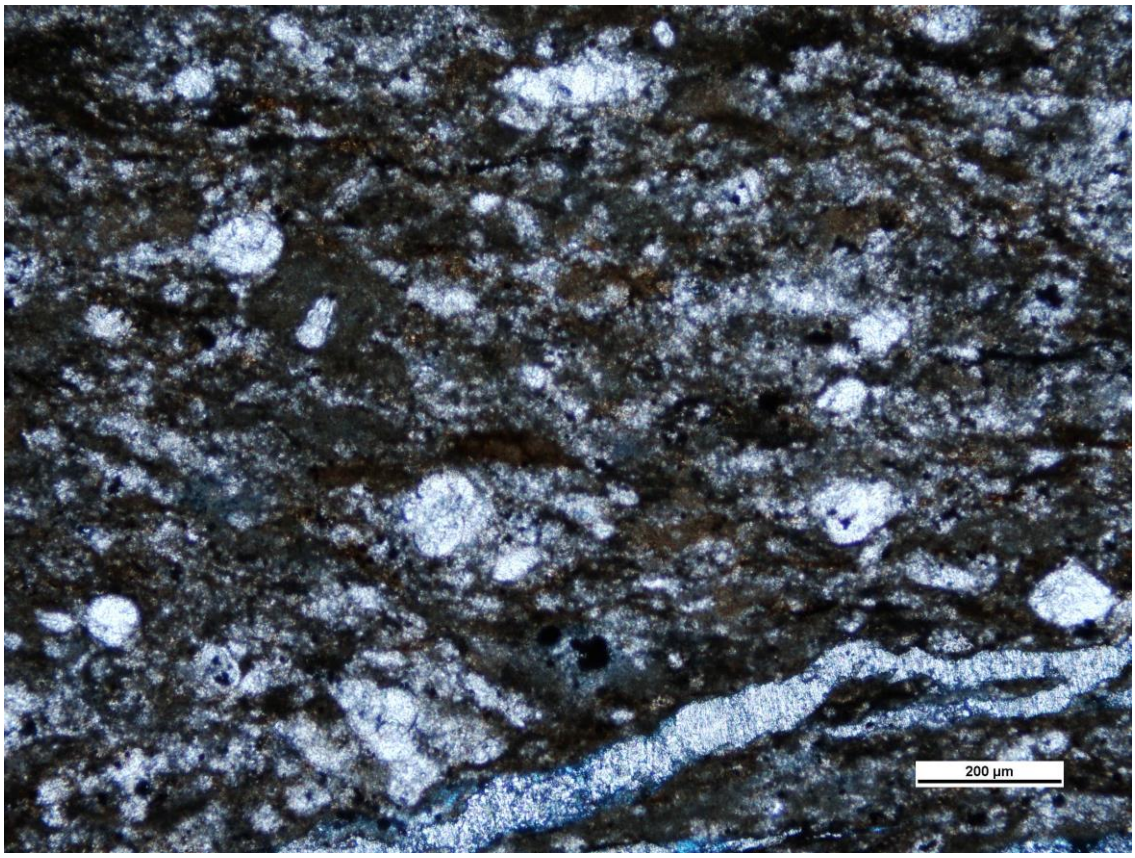

Height Above Buda:	108.5 feet
Skeletal Grain Types	Abundance
Planktonic Foram.	80%
Bivalve Fragments	10%
Organics	5%
Pyrite	5%

Other Diagenetic Features:
Flattened organic matter. Calcite filled fractures.

Rock Name:
Foraminiferal Mudstone

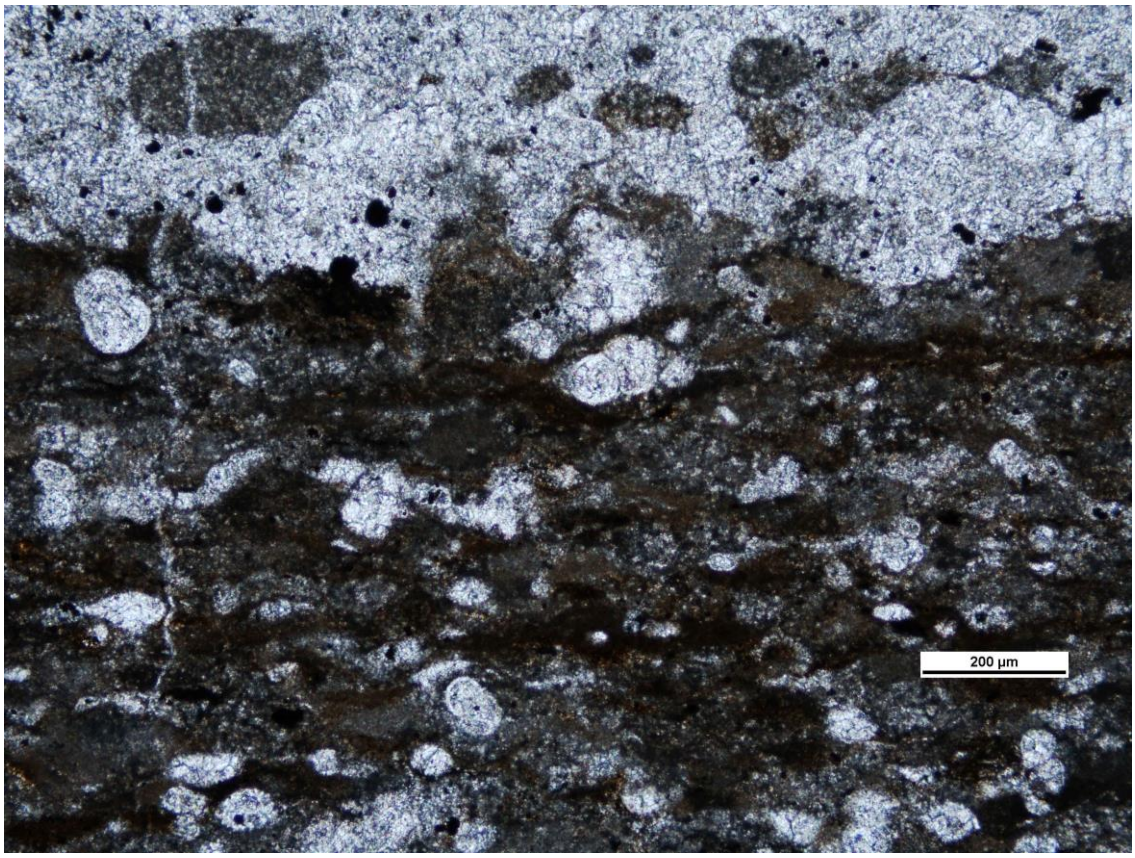

Height Above Buda:	112.6 feet
Skeletal Grain Types	Abundance
Planktonic Foram.	85%
Organics	10%
Pellets	5%
Pyrite	<1%

Other Diagenetic Features:
Organics and pellets are flattened. Calcite filled fractures.

Rock Name:
Foraminiferal Wackestone-Packstone

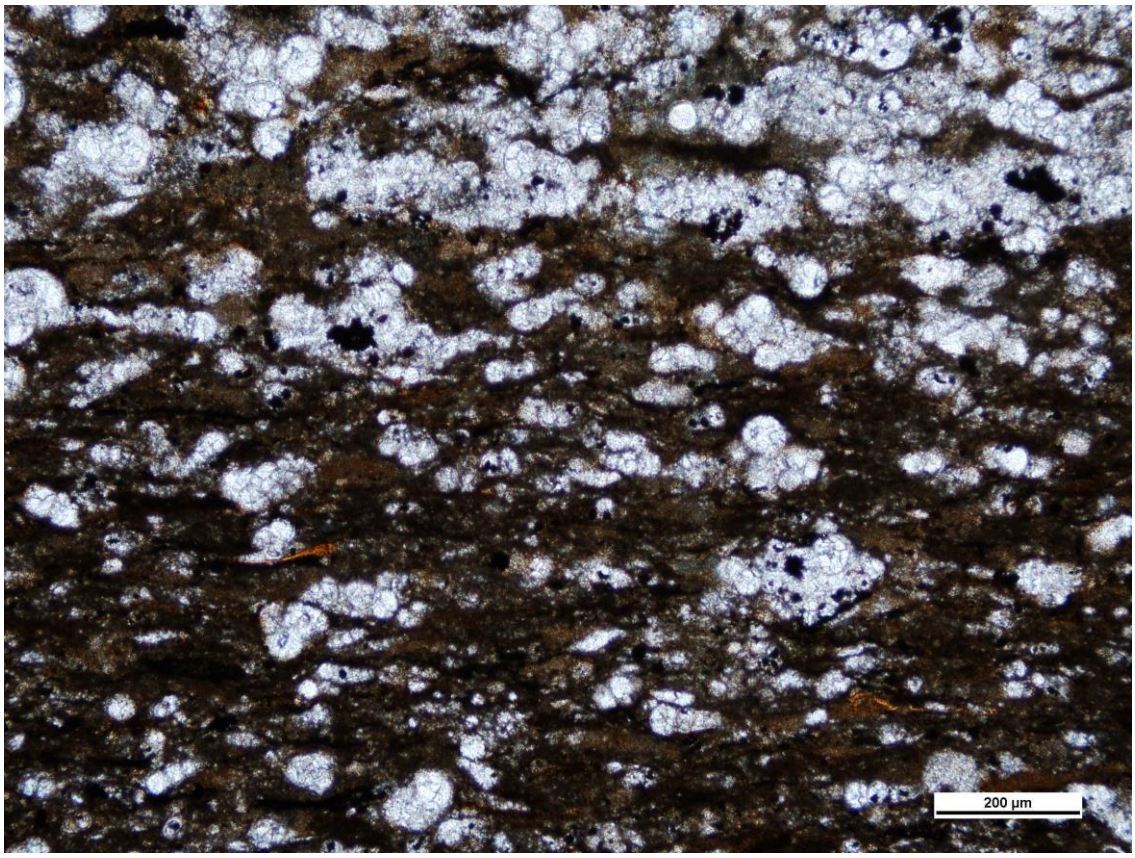

Height Above Buda:	115.5 feet
Skeletal Grain Types	Abundance
Planktonic Foram.	95%
Organics	5%
Pyrite	<1%
Fish Bones	<1%

Other Diagenetic Features:
Calcite filled fractures

Rock Name:
Foraminiferal mudstone-wackestone

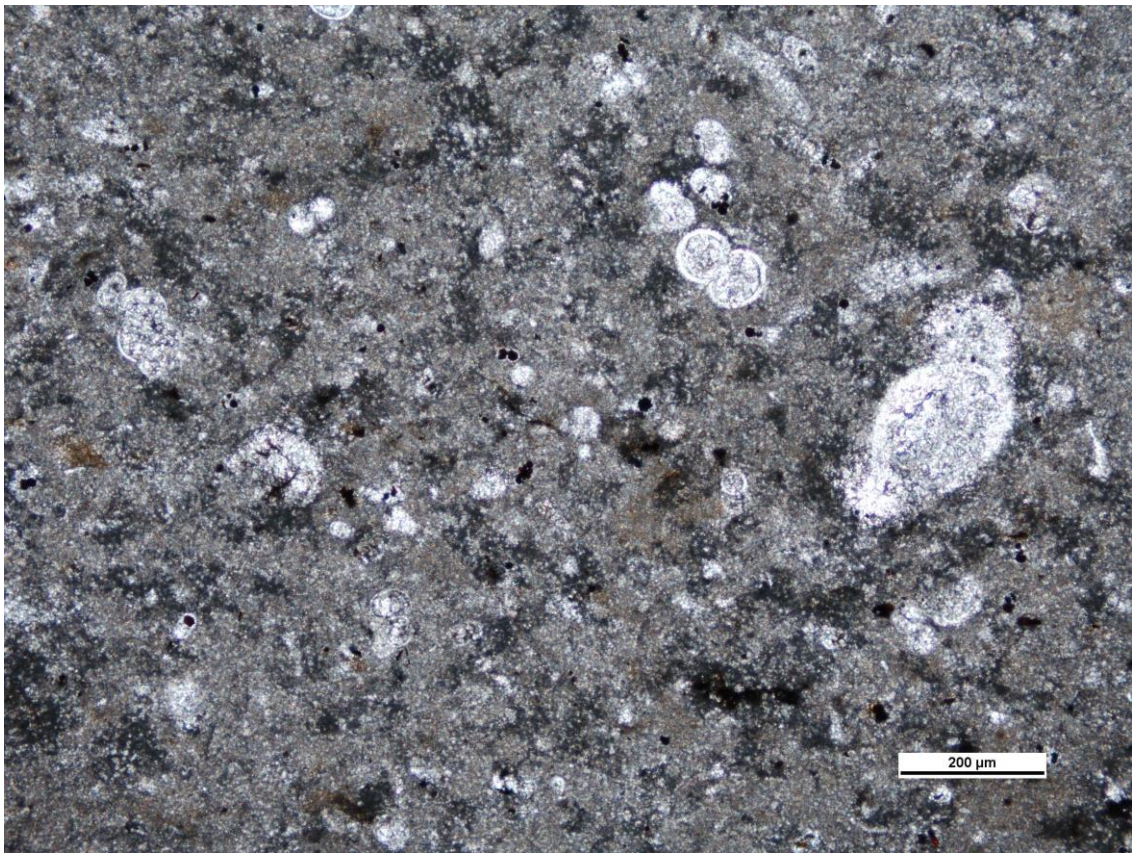

Height Above Buda:	121.0 feet
Skeletal Grain Types	Abundance
Planktonic Foram.	90%
Pellets	5%
Bivalve Fragments	5%
Pyrite	<1%

Other Diagenetic Features:
Burrows are darker than the surrounding matrix. Calcite filled fractures.

Rock Name:
Foraminiferal Wackestone-Packstone

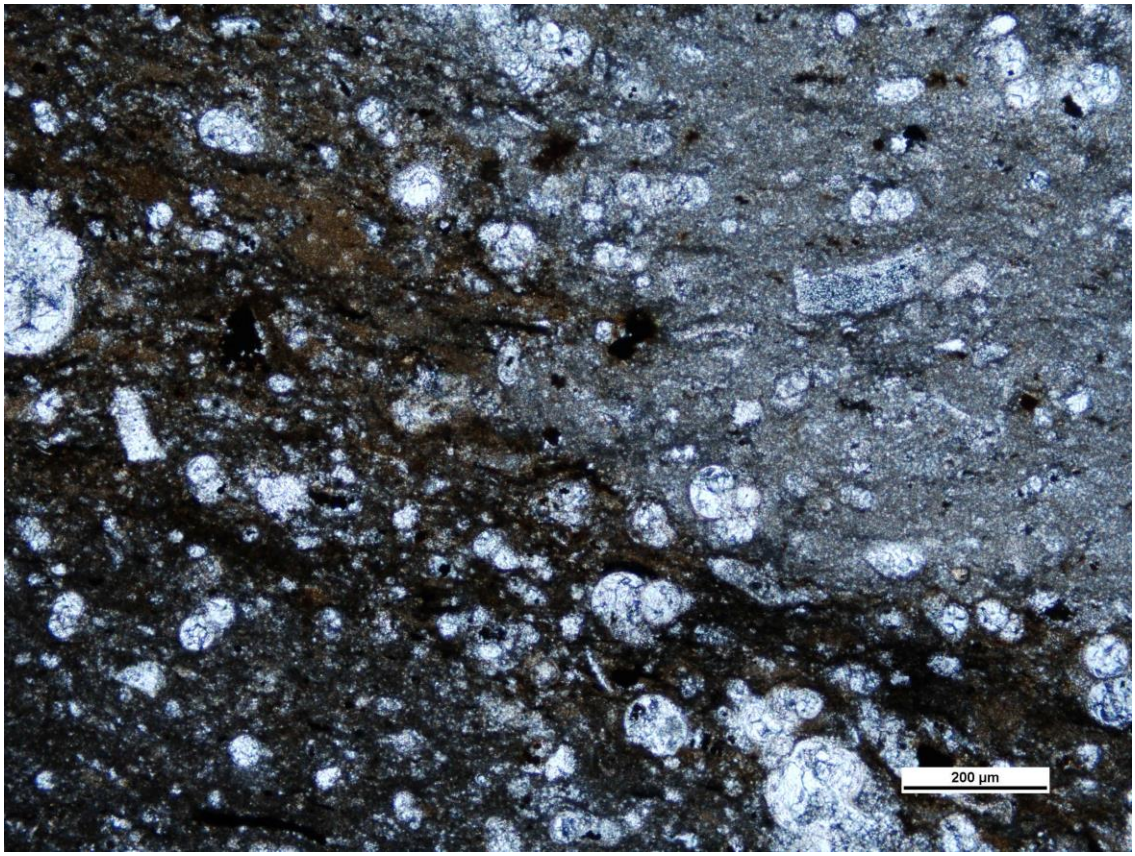

Height Above Buda:	122.0 feet
Skeletal Grain Types	Abundance
Planktonic Foram.	95%
Bivalves	5%
Ostracods	Rare
Pyrite	<1%
Organics	<1%

Other Diagenetic Features:
Burrows darker than the surrounding matrix. Pyrite replacement of some grains.

Rock Name:
Foraminiferal Wackestone-Packstone

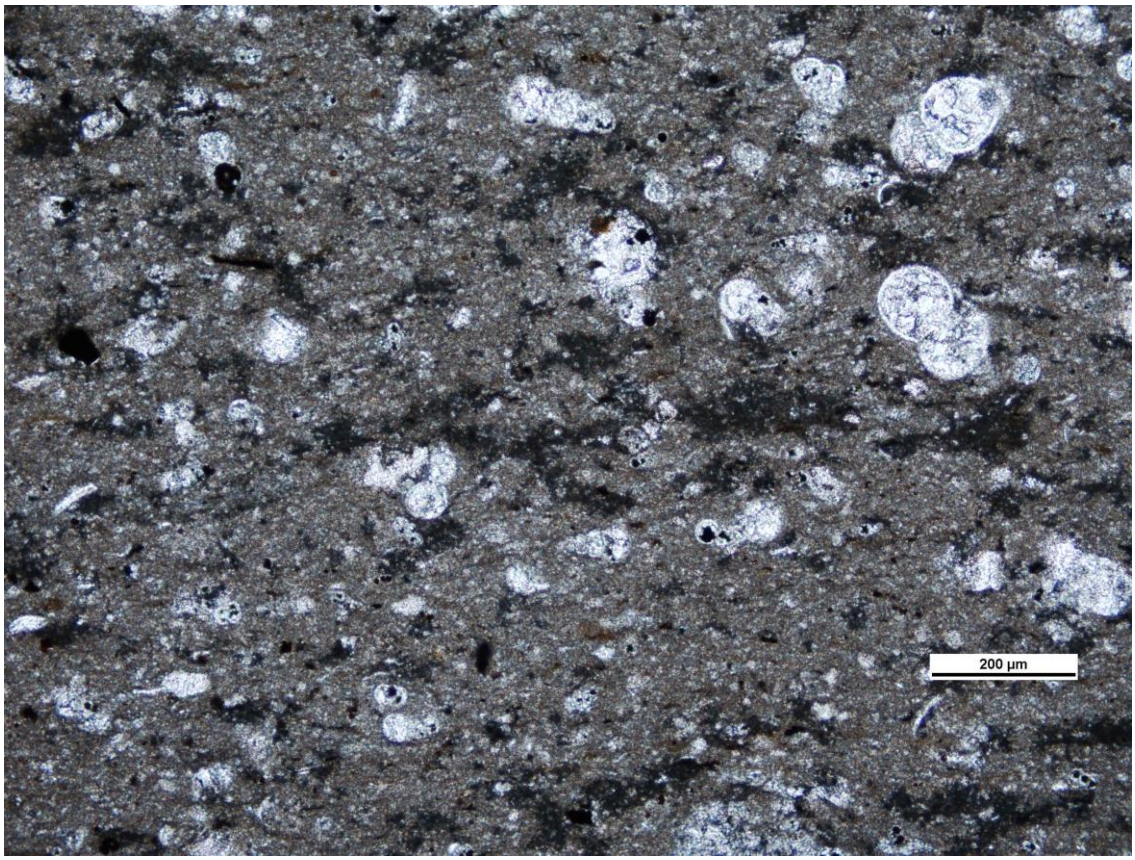

Height Above Buda:	125.5 feet
Skeletal Grain Types	Abundance
Planktonic Foram.	95%
Bivalve	<5%
Pyrite	<1%

Other Diagenetic Features:
Burrowed matrix is a darker color than surrounding matrix. Burrows are flattened.

Rock Name:
Foraminiferal Wackestone-Mudstone

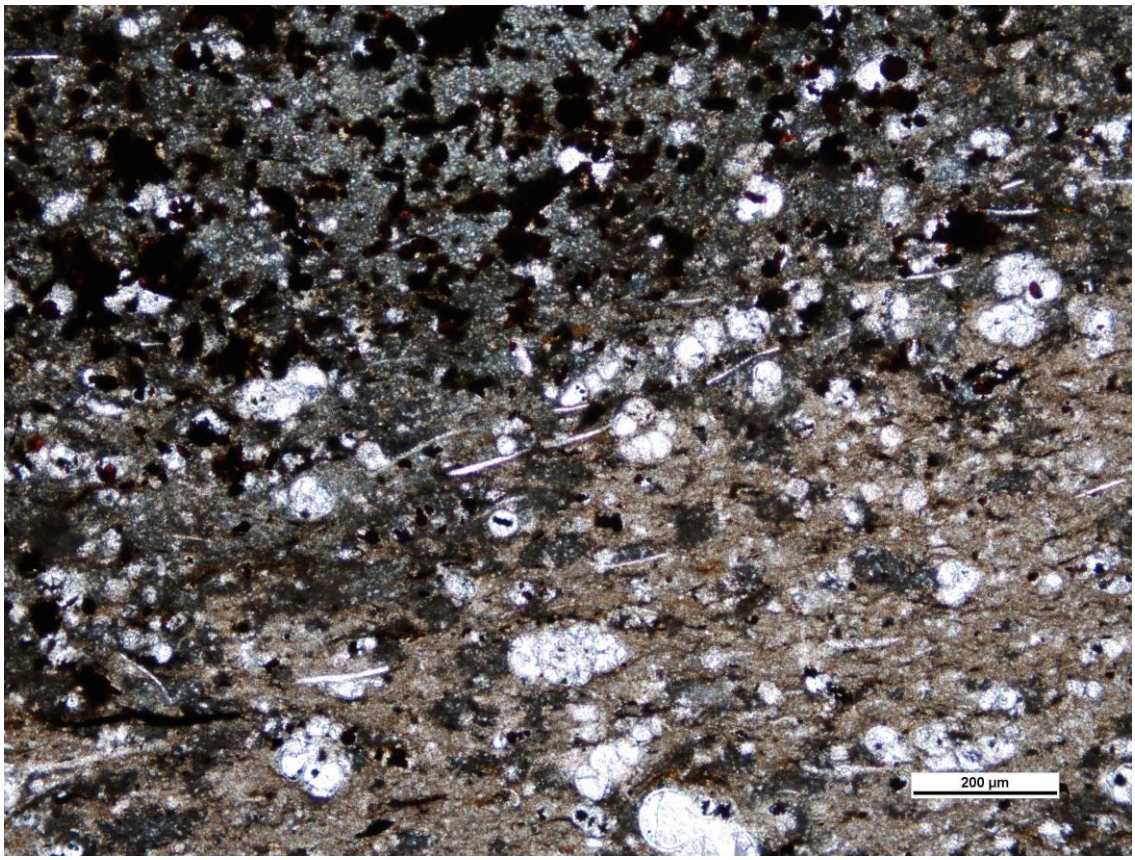

Height Above Buda:	133.0 feet
Skeletal Grain Types	Abundance
Planktonic Foram.	80%
Pyrite	15%
Bivalves	5%

Other Diagenetic Features:
There is more pyrite in the burrows.

Rock Name:
Foraminiferal Wackestone-Packstone

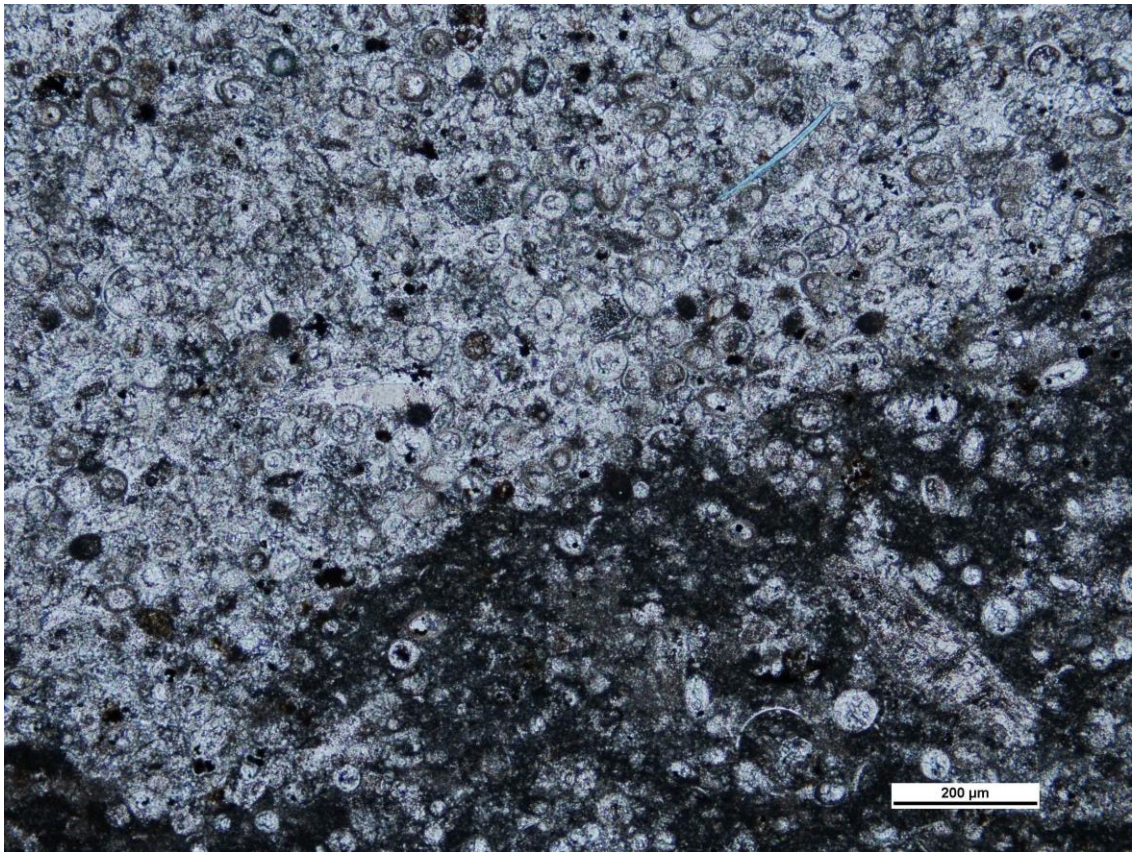

Height Above Buda:	134.0 feet
Skeletal Grain Types	Abundance
Foraminifera	60%
Pellets	30%
Bivalves	10%

Other Features:
Nodular bedding. Highly bioturbated.

Rock Name:
Nodular Foraminiferal Packstone

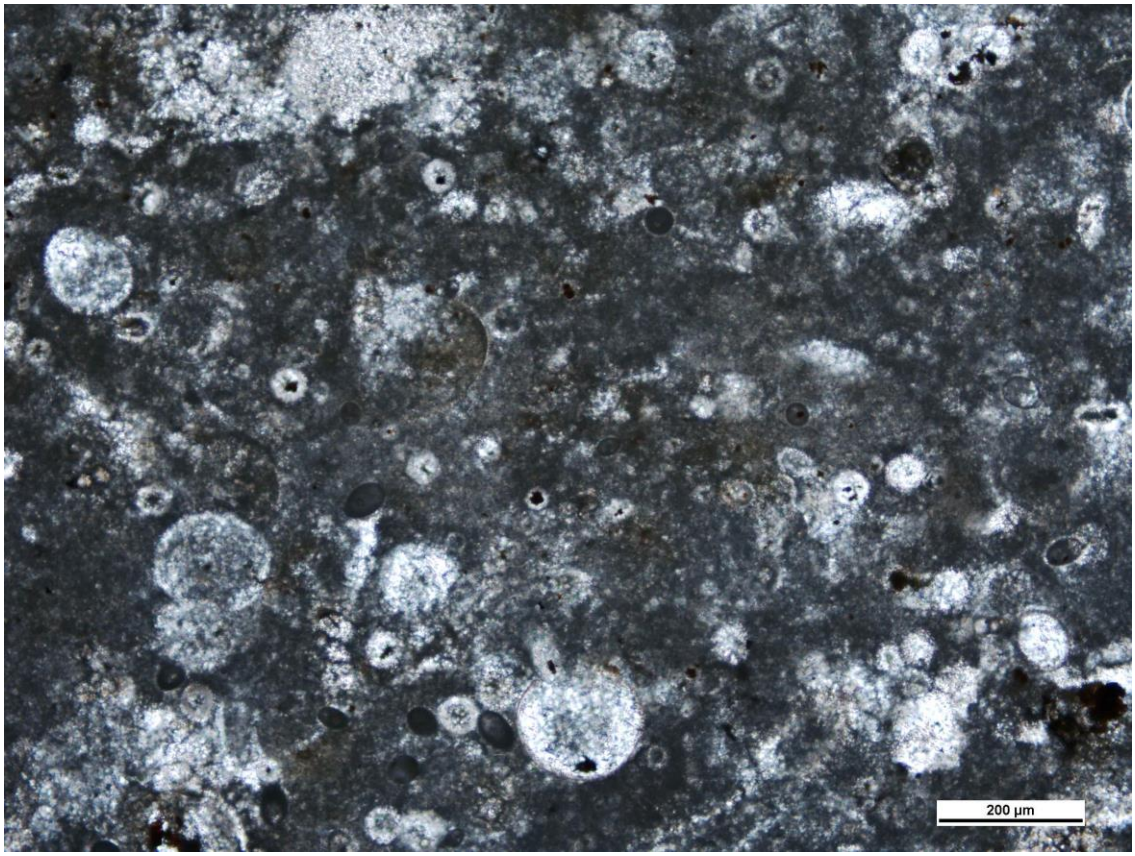

Height Above Buda:	135.2 feet
Skeletal Grain Types	Abundance
Foraminifera	80%
Pellets	15%
Bivalves	5%
Pyrite	<1%

Other Diagenetic Features:
Pyrite replaces some grains.

Rock Name:
Foraminiferal Wackestone-Packstone

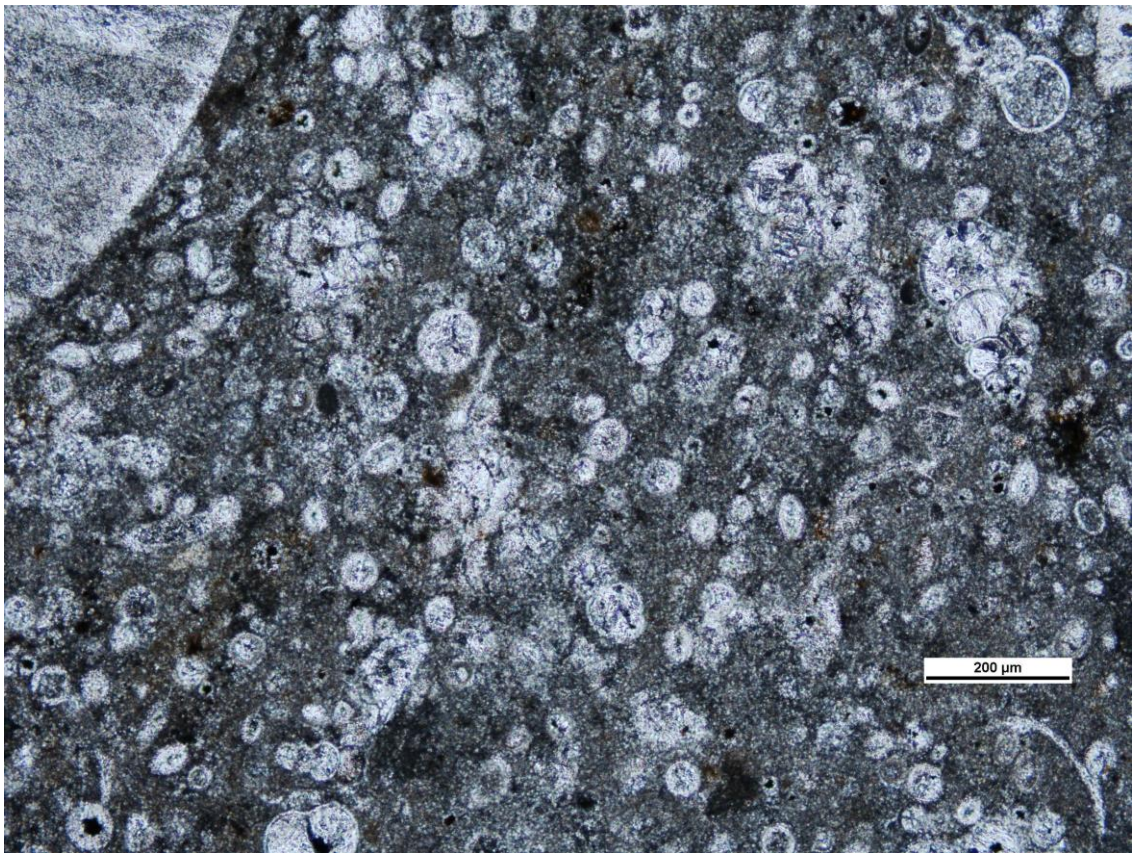

Height Above Buda:	136.9 feet
Skeletal Grain Types	Abundance
Foramifera	90%
Pellets	5%
Bivalves	5%
Pyrite	<1%

Other Diagenetic Features:
Pyrite replacement in some grains

Rock Name:
Foraminiferal Packstone-Wackestone

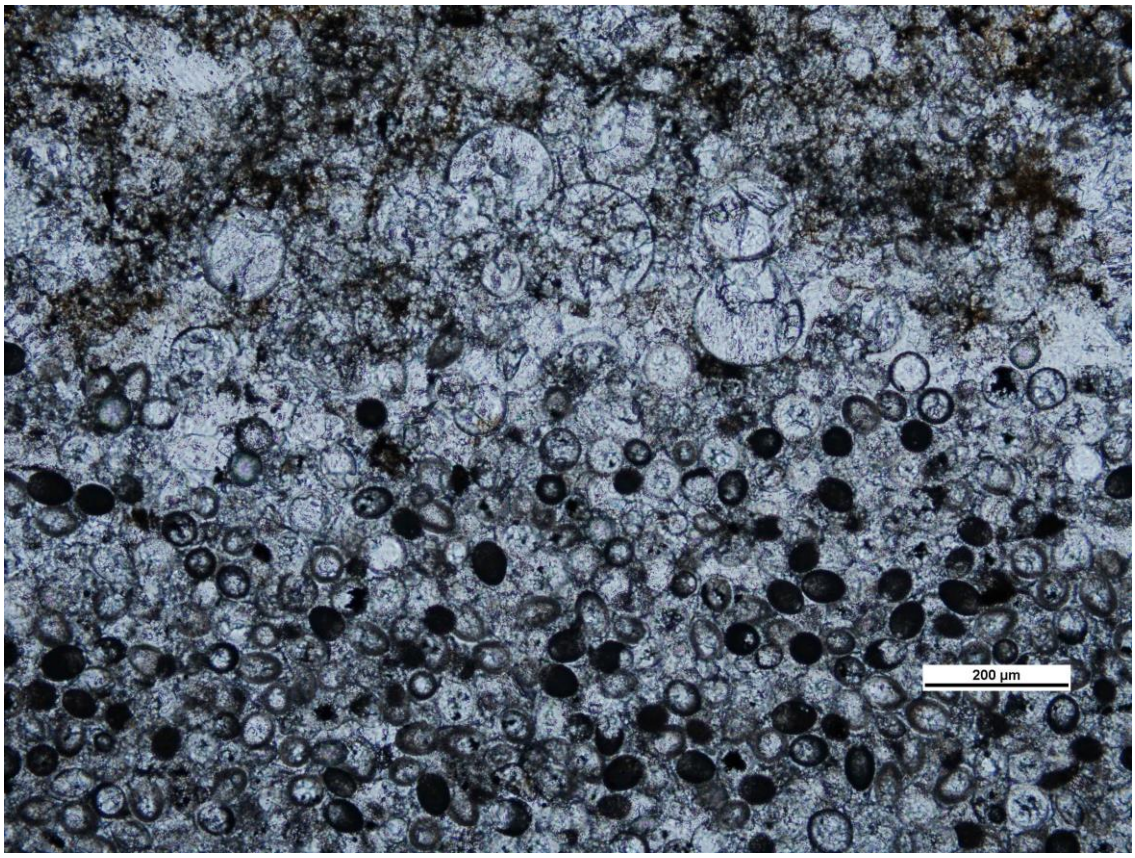

Height Above Buda:	141.0 feet
Skeletal Grain Types	Abundance
Pellets	60%
Foramifera	40%
Pyrite	<1%

Other Diagenetic Features:
Some grains are micritized. Forams are recrystallized.

Rock Name:
Pelloidal Packstone

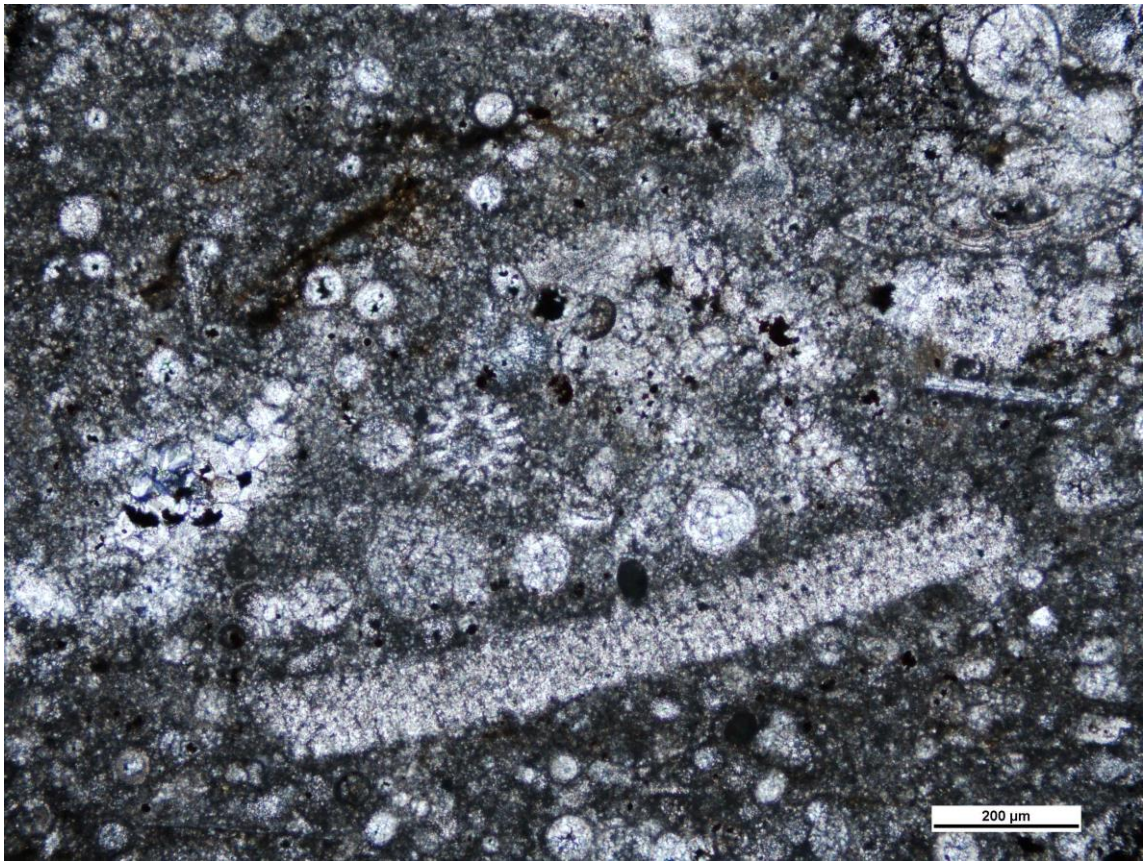

Height Above Buda:	143.0 feet
Skeletal Grain Types	Abundance
Foraminifera	50%
Pellets	30%
Bivalves	10%
Echinoids	10%
Pyrite	<1%
Fish Bones	Rare
Dasyclad Algae	Rare

Other Diagenetic Features:
Recrystallized grains.

Rock Name:
Foraminiferal Packstone-Wackestone

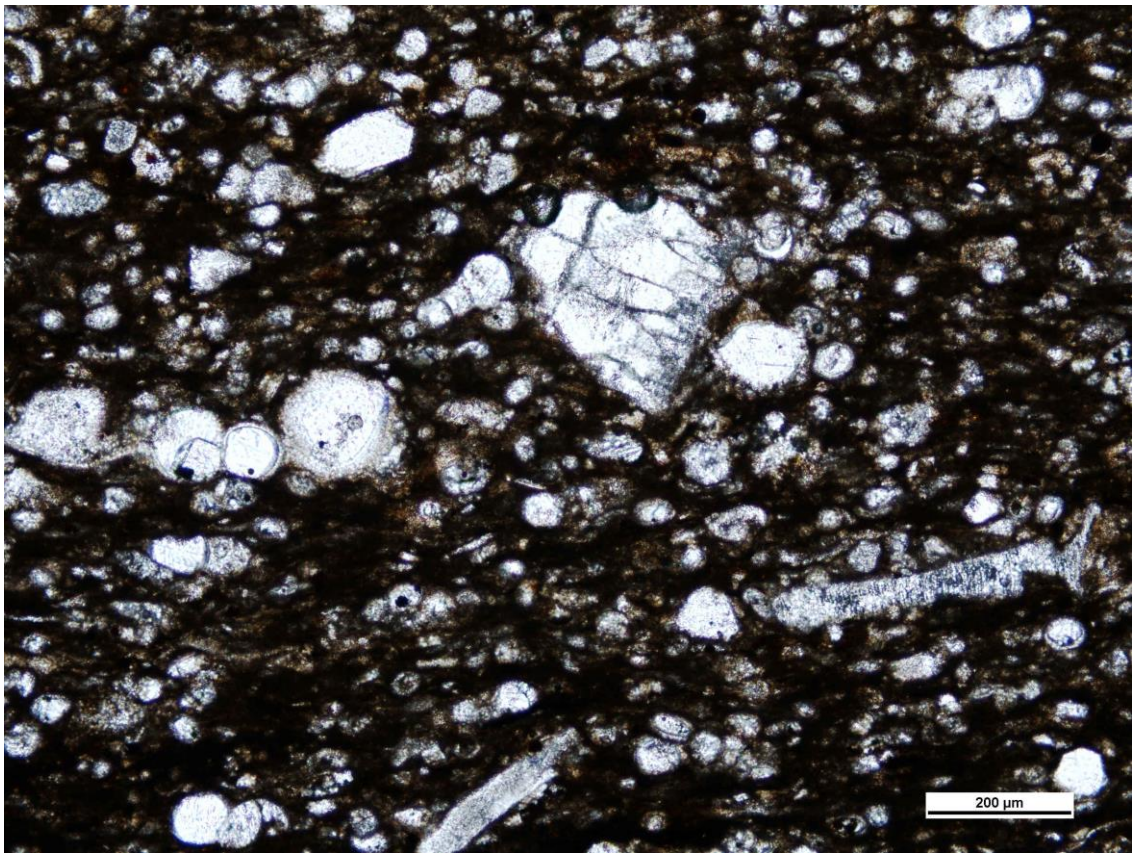

Height Above Buda:	147.4 feet
Skeletal Grain Types	Abundance
Planktonic Foram.	40%
Bivalves	20%
Pellets	20%
Echinoids	10%
Fish Bones	5%
Organics	5%

Other Diagenetic Features:
Recrystallized forams. Flattened organics.

Rock Name:
Foraminiferal Wackestone-Packstone

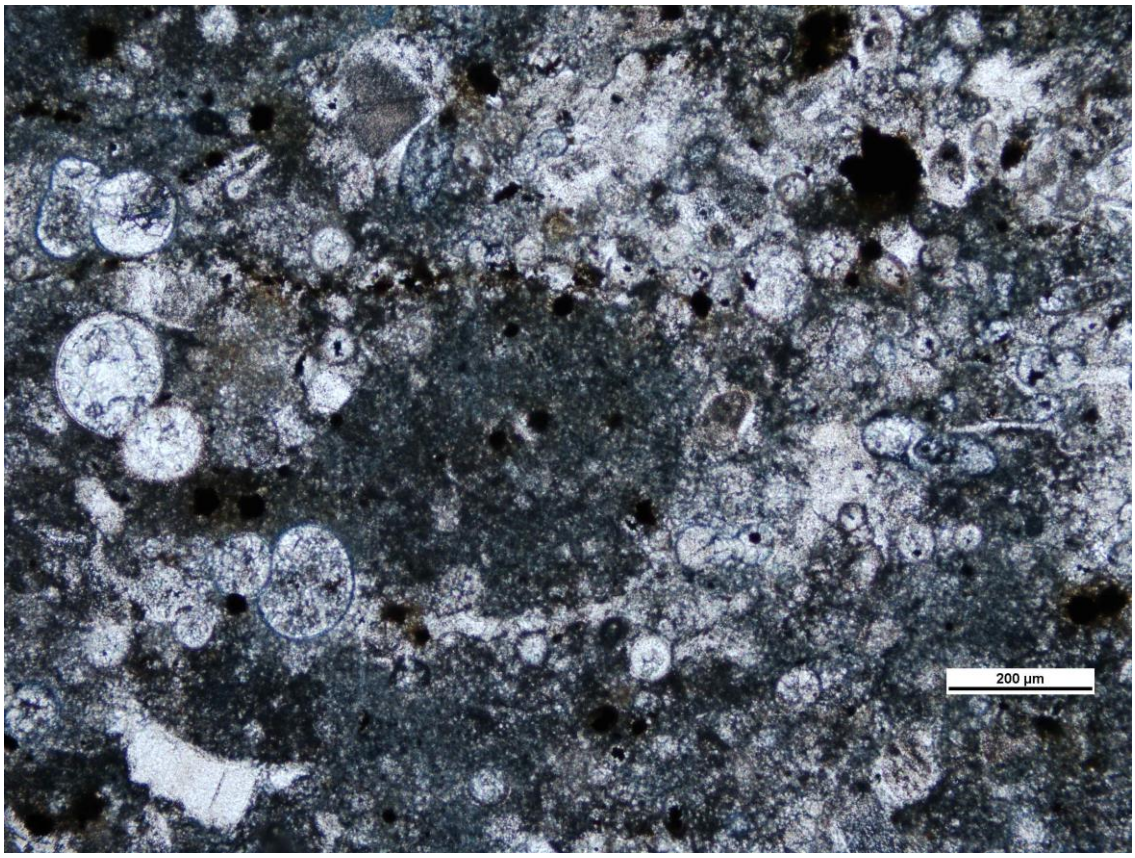

Height Above Buda:	149.2 feet
Skeletal Grain Types	Abundance
Planktonic Foram.	80%
Bivalves	10%
Pyrite	5%
Echinoids	5%

Other Diagenetic Features:
Burrows are darker than surrounding matrix.

Rock Name:
Foraminiferal Packstone-Wackestone

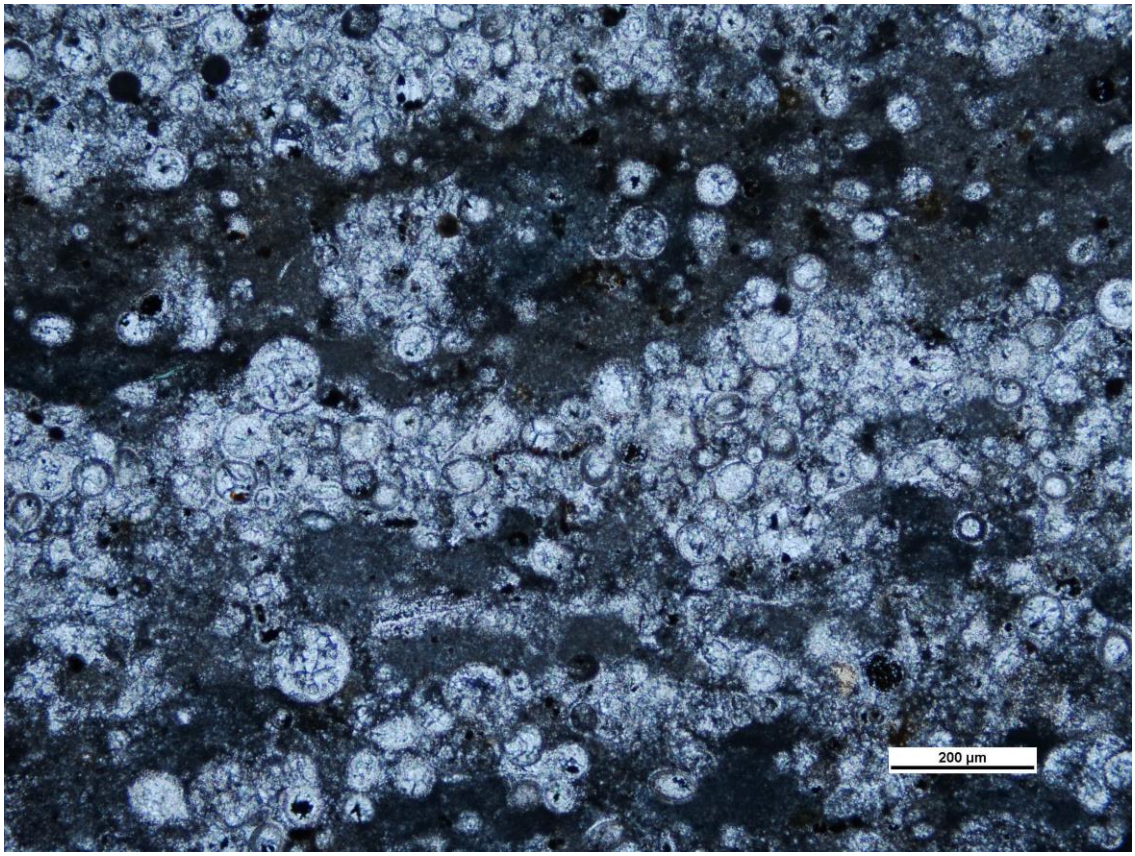

Height Above Buda:	152.3 feet
Skeletal Grain Types	Abundance
Planktonic Foram.	90%
Pellets	10%
Pyrite	<1%
Bivalve	<1%

Other Diagenetic Features:
Forams are recrystallized. Some are partially replaced with pyrite.

Rock Name:
Ripple Laminated Foraminiferal Packstone

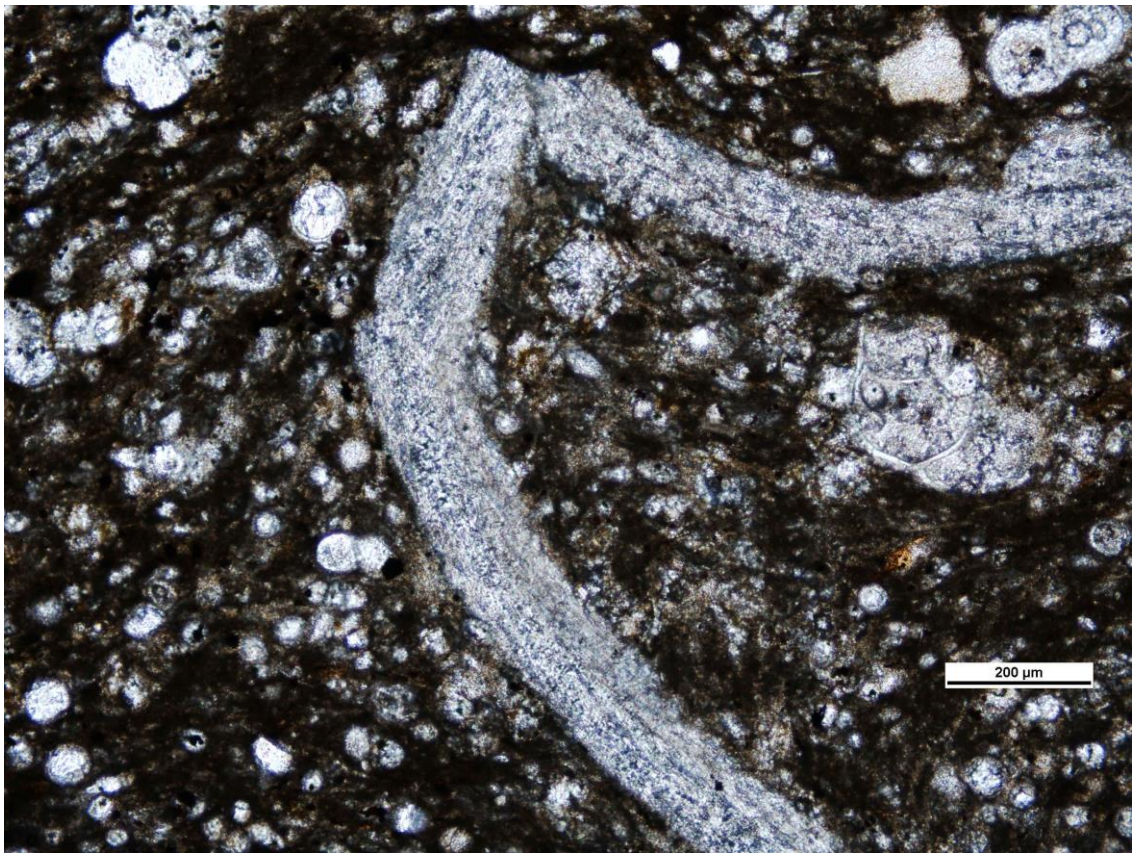

Height Above Buda:	153.7 feet
Skeletal Grain Types	Abundance
Planktonic Foram.	50%
Pellets	30%
Bivalves	20%
Pyrite	Rare
Fish bones	Rare

Other Diagenetic Features:
Some bivalves are recrystallized. Calcite filled fractures.

Rock Name:
Ripple Laminated Foraminiferal Packstone

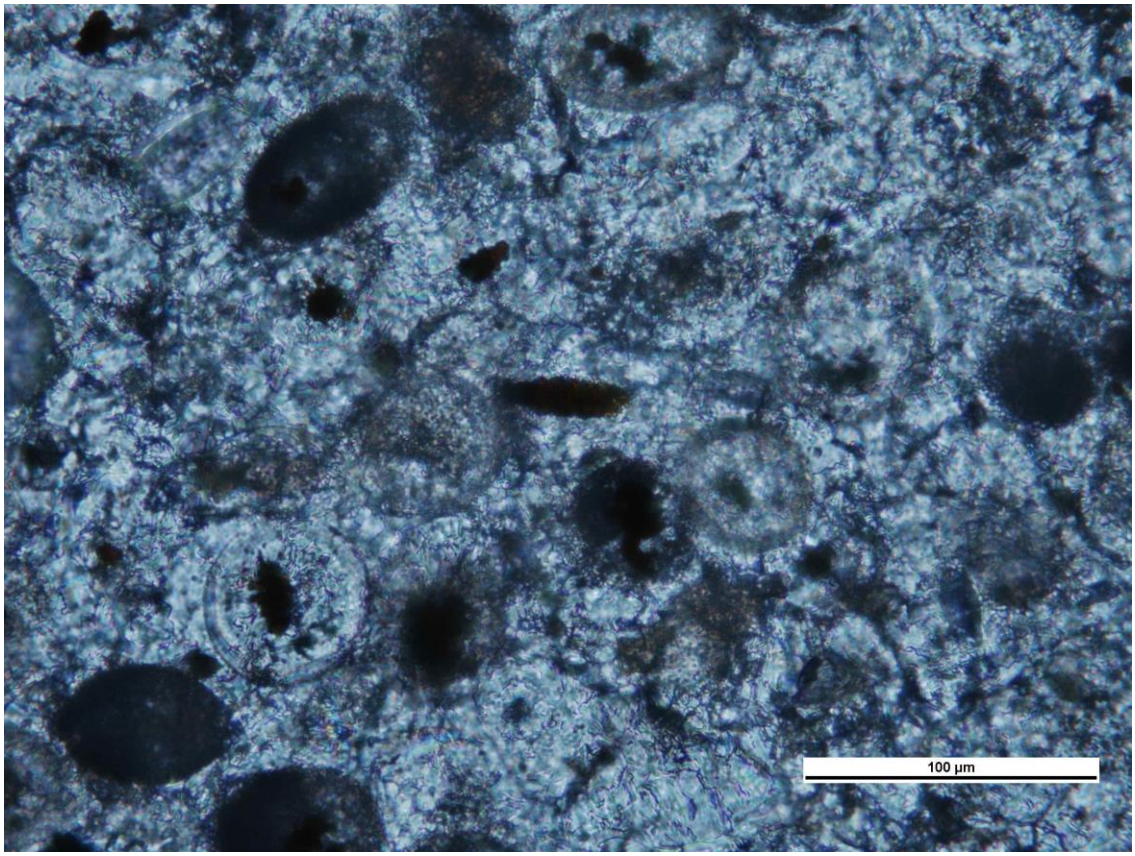

Height Above Buda:	154.4 feet
Skeletal Grain Types	Abundance
Foraminifera	80%
Pellets	20%
Bivalves	<1%
Pyrite	<1%

Other Diagenetic Features:
Moldic porosity within some lamina. Some grains pyritized.

Rock Name:
Foraminiferal Packstone.

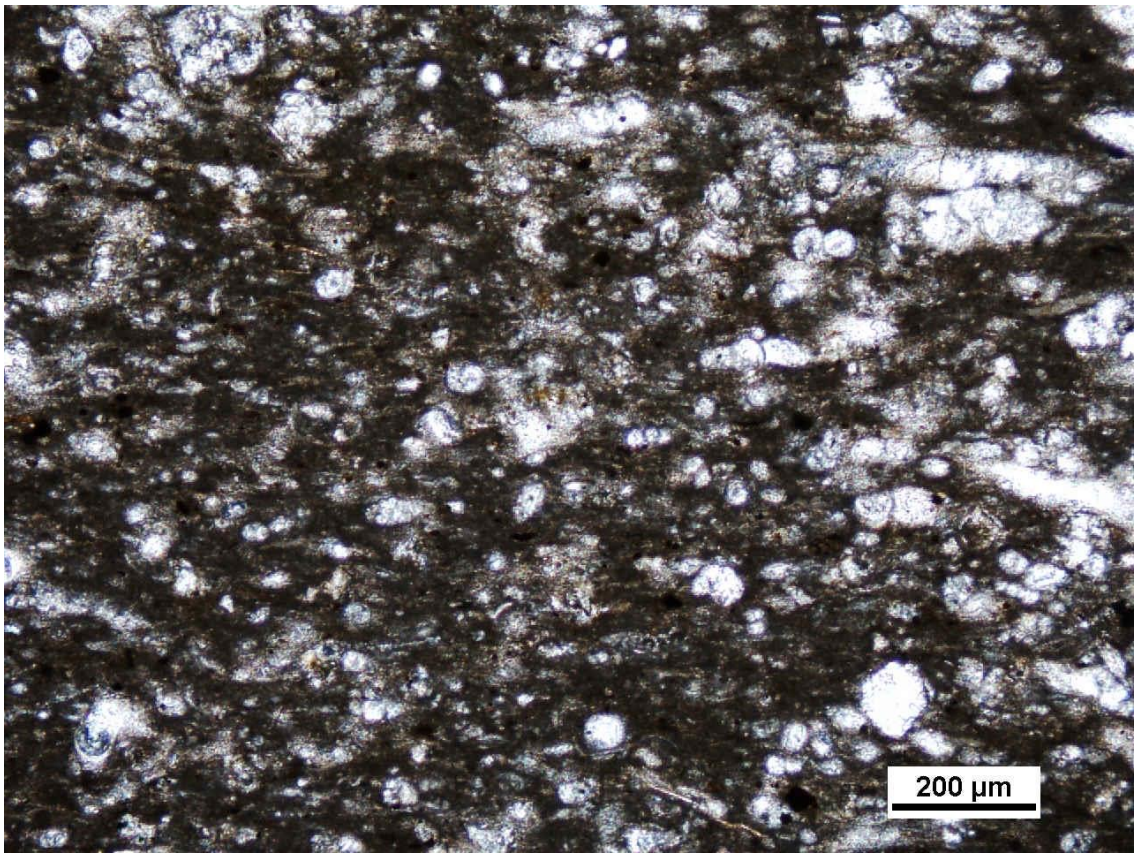

Height Above Buda:	154.7 feet
Skeletal Grain Types	Abundance
Planktonic Foram.	90%
Bivalves	10%
Pyrite	<1%
Fish Bones	Rare

Other Diagenetic Features:

Rock Name:
Foraminiferal Wackestone-Packstone

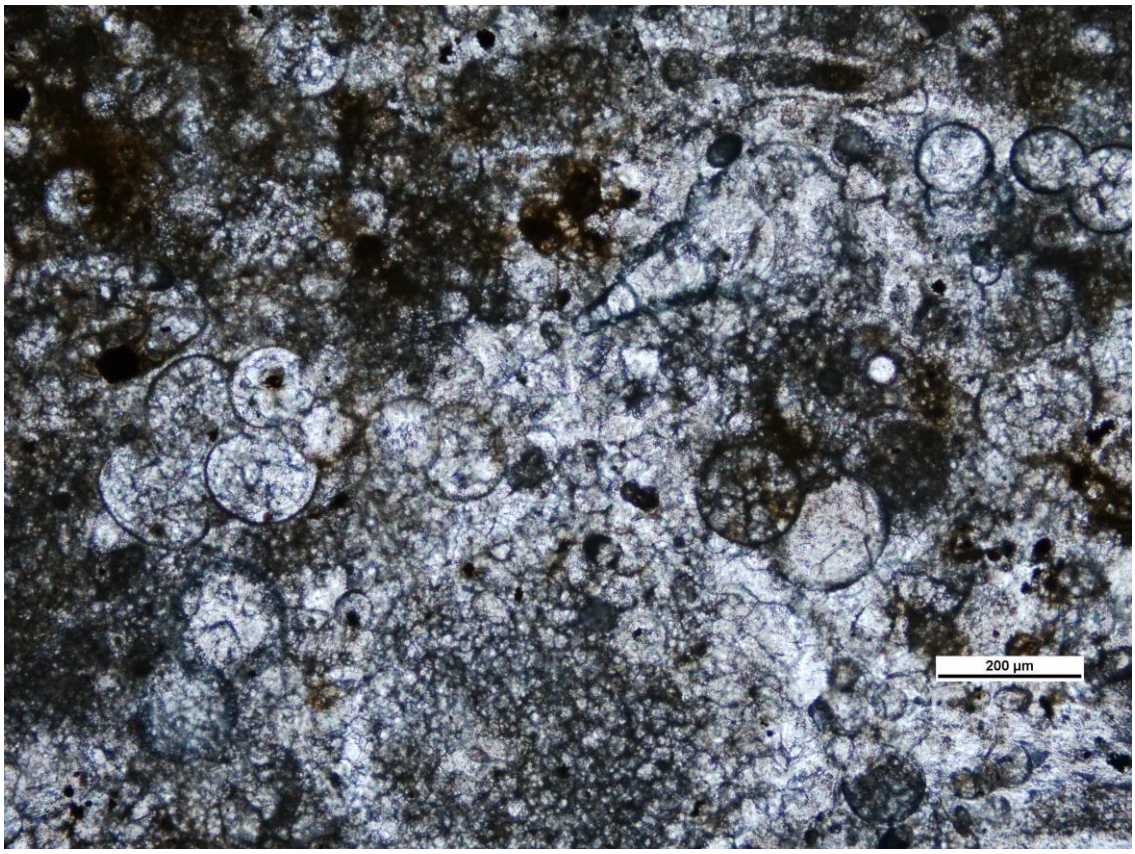

Height Above Buda:	157.3 feet
Skeletal Grain Types	Abundance
Planktonic Foram.	90%
Pellets	5%
Bivalves	5%
Pyrite	<1%
Radiolaria	Rare

Other Diagenetic Features:
Heavily recrystallized. Pyrite replacement of some grains.

Rock Name:
Foraminiferal Packstone- Wackestone

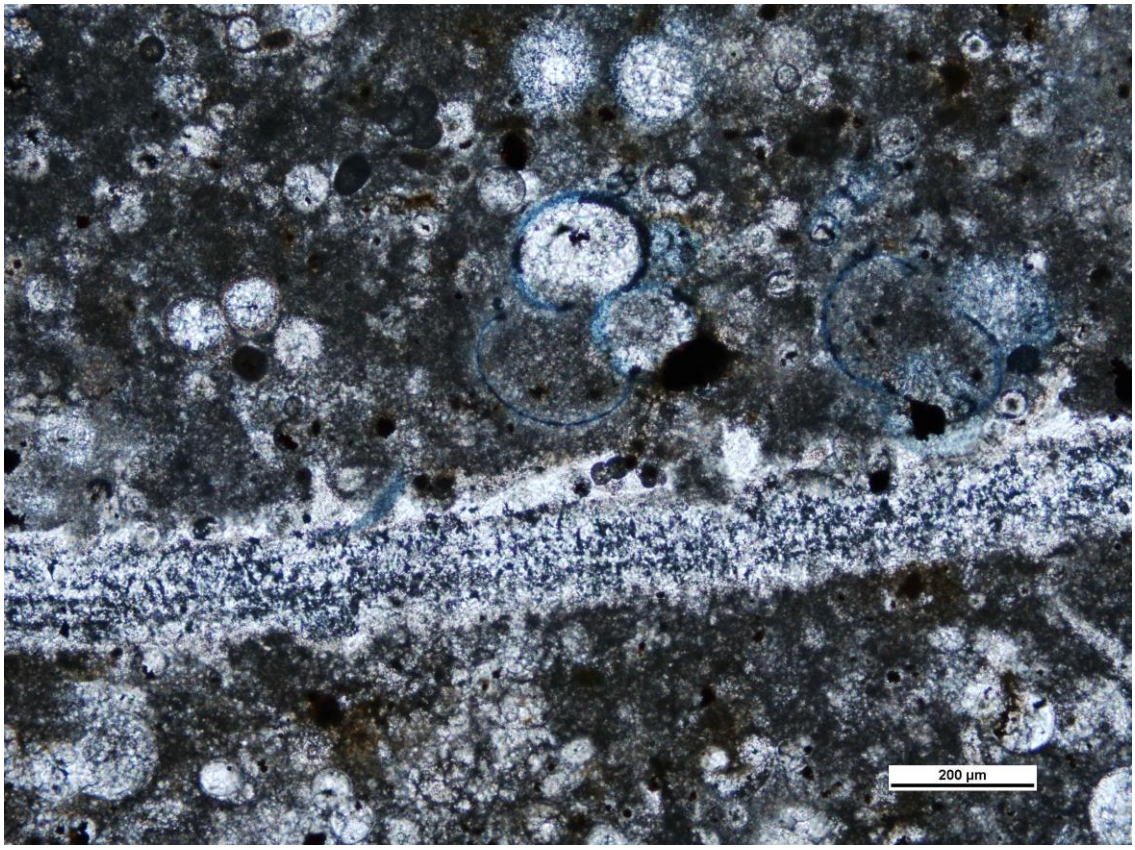

Height Above Buda:	159.3
Skeletal Grain Types	Abundance
Planktonic Foram.	40%
Echinoids	30%
Bivalves	20%
Pellets	10%
Pyrite	5%

Other Diagenetic Features:
Moldic porosity is common.

Rock Name:
Foraminiferal Wackestone-Packstone

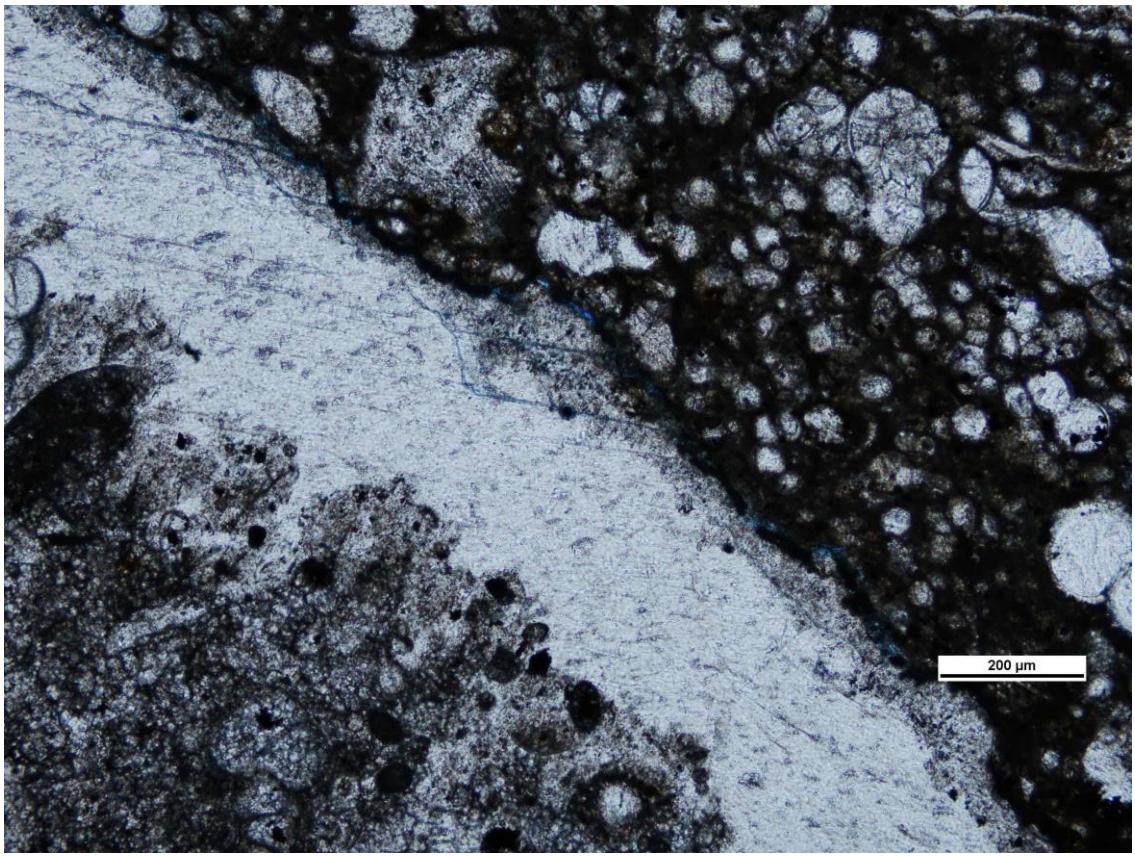

Height Above Buda:	160 feet
Skeletal Grain Types	Abundance
Planktonic Foram.	80%
Echinoids	10%
Bivalves	5%
Pellets	5%

Other Diagenetic Features:

Rock Name:
Foraminiferal Packstone

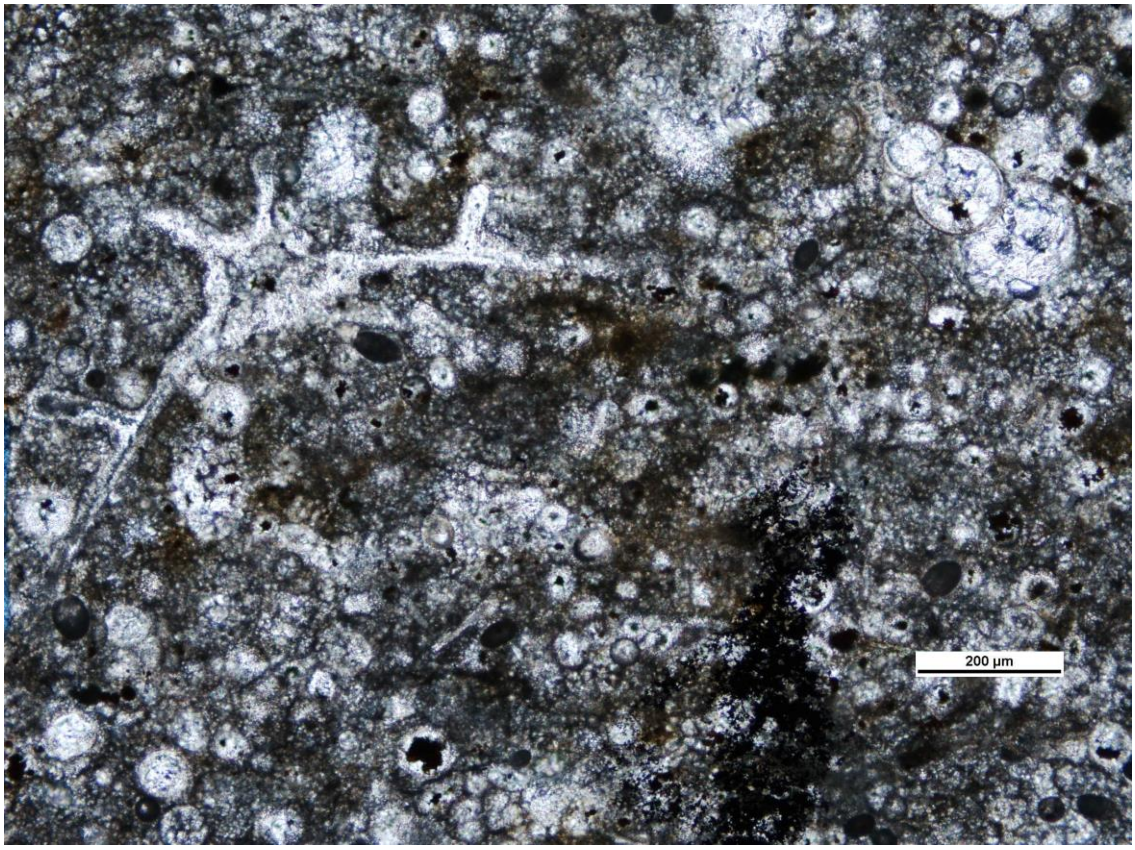

Height Above Buda:	165.0 feet
Skeletal Grain Types	Abundance
Planktonic Foram.	80%
Pellets	10%
Pyrite	5%
Bivalves	5%
Fish bones	<1%

Other Diagenetic Features:
Recrystallized forams and bivalves.
Pyritized grains.

Rock Name:
Foraminiferal Packstone-Wackestone

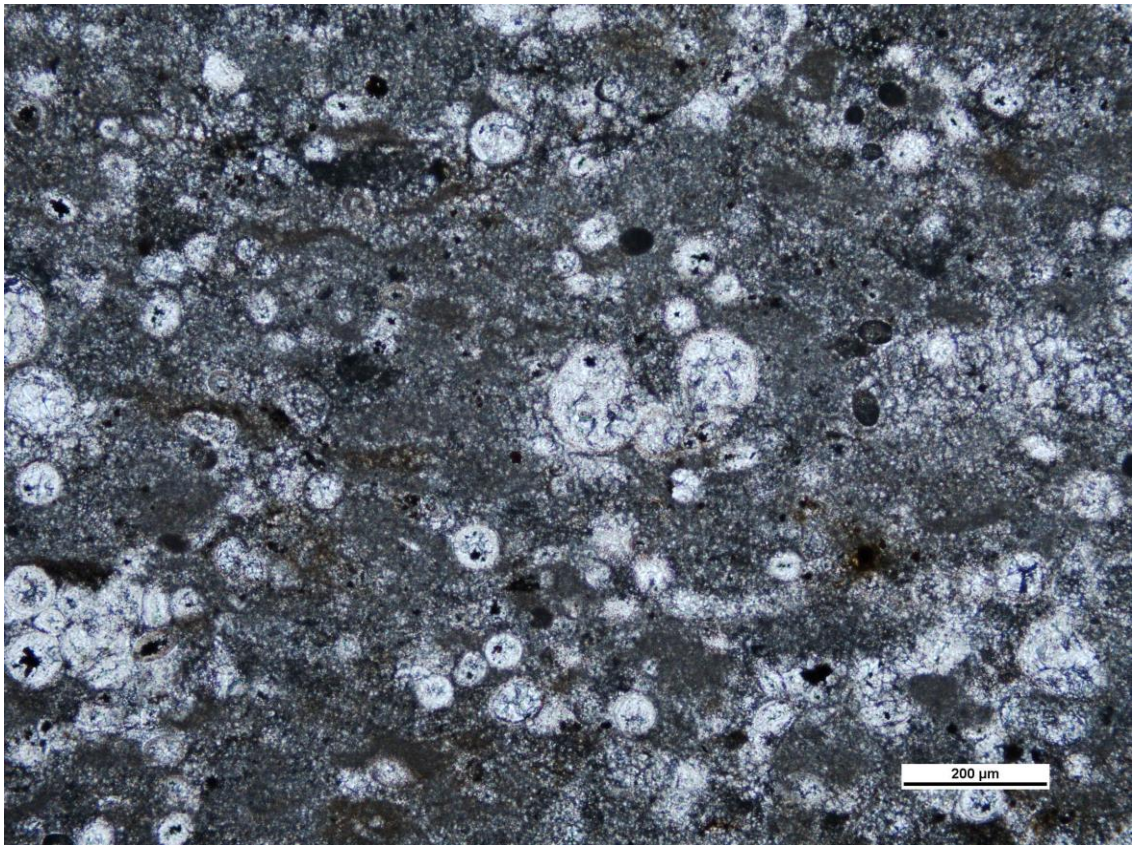

Height Above Buda:	167.0 feet
Skeletal Grain Types	Abundance
Planktonic Forams	95%
Pellets	5%
Bivalves	<1%
Pyrite	<1%

Other Diagenetic Features:
Recrystallized forams. Pyritized grains.

Rock Name:
Ripple Laminated Foraminiferal Wackestone.

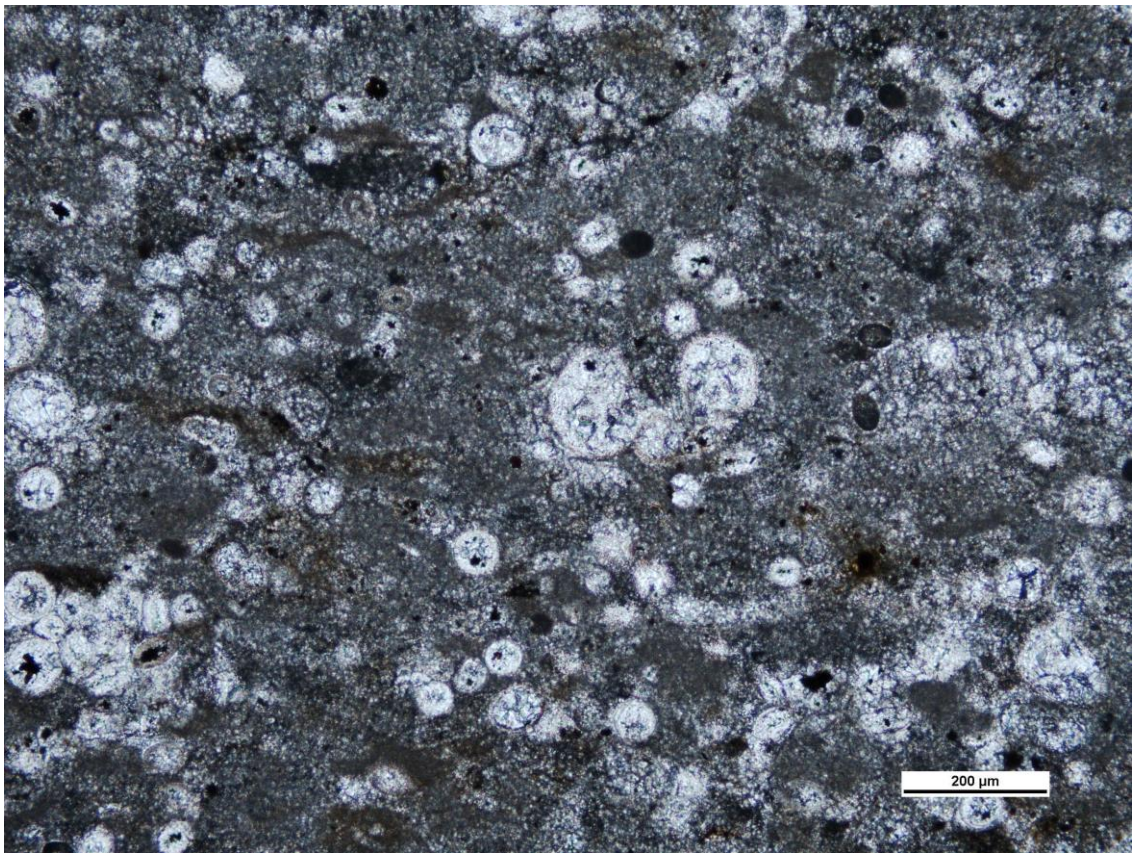

Height Above Buda:	167.0 feet
Skeletal Grain Types	Abundance
Planktonic foram.	85%
Pellets	10%
Pyrite	5%
Bivalves	<1%

Other Diagenetic Features:
Pyritized grains. Recrystallized forams.

Rock Name:
Ripple Laminated Foraminiferal Packstone-Wackestone

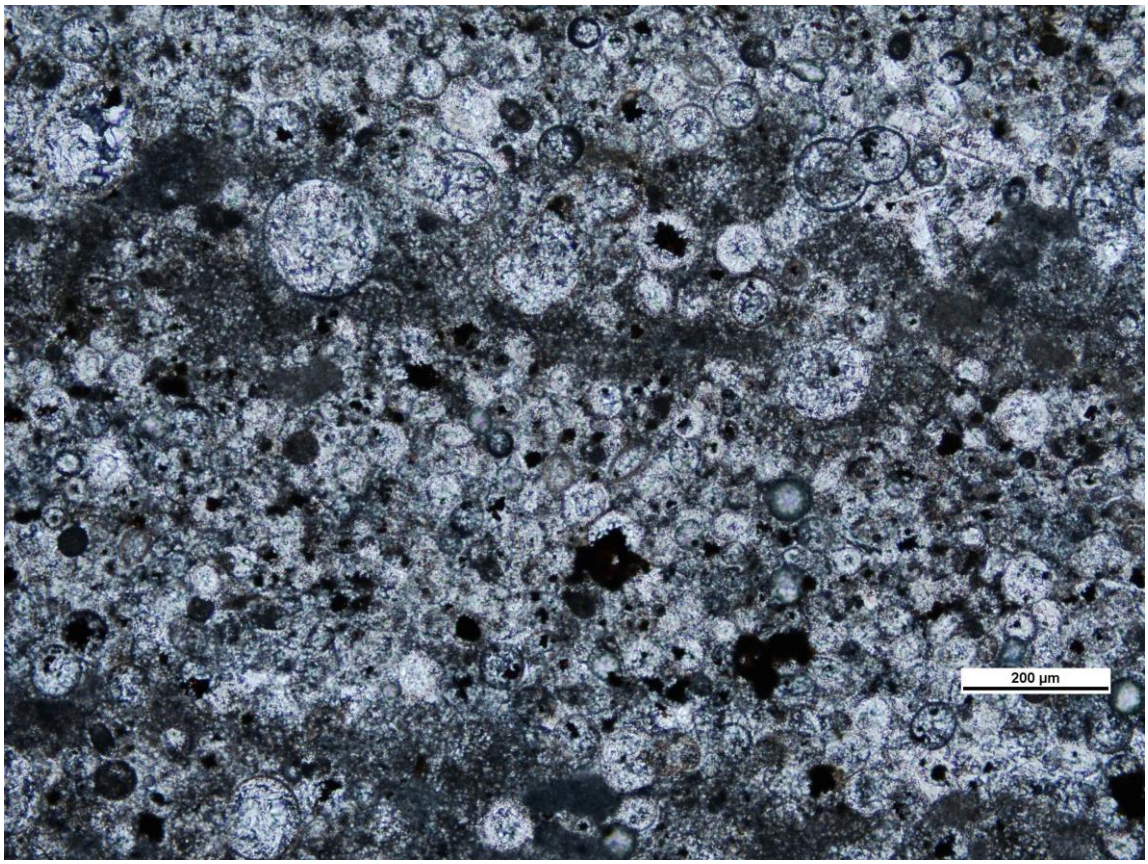

Height Above Buda:	168.6 feet
Skeletal Grain Types	Abundance
Planktonic Foram.	90%
Pellets	5%
Pyrite	5%
Bivalves	<1%
Echinoids	Rare

Other Diagenetic Features:

Rock Name:
Ripple Laminated Foraminiferal Packstone

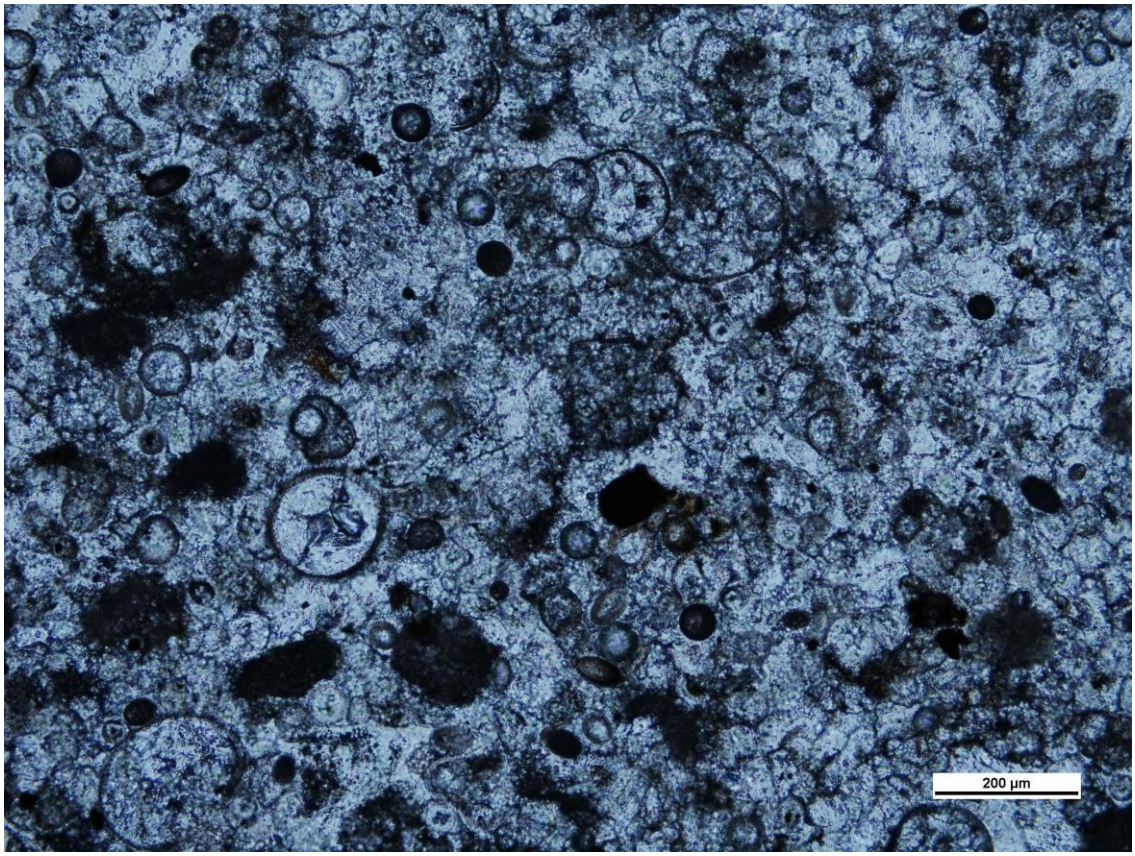

Height Above Buda:	170.6 feet
Skeletal Grain Types	Abundance
Planktonic Foram.	85%
Pellets	10%
Pyrite	5%
Bivalves	Rare
Echinoids	Rare
Other Diagenetic Features:	

Rock Name:
Foraminiferal Packstone

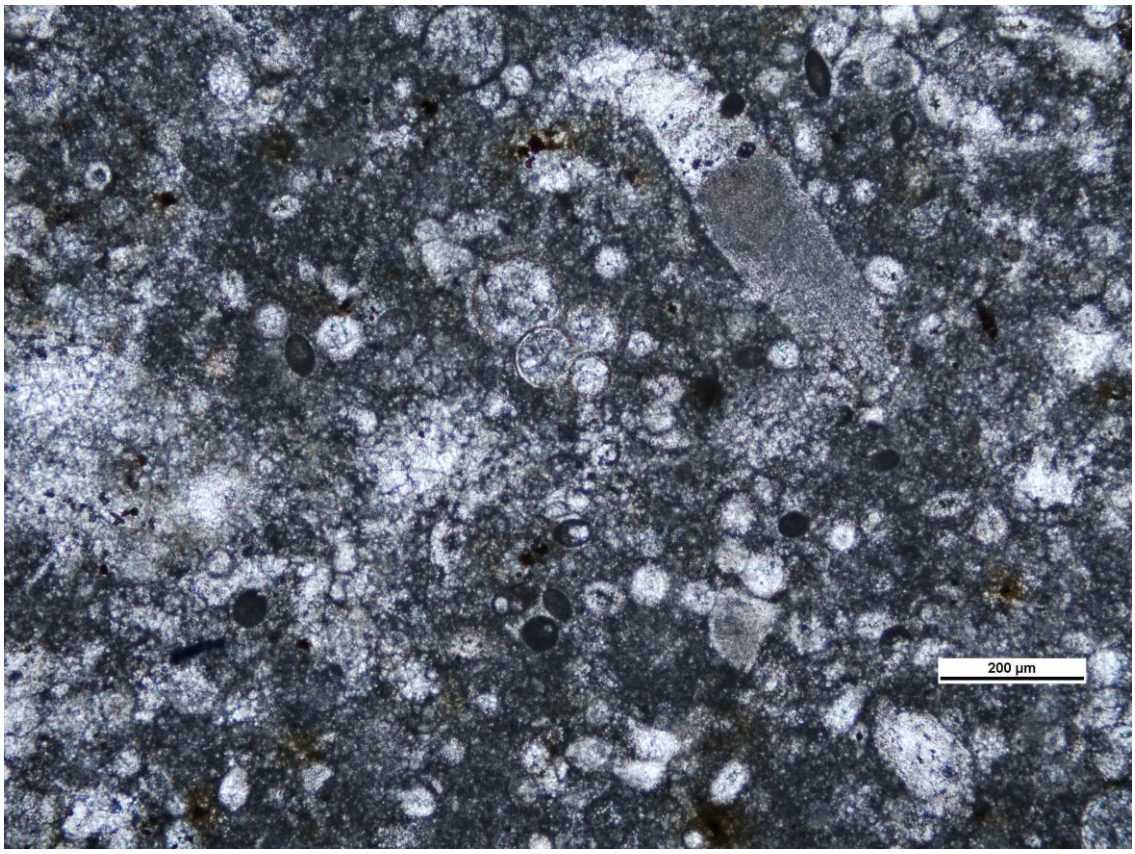

Height Above Buda:	171.3
Skeletal Grain Types	Abundance
Planktonic Foram.	60%
Pellets	30%
Bivalves	10%
Echinoids	Rare
Fish Bones	Rare
Pyrite	Rare

Other Diagenetic Features:
Recrystallized forams. Phosphatized fish bones.

Rock Name:
Foraminiferal Packstone-Wackestone

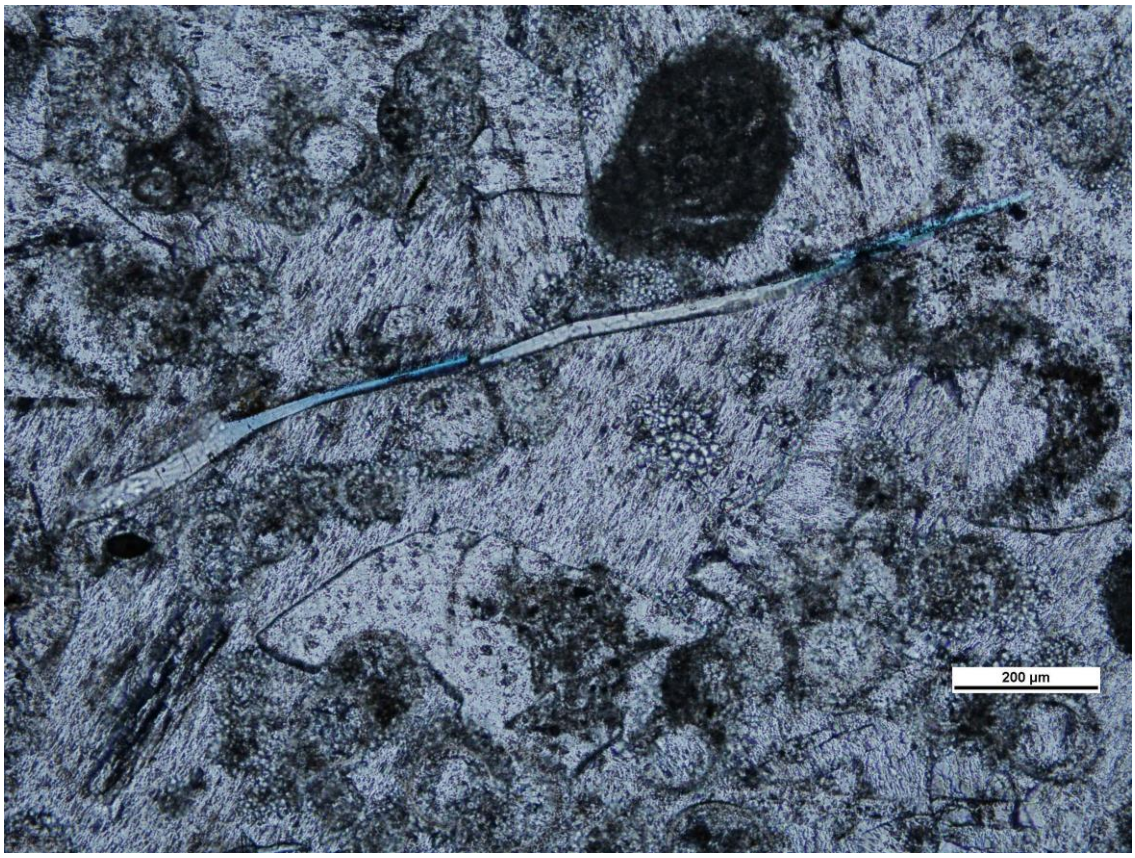

Height Above Buda:	178.5
Skeletal Grain Types	Abundance
Bivalves	40%
Ammonites	20%
Bryozoans	20%
Pellets	20%

Other Diagenetic Features:
Some moldic porosity.

Rock Name:
Skeletal Packstone

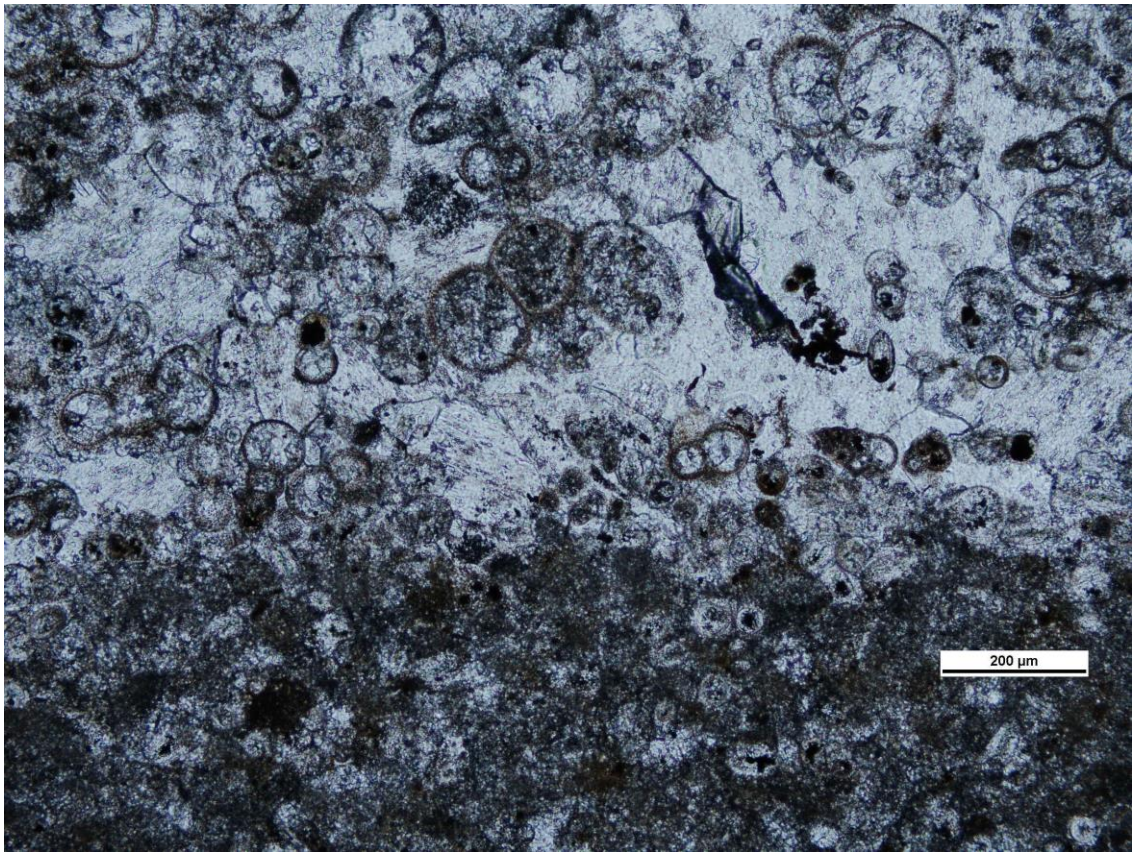

Height Above Buda:	182.9 feet
Skeletal Grain Types	Abundance
Planktonic foram.	85%
Pellets	10%
Pyrite	5%
Echinoids	Rare
Bivalves	Rare

Other Diagenetic Features:
Recrystallized forams. Pyritized grains.

Rock Name:
Ripple Laminated Foram Packstone